UNIVERSITY OF OKLAHOMA

GRADUATE COLLEGE

# THE ADVANCEMENT OF NARROW OPEN TUBULAR LIQUID CHROMATOGRAPHY

A DISSERTATION

SUBMITTED TO THE GRADUATE FACULTY

in partial fulfillment of the requirements for the

Degree of

DOCTOR OF PHILOSOPHY

By

PILIANG XIANG

Norman, Oklahoma

2021

THE ADVANCEMENT OF NARROW OPEN TUBULAR
LIQUID CHROMATOGRAPHY

A DISSERTATION APPROVED FOR THE
DEPARTMENT OF CHEMISTRY AND BIOCHEMISTRY

BY THE COMMITTEE CONSISTING OF

Dr. Zhibo Yang, Chair

Dr. Mark A. Nanny

Dr. Yihan Shao

Dr. Si Wu

This doctoral dissertation is dedicated to my family.

# Acknowledgements

I would like to thank my parents for their never-ending, priceless support in my entire life. I would also like to thank my best friend PJ Stephany for his support.

I would like to express my sincere gratitude to both my current advisor, Dr. Zhibo Yang, and my previous advisor Dr. Shaorong Liu. I appreciate that during this hard time, Dr. Yang became my committee head without hesitation to help me finish my doctoral program. The opportunities Dr. Liu provided me while I was in his lab was extremely precious. Without the help and support of Dr. Liu, all my research achievements would have been impossible.

I would like to thank my committee members, Dr. Si Wu, Dr. Mark Nanny, and Dr. Yihan Shao for their kindness and great advice on conducting my research projects. The "3×Time Rule" mentioned by Dr. Nanny was helpful.

I would like to give special thanks to Environmental Molecular Sciences Laboratory of Pacific Northwestern National Laboratory (PNNL) and Dr. Ying Zhu from PNNL. During my short stay in summer 2019 in PNNL, PNNL and its kind people and Dr. Zhu's help gave my research progress an important boost.

I would like to thank all the previous lab members in Dr. Liu's lab. They are Dr. Zaifang Zhu, Dr. Apeng Cheng, Dr. Kyle Lynch, Dr. Jiangtao Ren, Dr. Huang Chen, Dr. Yu Yang, Mitchell Weaver, Matthew Beckner and Zhitao Zhao.

# Table of Contents

# List of Figures

# List of Abbreviations

3-(2-furoyl)quinoline-2-carboxaldehyde (FQCA)
3-benzoyl-2-quinolinecarboxaldehyde (BQCA)
Analog to Digital Converter (ADC)
Bare Open Tubular (BOT)
Capillary Electrophoresis (CE)
Collision Induced Dissociation (CID)
Electroosmotic Pump (EOP)
Electrospray Ionization (ESI)
Escherichia coli (E. coli)
False Discovery Rate (FDR)
Flow Injection Analysis (FIA)
Flow Injection Chromatography (FIC)
Gas Chromatography (GC)
Hemoglobin (Hb)
High-Performance Liquid Chromatography (HPLC)
Horse Blood agar (Hba)
Hydrodynamic Chromatography (HDC)
inner diameter (i.d.)
Laser-Induced Fluorescence (LIF)
Limits of Detection (LOD)
Liquid Chromatography (LC)
Mass Spectrometry/Mass Spectrometer (MS)
Match Between Runs (MBR)
Mobile Phase A (MA)
Mobile Phase B (MB)
*narrow* Open Tubular Column (*n*OTC)
*narrow* Open Tubular Liquid Chromatography (*n*OTLC)
Octadecyltrimethoxysilane (OTMS)
Open Tubular Liquid Chromatography (OTLC)
outer diameter (o.d.)
picoliter-scale Liquid Chromatography (picoLC)
Poly(styrene-divinylbenzene) (PS-DVB).
Polyethoxysiloxane (PES)
Polymerase Chain Reaction (PCR)
Polymethyloctadecylsiloxane($PMSC_{18}$)
Porous Layer Open Tubular (PLOT)
Pounds per Square Inch (PSI)

Sequential Injection (SI)
Sequential Injection Chromatography (SIC)
Tetraethoxysilane (TES)
Total Ion Current (TIC)
Tris-EDTA (TE) buffer
Ultra-Performance Liquid Chromatography (UPLC)
Ultraviolet-Visible (UV-Vis)
Wall Coated Open Tubular (WCOT)
Wall-Layer Electrostatic Interaction (WaLEI)
Yeast Peptone Dextrose (YPD)

# Abstract

Liquid Chromatography (LC) is a century-old technology used for preparative and analytical separation. Since 1960s, High-Performance Liquid Chromatography (HPLC) has undergone quick development, resulting in shorter separation time and higher resolving power. While HPLC evolved, implementing Open Tubular (OT) columns in LC started to catch people's attention in around 1980. At that time, OT columns (OTCs) were primarily used in Gas Chromatography (GC), and they were regarded as the best choice to achieve high separation efficiency in GC. However, since substances diffuse much slower in liquids than in gases, an Open Tubular Liquid Chromatography (OTLC) column must have a small inner diameter (i.d.), to achieve high separation efficiency. Despite theoretical calculations predicting the best OTLC column i.d. to be 1 ~ 2 μm, researchers did not report OTLC with i.d. smaller than 5-μm for a long time.

As technology evolves, narrower OTCs implementation becomes more common. Luckily, we are one of the pioneers that explored *narrow* Open Tubular Liquid Chromatography (*n*OTLC) with 2-μm-i.d. capillaries. In our first publication, we achieved a high efficiency separation of 11 fluorescently derivatized amino acids with *n*OTLC. Since then, we improved the column preparation and greatly enhanced the separation efficiency of the *n*OTLC.

This thesis focuses on optimizing the *n*OTLC for high efficiency separation, high speed separation, high throughput separation and coupling *n*OTLC with mass spectrometry for single cell bottom-up proteomics.

# Chapter 1: Introduction

## 1. Background

Liquid Chromatography (LC) is a century-old technology used for preparative and analytical separation. Before the introduction of High-Performance Liquid Chromatography (HPLC), LC separation time would take up to a few days due to long columns and gravity driven flow.[1] Since the first HPLC published by Csaba Horváth and other reseachers,[1, 2] HPLC has undergone drastic improvement with shorter separation times and higher resolving power.[3] Together, the advancement of analytical instrumentation and the improvement of stationary phase, such as utilizing smaller and more uniform packing particles and better packing technology, have played a significant role in developments.[1, 4] While HPLC evolved, implementing Open Tubular (OT) column in LC started to catch people's attention around 1980. Although earlier implementations of *narrow* OT column (*n*OTC) in LC often had an i.d. of 50 μm or larger, most studies that summarized in this thesis were carried out using columns with an i.d. smaller than 10μm.

OTCs are primarily used in Gas Chromatography (GC), and regarded as the best way to achieve high separation efficiency in GC[5]. The major difference between GC and LC is that the mass transfer rates of analytes in a liquid phase is much slower than those in a gas phase. Therefore, OTCs for LC must have significantly smaller diameters than GC to achieve desired efficiencies.[5, 6] Studies suggested that in order to achieve a performance comparable to packed columns, the i.d. of OTCs should be 10 ~ 30 μm.[7, 8] Although some earlier publications suggested that the i.d. should go down to 5 ~ 10 μm[8, 9], Jorgenson *et al*.[5] performed a

theoretical analysis, based on limited elution pressures and analysis time to investigate the impact on the i.d. of OTCs. They used a variant of the standard Hagen–Poiseuille equation, a conditional Golay's equation, and other factors (retention time and capacity factor) to correlate theoretical plates *N*, column radius, pressure, and separation time. The study suggested that OTCs with i.d. between 1 μm and 2 μm are expected to have the optimal performance.[5]

Although capillaries with small i.d. have been the preferred option for OTLC separations, there are multiple complications all the way from column preparation to detection. An obvious challenge is that the small channel is vulnerable to clogging. In addition, sample injections are more difficult to perform than using a traditional packed column. For example, a 2-μm i.d. OTC could only load a few hundred picoliters sample,[10-12] while a standard HPLC systems takes a few micro liters. Hence, the HPLC injection technique cannot be directly applied to a narrow i.d. OTC. Additionally, among all the challenges, adopting proper analyte detection instrumentations is perhaps the major cause that limited the development of narrower OTCs[13]. Eluted analytes in *n*OTC have such small volumes that a tradition UV-Vis detector is improper for *n*OTLC systems without major modification. To allow for UV-Vis detection, the OTCs must have a relatively large i.d. (e.g., 10 μm). To the best of my knowledge, all *n*OTCs with an i.d. smaller than 5 μm must be couple with more sensitive detectors such as Laser-Induced-Fluorescence (LIF) detectors and mass spectrometers (MS).

During the wave of OTLC development in late 1970s, most studies utilized capillaries with an i.d. of at least 50 μm[14-18] and ultraviolet-visible (UV-Vis) absorbance as detection. A few researchers have explored capillaries with smaller i.d. down to 32 μm[5] with an on-

column fluorometer. In 1980s, there were more publications about sub-10-μm OTCs in LC. For example, Tsuda *et al*.[18] reported one of the first OTLC separations using a 6-μm-i.d. soda-lime glass capillary. The smaller capillary however, did not present better performance than the similarly prepared OTC with a wider diameter and longer length.

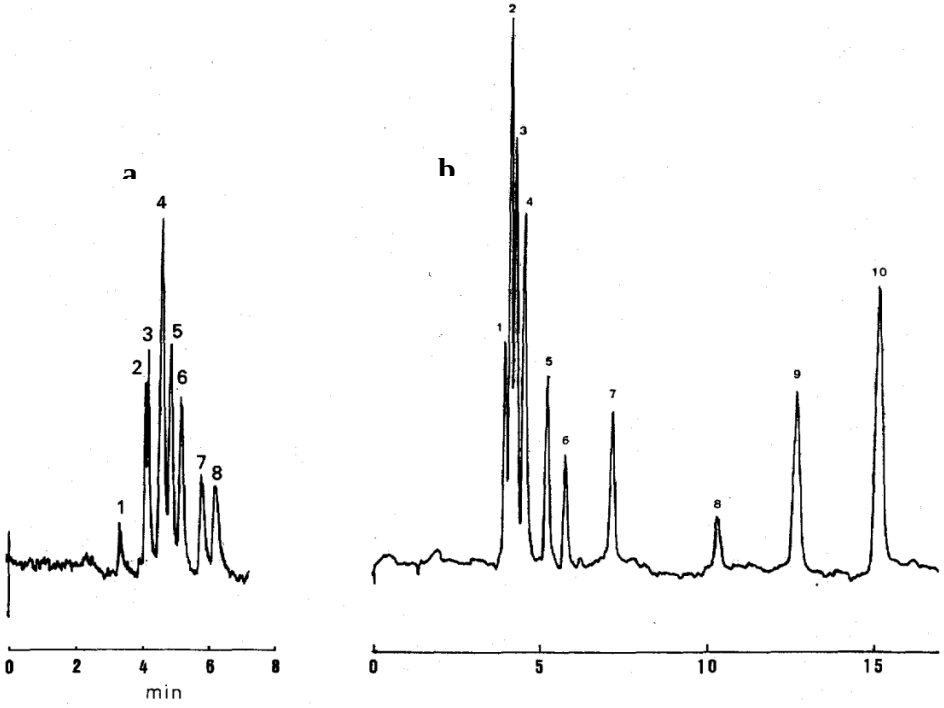


**Figure 1.1 One of the first <10-μm i.d. *n*OTLC separation.**

[a] Chromatogram obtained by using a 6-pm i.d. column of length 220 cm. Mobile phase: n-hexane containing acetonitrile (0.7%), methanol (0.7%), dichloromethane (0.3%) and water (0.01%). Sample: (1) o-, (7) m- and (8) p-chloroaniline; (2) 3-chloro-p- and (4) 4-chloro-o- and 6-chloro-o-toluidine; (3) o-, (5) m- and (6) p-toluidine. Inlet pressure: 110 atm. UV detection at 235 nm. [b] same as (a) except for the 11-μm column i.d. Figure reproduced from ref 18 with permission.

Most researchers either used modified UV-Vis absorbance detection[19] or LIF detection, including UV-LIF detection[20-22]. One publication reported fabricated micro-channels on a glass wafer with a conductometric detector[23]. While LIF is the preferred detector for its higher sensitivity, there are several drawbacks. A disadvantage is that analytes must have fluorescence emission. Studies during this period used either UV-LIF or analytes with intrinsic fluorescence in visible light. In 1989, a paper published by Beale and coworkers[24] reported an

effective method to introduce a fluorogenic group to primary amines. The compound, 3-benzoyl-2-quinolinecarboxaldehyde (BQCA), reacts with primary amines and an appropriate nucleophile (e.g., cyanide) under a mild condition (pH = 8, room temperature) and produces highly fluorogenic derivatives with excitation wavelength around 455 nm (e.g., glycine derivative). These excitation maxima are close to the He-Cd laser line at 443 nm. A year later, this research group published another paper,[25] reporting a modified derivatization reagent, 3-(2-furoyl)quinoline-2-carbaldehyde (FQCA). Replacing the phenyl group with a stronger electron donor, a furyl group, resulted in a redshift in both the excitation and emission spectrum of the amine derivative. The product of FQCA and methionine has a maximum excitation wavelength at 480 nm (e.g., a methionine derivative) which is ideal for the argon-ion laser line at 488 nm. This amine derivatization protocol is valuable for LIF detection in *n*OTLC.

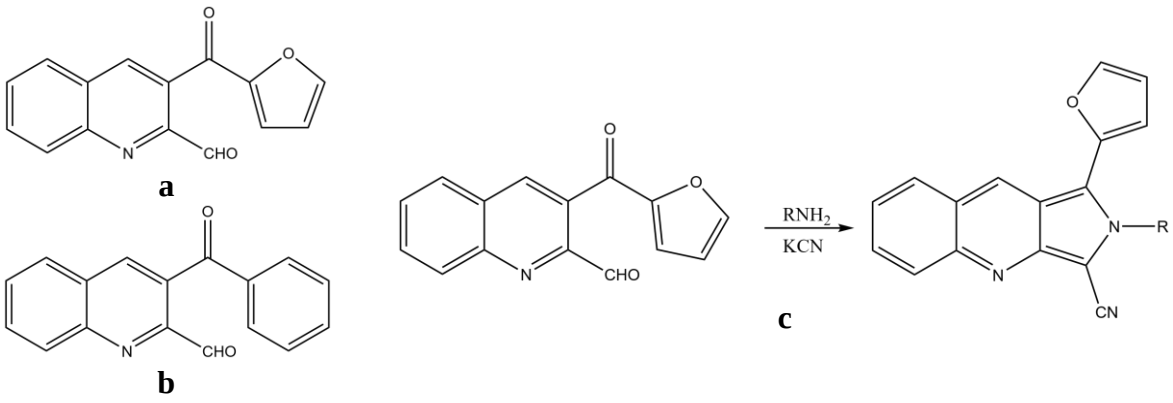


**Figure 1.2 The structure of BQCA and FQCA and the derivatization reaction of primary amines**

[a], [b] The structure of BQCA and FQCA respectively. [c] The derivatization reaction of primary amines with FQCA and potassium cyanide, reproduced from ref 25.

Decades after 1980, studies on *n*OTLC have progressed even further. In 1991, Göhlin *et al*. coated a 5-μm-i.d. fused silica capillary with immobilized polymethyl-octadecylsiloxane. More than 900,000 plates were achieved in 25 min with a 164-cm OTC[26]. Crego *et al*. chemi-

cally bounded octadecylsiloxane (C18) on a 5-μm-i.d. fused silica capillary[13] and reported 0.5 × $10^6$ plates per meter and 1000 plates per minute[13]. Swart *et al*. coated 5-μm-i.d. fused silica capillaries with *in situ* photo polymerization[27, 28]. This method allows for forming thick (up to 1.9 μm) films on the capillary walls which increases the amount of sample loaded on the column, making it possible for UV-Vis detection. In 2007, Luo *et al*. demonstrated an automated 1D and 2D PLOT separation using 10-μm-i.d. columns for LC-MS analysis.[29] With this experimental setup, they were able to identify >300 unique proteins from ~75 ng of samples. Shortly after, Yue *et al*. coupled a longer 10-μm-i.d. column with a mass spectrometer.[30] As a result of the improved condition, attomole to sub-attomole detection limit was achieved. In addition, using 50 ng in-gel tryptic digest sample, they identified >550 unique proteins. Interestingly, within a few years, Liu's group was able to demonstrate separations of DNA inside uncoated nanocapillaries with pressure driven flow[31-36]. Wang *et al*. in Liu group also employed a 1.5-μm-i.d. uncoated capillary, successfully separating proteins.[37] The negatively charged capillary wall together with the parabolic flow caused the separation of dyes based on their charging state. Anions tend to stay in the center of the capillary and move faster, while cations prefer to stay closer to the capillary wall and will move slower. For large molecules, the hydrodynamic effect is more significant. Larger molecules have a higher chance of staying in the middle of the capillary where the eluent flows faster. Larger capillaries with an i.d. of 10 μm were also coated with a porous layer stationary phase and coupled with MS for glycan analysis[38] and intact protein separation[39].

Despite the bare narrow capillaries (2-μm-i.d. or smaller) that separated molecules based

on hydrodynamic chromatographic principles, narrow capillaries with coated inner wall remained almost unexplored until late 2010s. This period is probably the most exciting one for *n*OTLC development. In 2017, Li *et al*. published a paper describing a separation of amino acid enantiomers with a 0.9-μm-i.d. porous layer *n*OTLC with LIF detection[40]. The amino acid enantiomers were derivatized with 4-fluoro-7-nitro-2,1,3-benzoxadiazole (NBD-F), while the column stationary phase contains O-9-[2-(methacryloyloxy)-ethylcarbamoyl]-10,11-dihydroquinidine, a chiral selector.

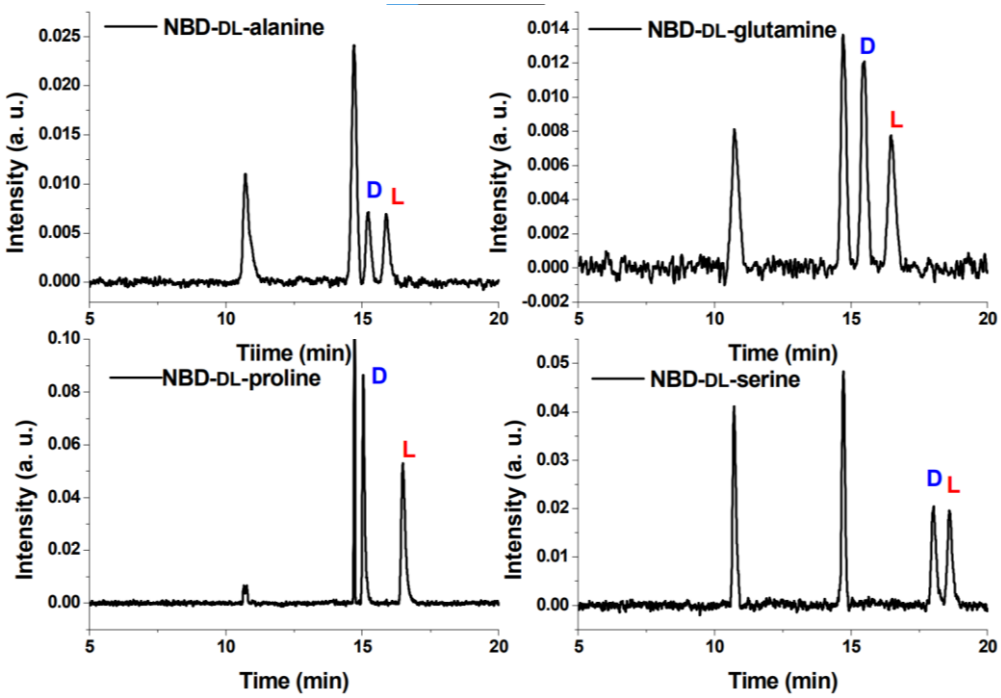


**Figure 1.3 Separations performed with a 0.9-μm-i.d. PLOT column**

Enantioseparation chromatograms of NBD-amino acid enantiomers on the poly(MQD-co-HEMA-co-EDMA) pico-PLOT column. Conditions: mobile phase: ACN/0.1 mol·L$^{-1}$ ammonium formate (80/20, v/v) (apparent pH = 6.0). Reproduced with permission from Ref 40.

Chen *et al*.[41] reported the first reverse phase (octadecyltrimethoxysilane, OTMS) *n*OTLC with LIF detection for highly effective separation of FQCA derived amino acids. This *n*OTLC exhibited an efficiency of more than $10^7$ plates/meter. The authors also observed a focusing effect. Later, Yang *et al*. studied the focusing effect,[42] and concluded that the focus-

ing effect was caused by the combination of a reversed gradient and a normal gradient. Briefly, the diffused analytes in the reversed gradient at the front trend to stay on stationary phase due to the gradually decreasing elution power of the incoming eluent. Once the normal gradient arrived, the analytes started to move, which is a common phenomenon in regular gradient HPLC practice.

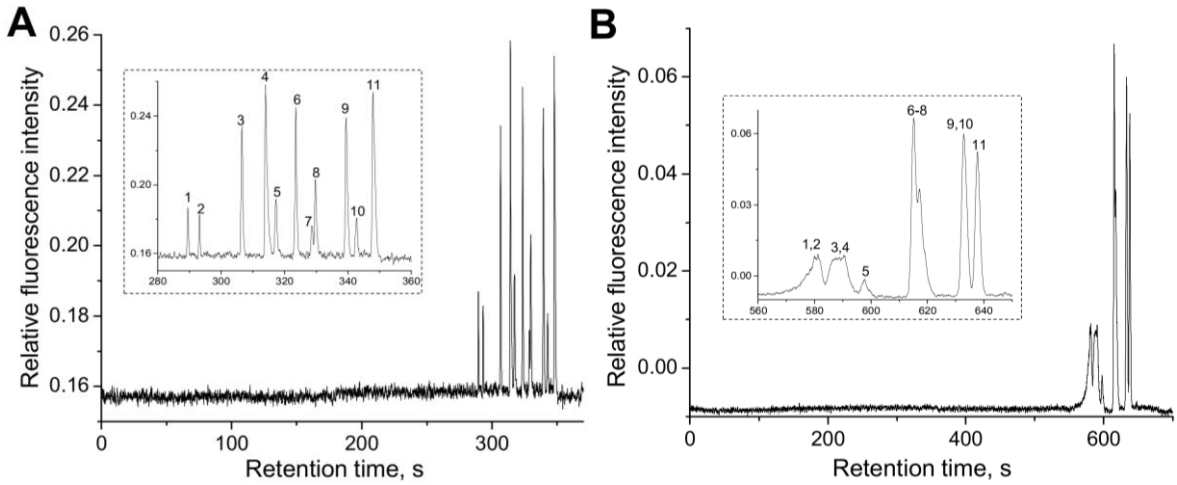


**Figure 1.4 Comparison of 11 separation with 2-μm-i.d. and 5-μm-i.d. *n*OT columns**

Both 2-μm-i.d. column (A) and 5-μm-i.d. column (B) had a total length of 48 cm and an effective length of 44 cm. The amino acids were 1) histidine, 2) asparagine, 3) glycine, 4) tyrosine, 5) arginine, 6) alanine, 7) tryptophan, 8) valine, 9) isoleucine, 10) phenylalanine and 11) leucine. Figure reproduced from ref 41 with permission.

Yang *et al*.[43] later coated a longer *n*OTC (2-μm-i.d. × 80-cm, 75-cm effective) and performed separations with pepsin/trypsin digested *E.coli* lysate. With a 3-h linear gradient, ~440 peaks were identified, corresponding to an estimated peak capacity of 1640 in 172 min. The peak capacity reaches up to 1830 within 245 min. As a follow-up experiment, Yang *et al*. modified a thermoelectric plate to heat up a 2-μm-i.d. × 160-cm-length *n*OTC.[44] At 70 ℃, the chromatogram had a significantly increased peak capacity of 2720 within 143 min. In a later publication, a short *n*OTC demonstrated[10] potentially one of the fastest LC separations of six amino acids in less than one second. With tweaked setup, high-throughput separations with *n*OTCs were also achieved. The sampling frequency reached up to 1800 samples·$h^{-1}$ and 24

samples·h$^{-1}$ for a mixture of three amino acids and cytochrome C tryptic digest, respectively. The successful coupling of *n*OTLC and MS potentially showed one of the most sensitive LC-MS setups: more than 1000 unique proteins identified reliably with only dozens of picograms of peptides loaded on the *n*OTC.[12]

## 2. Types of *narrow* OT columns

### 2.1. *narrow* Bare Open Tubular Columns

The inner surface of a *narrow* Bore Open Tubular (BOT) column is uncoated. Unlike a Wall Coated Open Tubular (WCOT) column, a *n*BOT column separates analytes based on hydrodynamic chromatography (HDC) mechanism[31-35] or the wall-layer electrostatic interaction (WaLEI) mechanism, which is based on the Coulomb force between the surface charge (or ζ potential) of the capillary inner wall and the analytes under certain pH conditions.[33]

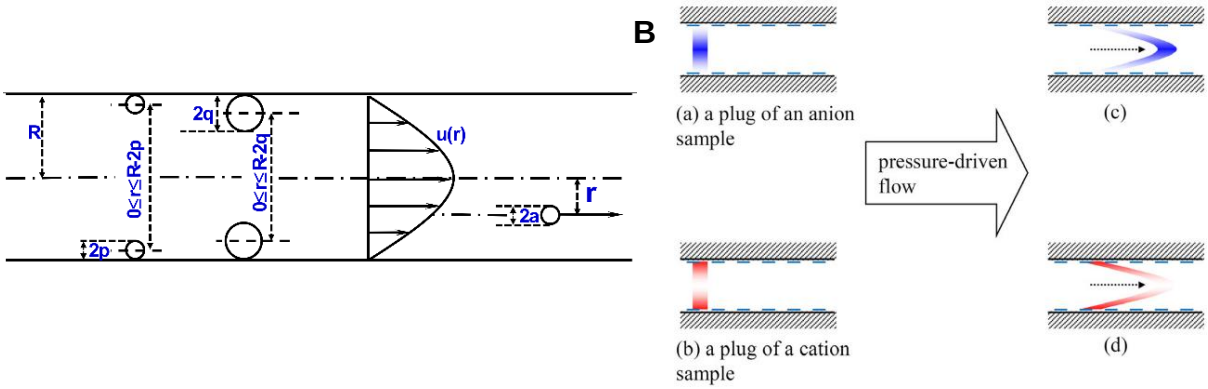


**Figure 1.5 Mechanisms of HDC and WaLEI**

A) Hydrodynamic chromatography (HDC) mechanism. Figure reproduced from ref 32 with permission. B) Wall-layer electrostatic interaction (WaLEI) mechanism. Figure reproduced from ref 33 with permission.

HDC is the primary mechanism that causes large molecules (e.g., DNAs or proteins) to separate in a *n*BOT column. In the early studies of HDC, Small used a packed-bed column to separate colloidal particles.[45] The author observed that the transport rate of the colloidal particles is dependent on the size of the colloid, the size of the packing bed, and the ionic com-

position of the aqueous phase. Multiple publications from Liu's group demonstrated high resolution separation (> a million plates per meter) of a wide range of DNA fragments in a single run without sieving matrix.[31-35]

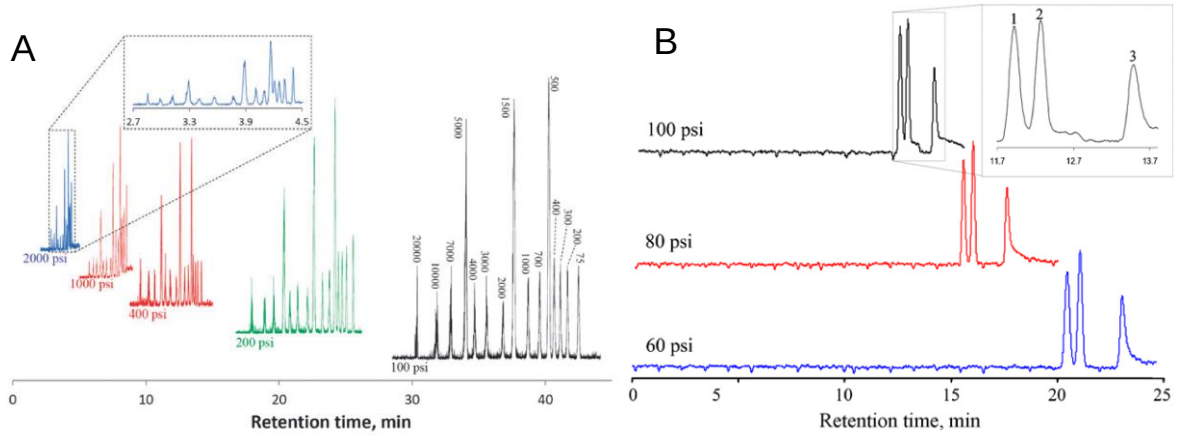


**Figure 1.6 Examples of HDC separation and WaLEI separation**

(A) Typical chromatograms at different elution pressures. The eluent was 5 mM $NH_4Ac/NH_4OH$ (pH = 8.0). The sample contained 15 DNA fragments, and the total DNA concentration was 20 ng·mL$^{-1}$; 3.2 ng·mL$^{-1}$ for the 1.5 kbp fragment, 3 ng·mL$^{-1}$ for the 0.5 and 5 kbp fragments, 1 ng·mL$^{-1}$ for the 0.075, 0.2, 0.3, 0.4, 0.7, and 1 kbp fragments, and 0.8 ng·mL$^{-1}$ for the 2, 3, 4, 7, 10, and 20 kbp fragments, respectively. The injection volume was estimated to be 2.4 pL. The inset shows an expanded view of the fast separation. Figure reproduced from ref 46 with permission. (B) Comparison of three separation traces obtained under different separation pressures. The separations were carried out using a 44-cm-long (39-cm effective length) and 800-nm-radius fused silica capillary under the indicated pressures. Sample injection condition: 0.55 MPa for 10 s; eluent composition: 100 μM borax. Peak identification: 1) BCECF (-4 charged), 2) fluorescein (-2 charged) and 3) rhodamine B (neutral). Figure reproduced from ref 33 with permission.

The separation of small charged molecules is induced by WaLEI.[33] Under appropriate pH conditions, the silanol groups on the inner wall of the capillary dissociate and make the inner wall negatively charged. The inner wall attracts cations and repulses anions; hence cations reside closer to the capillary wall whereas anions prefer the center region of the capillary. The charge state on molecules is also an important factor. For example, a cation with higher charge state stays closer to the capillary wall than a cation with lower charge state. A similar principle applies to anions: an anion with a higher charge state gets pushed further to the cen-

ter of the capillary than an anion with a lower charge. When a pressure-driven flow is introduced, the fluid closer to the center of the capillary flows faster than that near the capillary wall, creating the following movement speed: anions with more charges > anions with less charges > neutral > cations with less charges > cations with more charges. Figure 1.6 B presents chromatograms using a 1.6-μm-i.d. BOT column for separating three fluorescence dyes: 2',7'-Bis(2-carboxyethyl)-5(6)-carboxyfluorescein (BCECF, −4 charged), fluorescein (−2 charged), and rhodamine B (neutral). The key to such separation is a stable ζ potential on the inner wall and hence stable pH and temperature are required.

### 2.2. *narrow* Porous Layer Open Tubular Column

Theoretical calculation indicated that to achieve very high performance with *n*OTLC,[5, 8, 9] the i.d. of the capillary must be as narrow as 1 to 2 μm. In the past decades, people devoted much effort to fabricating smaller i.d. OTCs. One of the concerns of using a small i.d. OTC is its low sample loadability. To address this issue, people prepared porous layer stationary phases in the capillary to increase the surface area which increases the sample loaded on the column. The porous layer on the inner wall of the capillary can either be inorganic silica [21] or organic copolymers[13, 26, 29, 30, 47]. The narrow bore capillaries are generally pulled under high heat, hence the density silanol groups on a non-activated capillary is low. To increase the density of silanol group anchors, the capillaries are treated with basic solutions before coating.

Tock *et al.*[21, 48] used a dynamic coating procedure: precipitate silica from a solution of polyethoxysiloxane (PES) and form a stable porous silica layer on the inner wall of the capillaries. The preparation of PES was adopted from a procedure described by Unger *et al.*[49] by

hydrolytic polycondensating of tetraethoxysilane (TES). The procedure of coating such capillaries indicated in Figure 1.7. First, the inner surface of the capillary was activated with KOH solution. Next, the PES solution was prepared by adding 5.7 mL water (0.32 M) containing 60 μM HCl to 50 mL of TES (0.22 M) dissolved in 30 mL of dry ethanol. The mixture was vigorously stirred for 1 hour and then refluxed for 6 hours. Ethanol and HCl were then evaporated in vacuum to create pure PES. The KOH-activated capillary was dynamically coated by fitting the capillary with a 25 cm long plug of pure PES. The plug was passed though the column with helium at a linear velocity of 30 $cm \cdot h^{-1}$. The PES-layer was converted into silica by treatment of gaseous ammonia in a helium stream for one day at room temperature. The capillary was flushed with 0.01 M ammonia for half an hour, rinsed with water for 3 hours, and then dried for at least two hours at 200–250℃ while purged with helium. In this study, the authors[21] adopted the liquid-solid chromatography. The stationary phase was generated by pumping cyclohexane saturated at 20℃ with γ-butyrolacton through the capillary. As suggested, the porous silica surface can be easily modified by reaction the silanol groups with silane reagents.[21]

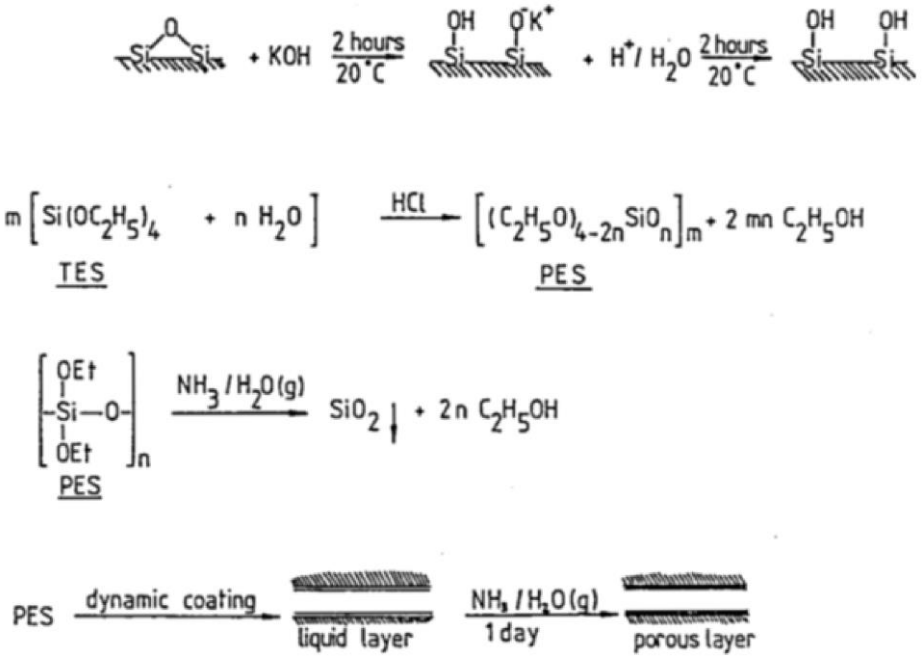


**Figure 1.7 Schematically representation of etching and PES procedure**

Figure reproduced from ref 21 with permission.

Crego *et al.*[13] converted a protocol that produced 50-μm-i.d. PLOT columns to a method for preparing 5-μm-i.d. columns. The porous layer was formed by hydrolysis and polycondensation of tetraethyl orthosilicate (TEOS) in a water-ethanol solution. The porous silica was then silanized with octadecylsilane. The thickness of the porous layer could be controlled by adjusting pregelling time. Despite the 5-μm-i.d. columns having thinner coating than the 10-μm-i.d. columns, they exhibited higher retention values. This study suggests that, instead of simply increasing the coating thickness, decreasing capillary i.d. is a more effective choice for stronger retention.[13]

The other method to generate a porous layer was reported by Folestad *et al.* [47] They coated narrow (down to 5-μm i.d.) OTCs with polysiloxane gum phase PS-255 (methylvinyl silicone), generating a film whose thickness was 0.056 μm. Briefly, PS-255 pentane solution and polymerization initiator were well mixed, the mixture was then driven inside the capillary by

high pressure helium. The capillary was then slowly depressurized. The capillary was immersed in a room-temperature water bath with the capillary end connecting to vacuum. Trace amount of pentane was removed by flushing the capillary with helium gas. To immobilize the silicone gum phase, the capillary was flame sealed and subsequently heated in oven. Later, Göhlin *et al*. reported a method, similar to static evaporative coating technique, to coat narrow fused silica OTCs with immobilized polymethyloctadecylsiloxane($PMSC_{18}$) stationary phase.[26] The film thickness of the stationary phase on the *n*OTC ranged from 0.014 to 0.028 μm. High efficiency separations were demonstrated with such *n*PLOT columns (Figure 1.8). More than $3\times10^5$ plates were reached in 3 min (Figure 1.8 A). Under a close to optimum flow rate (Figure 1.8 B) more than $8\times10^5$ plates were achieved.

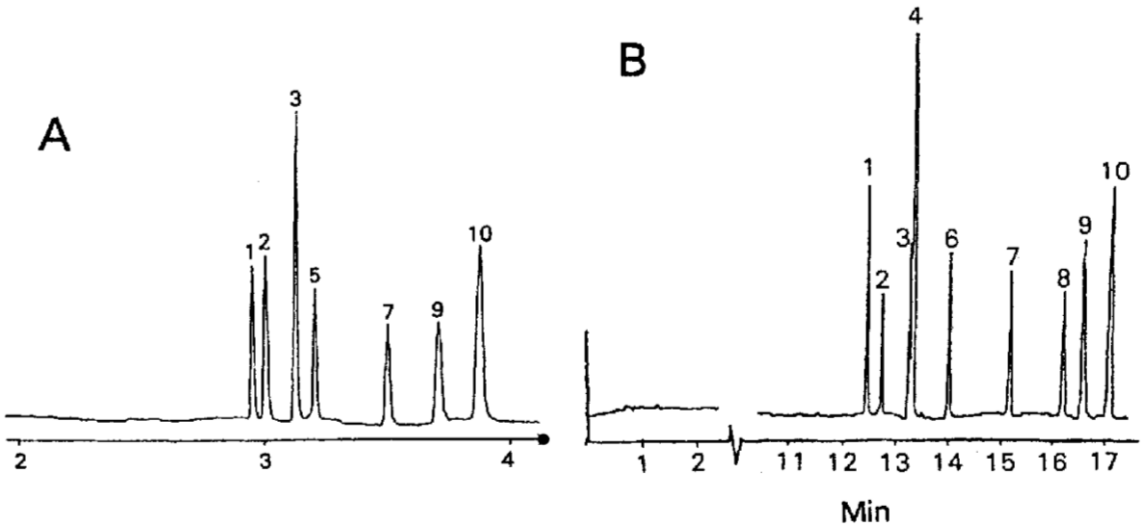


**Figure 1.8 High efficiency reversed-phase separations on a 5.8-μm-i.d. $PMSC_{18}$ coated OT columns**

Conditions: (A) high flow rate, 0.8 $cm\cdot s^{-1}$ (13 $nL\cdot min^{-1}$), 144-cm length; (B) close to optimum flow rate, 0.2 $cm\cdot s^{-1}$ (4 $nL\cdot min^{-1}$), 164-cm length. Column phase ratio 0.011, film thickness 0.016 μm. 1:1 acetonitrile/phosphate buffer mobile phase (30 mM, pH 6.4). Solutes: (1) anthracene carboxylic acid, (2)propanolanthracene, (3) methoxyanthracene, (4) anthracene, (5) 9- methylanthracene, (6) dimethylanthracene, (7) 9-phenylanthracene, (8) phenylethynylanthracene, (9) propylenephenylanthracene, (10) n-butylanthracene. Figure reproduced from ref 26 with permission.

Yue *et al*.[30] prepared a 4.2-m × 10-μm-i.d. PLOT column with poly(styrenedivinylbenzene) (PS-DVB) by adopting a similar approach described by Folestad *et al*.[47] Briefly,

solutions of monomers were mixed with polymerization initiator. The capillary was filled with the mixture, sealed with septum, and heated in an oven for several hours. Yue *et al*. obtained a peak capacity of 400 in ~ 4h by coupling this PLOT column with MS.[30] Rogeberg *et al*. adopted a method similar to that described by Yue *et al*.[30] and prepared ~ 3m polystyrene divinylbenzene PLOT columns.[39] An SEM image of this PLOT column is shown in Figure 1.9.

The PLOT column with the smallest bore was reported by Li *et al*.[40] in 2017. To prepare this column, the 900-nm-i.d. capillary was firstly flushed with 1 M NaOH for 5h, followed by a 3h water flushing. After a subsequently acetone wash, the capillary channel was dried by high pressure $N_2$. The capillary was then filled with a mixture of 3-(trimethoxysilyl)-propyl methacrylate (γ-MAPS) and acetone (v/v=1) and kept in dark for 24h. Next, the capillary was flushed with acetone and dried with $N_2$. The polymerization solution was prepared by vibrating and ultrasonicating a mixture of 3.98% O-9-[2-(methacryloyloxy)-ethylcarbamoyl]-10,11-dihydroquinidine (MQD), 7.92% 2-hydroxyethyl methacrylate (HEMA), 7.98% ethylene glycol dimethacrylate (EDMA), 39.77% cyclohexanol, 40.00% 1-dodecanol and 0.35% 2,2′-azobisisobutyronitrile (AIBN). Before sealing both ends, the capillary was filled with the polymerization solution except for the last 6 cm at each end of the capillary. The polymerization lasted for 2h at 60°C. The authors separated amino acid enantiomers using this narrow PLOT column (Figure 1.10).

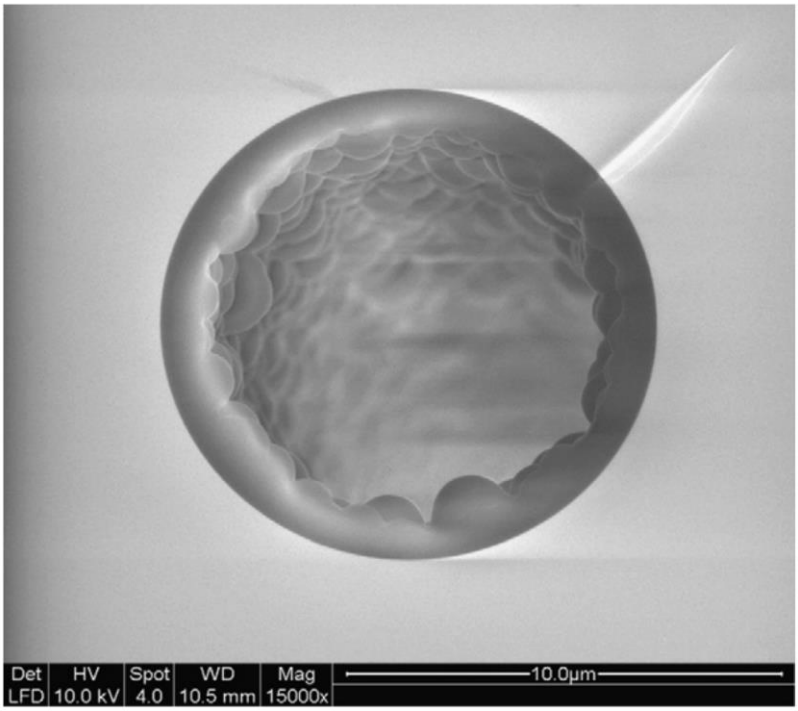


**Figure 1.9 SEM image of PLOT column used for separation of intact proteins**

Figure reproduced from ref 39 with permission.

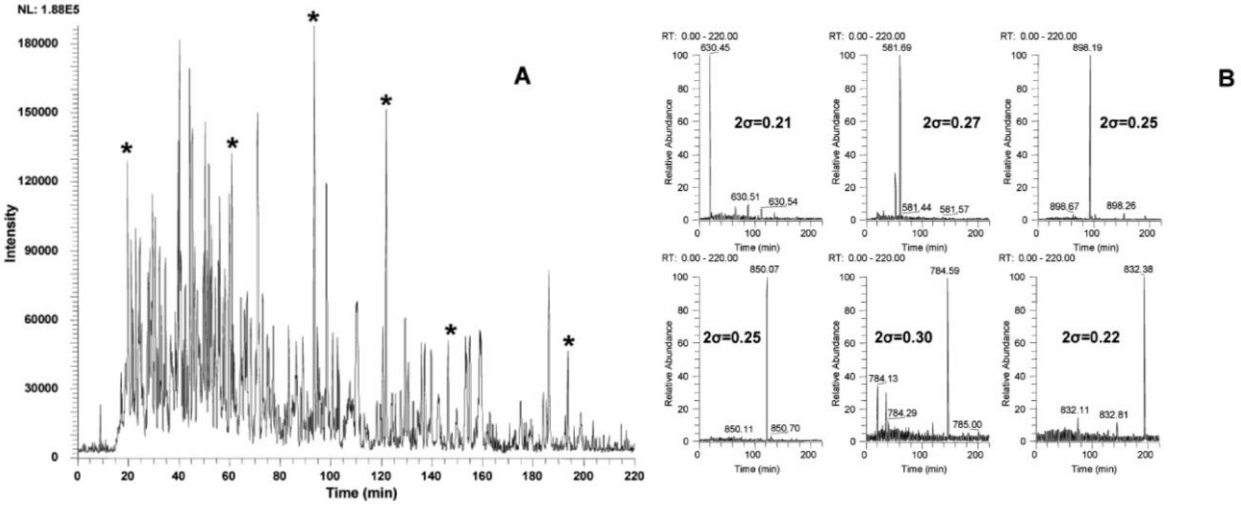


**Figure 1.10 Base peak chromatogram from the PLOTLC-MS analysis and extracted ion chromatograms of six highest intensity peaks**

Calculation of peak capacity for a 4.2 m × 10-µm-i.d. PS-DVB PLOT column. (A) Base peak chromatogram from the microSPE-nanoLC/ESI-MS analysis of a 4-ng tryptic in-gel digest of a single SDS-PAGE cut of *M. acetivorans*. (B) Extracted ion chromatograms of six high-intensity peaks used to calculate the peak capacity. A 4 cm × 50-µm-i.d. PS-DVB monolithic column was used as the microSPE precolumn. A 800-amol amount of sample was loaded onto the precolumn using a pressure bomb at a flow rate of 0.5 µL·min$^{-1}$. A 260-min gradient was used (mobile phase A (0.1% (v/v) formic acid in water) to 40% B (0.1% (v/v) formic acid, 10% (v/v) water in acetonitrile)). A peak capacity of ~400 was determined. Figure reproduced from ref 30 with permission.

### 2.3. *narrow* Wall Coated Open Tubular Columns

A WCOT column has a thin layer of non-porous stationary phase. Sample loadability has been a major concern for *n*WCOT columns.[50] For a smooth-surface WCOT column with an inner radius of *r* and a length of *h*, the ratio of surface area to volume is:

$$\frac{2\pi rh}{\pi r^2 h} = 2 \cdot \frac{1}{r}$$

Considering an ideal face-centered cubic (FCC) sphere packing in an HPLC column with the sphere radius of *r*, the side length of a primary cubic unit is $2\sqrt{2}r$. The volume of that primary cubic unit is $16\sqrt{2}r^3$. The volume that occupies by spheres is $4 \times \frac{4}{3}\pi r^3$. The surface area of the spheres is $4 \times 4\pi r^2$. Hence the surface area to volume ratio is:

$$\frac{4 \times 4\pi r^2}{16\sqrt{2}r^3 - 4 \times \frac{4}{3}\pi r^3} = \frac{\pi}{\sqrt{2} - \frac{\pi}{3}} \cdot \frac{1}{r} \approx 8.6 \cdot \frac{1}{r}$$

In an ideal condition, the surface area per mobile phase volume of a *n*OTC is 25% of that of a packed column whose packing spheres have a similar diameter as the i.d. of the *n*OTC. However, due to potential imperfect packing and non-smooth inner surface of a WCOT column, the actual value could be more than 25%. The volume that a *n*OTC holds is significantly less than a packed column. Therefore, the amount of sample handled by a *n*WCOT column is extremely low which requires ultrasensitive detection. This, unfortunately, deterred the development of *n*WCOT column.[13] Most of the publications studying *n*OTLC in recent years focused on PLOT column.[51-55]

The Liu group conducted a series of studies of *n*WCOT utilizing 2-μm-i.d. capillaries derived with octadecyltrimethoxysilane (OTMS).[10-12, 41-44, 56, 57] The *n*WCOT preparation method developed by Liu group have evolved since the first *n*OTLC publication in 2018. In

the earlier publications,[41-43] *n*OTCs were prepared by activating the capillary wall with 1 M NaOH solution at 100 ℃ for an hour or two. After NaOH reaction, the capillary was rinsed with water for an hour. Sequentially, the capillary was dried with $N_2$, followed by rinsing with acetone and drying by blowing $N_2$ through overnight. The coating procedure was done by flushing 50% OTMS dissolved in toluene through the capillary at 50℃ for 16 hours, followed by a toluene wash and then $N_2$ drying. With improved protocols in later publications,[10, 56] the column performance significantly increased while the preparation time dramatically decreased. The improvements included but not limited to: decreased NaOH activation temperature, skipped toluene flush after coating, and increased OTMS concentration in the coating mixture. Piranha solutions (3 parts of 98% $H_2SO_4$ and 1 part of 30% $H_2O_2$) have been adopted to replace NaOH for activating capillary inner wall.[12] Activating capillary inner wall with NaOH solutions will increase the i.d. of the capillary[11], which is unlikely to happen with piranha solutions. In addition, activating with piranha solutions provides other advantages. For example, unlike NaOH solutions, piranha solutions do not crystalize, which is helpful preventing column clogging since the solution dries up very quickly on the inlet or outlet of the capillary. Besides, the piranha solution dissolves most organic particles at the activation temperature, further reducing the possibility of column clogging. However, the highly corrosive piranha solutions must be handled with extreme caution. The high viscosity of piranha solutions also makes it harder to push the solutions through a narrow capillary. To overcome the viscosity issue, higher activation temperature should be selected. Yang *et al.*[57] performed systematical studies of the coating conditions. They determined that the optimum OTMS

concentration is in between 70% to 80%, the optimum coating temperature is ~60℃, and the best coating time is around 18 hours.[57]

Separations using *n*WCOT columns exhibited stunning performance. To the best of my knowledge, 2-μm-i.d. nWCOT columns achieved the highest reported peak capacity in 3 hours.[11] At elevated temperatures, the peak capacity could be further increased to a record value of 2720 in 3 hours.[44] Short *n*OTCs were used to produce one of the fastest, sub-second, baseline separation of six amino acids,[10] as well as high throughput separation up to 1800 samples·$h^{-1}$.[56] *n*OTLC was also coupled with MS successfully, demonstrating one of the first picoflow LC-MS separations with promising sensitivity: with only 75 pg of peptide digest loaded on the *n*OTC, ~1000 proteins were reliably identified, which corresponds to 10–100-fold increase of sensitivity compared to traditional packed capillary columns[12].

## 3. Sample Delivery Method

A distinct feature of *n*OTLC is its ultralow flow rates. Despite reports of *n*BOT column separation with EOP[58], almost all *n*OTLC used in published studies were operated under constant pressure mode, with wither a flow splitter or pressure chamber. Systems with both pressure chamber and flow splitter were also reported.[21, 22, 56]

### 3.1. Flow Splitter Style Sample Delivery

*n*OTCs are operated at very low flow rates (e.g., hundreds of picoliters per min),[10-12, 41-44, 56] which are well below the operating flow rate of any commercial HPLC/UHPLC pumps. Therefore, flow splitters are required to split excess flow from the pumps. Decades ago, several studies[21, 22, 48] started to implement flow splitting device in systems equipped with 5-μm-

i.d. capillaries (e.g., a splitter from Tsuda reported in 1983, Figure 1.11). Examples of recent designs of flow splitting setups are illustrated in Figure 2.1, Figure 3.2, and Figure 5.3.

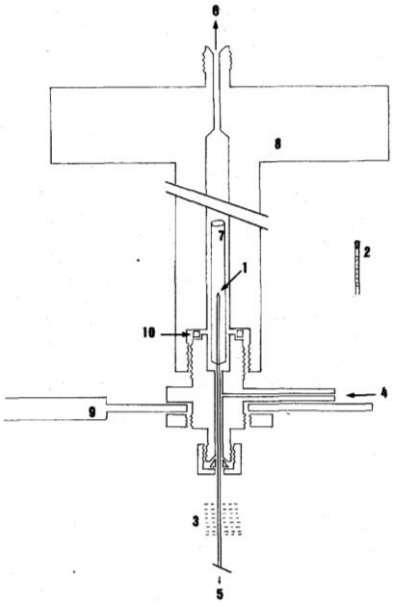


**Figure 1.11 An injection device for 5-μm-i.d. *n*OT column**

Apparatus for in-column injection. 1 = Head of capillary column; 2 = PTFE tubing, one of the ends of which was sealed; 3 = heating zone; 4-6 = directions of effluent flow; 7 = guard tube; 8 = cap; 9 = support; 10 = O-ring, made by PTFE resin. Figure reproduced from 19 with permission.

## 3.2. Pressure Chamber Sample Injection

A pressure chamber is a device that withstands high pressure and holds eluent or sample vials (Figure 3.1**)**. To perform a sample injection[31, 33], the *n*OTC is inserted in the pressure chamber, guided by a hypodermic needle. The needle is then pulled back to ensure a gas-tight seal on the septum. High pressure $N_2$ or He is applied inside the pressure chamber by poking a gas-line-connected needle through the septum. After a certain amount of time, the needle is removed. Another needle is inserted in the pressure chamber to release the pressure and stop sample injection. For separations with pressure chambers, the gas-line needle is generally left in the chamber to keep a stable pressure.

## 4. Detection

Due to the ultra-low amount of sample required by a *n*OTC, the detection of analytes is challenging. In fact, the requirement for sensitive detection is one of the major reasons that curbed the development and application of *n*OTLC. Although modified UV-Vis systems could be used for some PLOT column detection, they are not sensitive enough for *n*WCOT column detection. LIF, as one of the most sensitive detection methods in LC, is more suitable for *n*OTLC. However, as most analytes are not fluorogenic, they must be labeled or derived for LIF detection. For application purpose, MS is desired due to its sensitivity and its ability for structure identification of broad ranges of molecules. Despite challenging, an 80-cm long *n*OTC has been couple with MS successfully, providing unprecedent sensitivity.

### 4.1. UV-Vis Absorbance

UV-Vis absorbance detection, commonly used in conventional LC detection systems, has relatively low sensitivities. A *n*OTC must load significant amount of sample for on-column UV-Vis detection. PLOT columns are generally candidates for UV-Vis detection. Back to 1993, Crego *et al*. prepared 5-μm-i.d. and 10-μm-i.d. PLOT columns with coating thickness ranging from 0.1 μm to 0.7 μm. A customized UV detector was employed for analyte detection.[13] Swart *et al*.[27] prepared thicker coatings (up to 1.9 μm) in capillaries with i.d. ranging from 8 μm to 10 μm. The thick coating significantly increased the loading capacity of the column. Again, a customized UV-Vis detector was employed and successfully implemented for detecting separated methyl-substituted benzenes.

### 4.2. Laser-Induced Fluorescence

The high sensitivity of a LIF detector makes it a good candidate for *n*OTLC detection. LIF has been used in separation with ~5 μm *n*OTC since decades ago.[21, 59] Weaver *et al*. constructed a confocal LIF detector for *n*OTLC separations (Figure 1.12A, B).[60] Zhang *et al*. designed a confocal LIF detection system with visual and real-time imaging focusing (Figure 1.12 C).[61] Compared to the system developed by Weaver *et al*., this system has an extra light path for real-time image calibration, achieving an extremely low LOD: 6.76 yoctomoles or 4 molecules of fluorescein sodium.[61]

To the best of my knowledge, besides MS, all *n*OTLC with 2-μm or smaller i.d. adopted LIF as detection.[10-12, 40-44, 56] The highly sensitive LIF detector is ideal for optimizing or evaluating *n*OTC performance. However, LIF requires analytes to be fluorogenic, and it cannot provide detailed structural information of analytes.

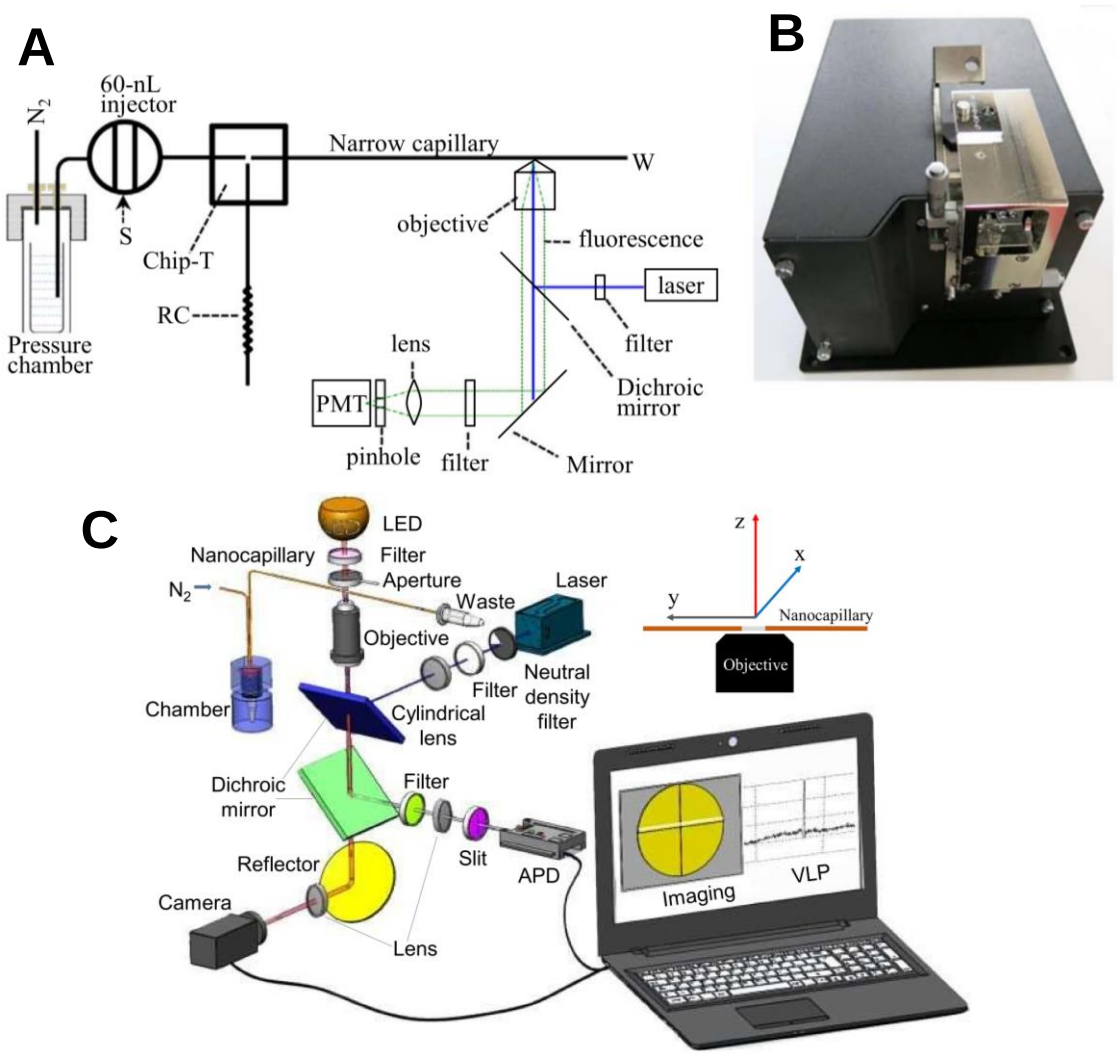


**Figure 1.12 Diagrams of two LIF systems**

(A) Schematic configuration of BaNC-HDC system. The narrow capillary had a total length of 47 cm (41 cm effective), an i.d. of 2 μm and o.d. of 150 μm. RC had a length of 6.5 cm an i.d. of 20 μm and an o.d. of 150 μm. (B) Picture of assembled LIF detector. Figure reproduced from 60 with permission. (C) Schematic graph of the confocal LIF detection system with visual and real-time imaging focusing. Figure reproduced from ref 61 with permission.

### 4.3. Mass Spectrometer

As mentioned above, *n*OTCs with i.d. ≤ 5 μm capillaries were much less frequently used in experiments compared to larger i.d. OTCs. Although MS provides exceptionally high detection sensitivities, very few studies have reported coupling *n*OTCs (with i.d. ≤ 5 μm) with MS (e.g., direct infusion, Capillary Electrophoresis (CE)-MS, and LC-MS). Since the appearance of electrospray ionization (ESI) in 1990s, ESI emitters with small orifices have been

studied in a variety of biomolecules. In an early work by Jon H. Wahl *et al.*[62] chemically modified 5-μm-i.d. capillary was used for CE-MS setup, and its performance was compared with a 500-μm-i.d. capillary. The protein mixture injected in the 500-μm-i.d. capillary and the 5-μm-i.d. capillary were 60 fmol and 600 amol respectively while the signal intensity only showed 2-4-fold difference. The sensitivity gain was estimated to be 25~50. Later, Gale *et al.*[63] used an HF etched, 5-μm-i.d. ESI emitter for shealthless infusion of samples at stable low flow rates. This ion source is more effective for a variety of proteins, peptides and oligonucleotides. It has other advantages such as lower electrospray potentials, smaller electrospray currents, reduced space-charge limiting effects, stable flow without varying analyte flow rate, and reduced interference from the sheath.[63] The sheathless design has a higher ionization efficiencies and higher signal intensities(typically 4-10 times higher).[63] Emmett *et al.* employed a micro-ESI source, operated at flow rates ranging from 300 to 800 nL·min$^{-1}$, to directly spray from a capillary needle. [64] The reduced flow rate caused narrower spray dispersion, leading to more analyte into the MS with less solvent. Nitrogen gas also helps reducing the background signal. Shen *et al.*[65] packed a 87-cm × 15-μm-i.d. capillary and performed nanoLC-MS separation with a tapered emitter (4.1μm orifice) at 20 nL·min$^{-1}$. Compared to a 75μm column with a tapered emitter (30μm orifice) operating at 300 nL·min$^{-1}$, the peptide detection sensitivity was significantly increased, allowing for detection of 10 zmol from a protein digest. Heemskerk *et al.*[66] developed a sheathless capillary electrophoresis-electrospray ionization-mass spectrometry (CE-ESI-MS) system to perform separation at flow rates as low as 6.6 nL·min$^{-1}$. Similarly, the authors observed increased ionization effi-

ciency at ultra-low flow rates for several synthetic peptides. A near equimolar ESI response was approached for flow rates below 15 nL·min$^{-1}$. One of the smallest orifices of ESI emitter was achieved by Yuill *et al*.[67] The authors laser pulled emitters with orifice diameters ranging from 37 to 70 nm. With 1.8 kV ESI voltage applied on the smallest emitter (diameter of 37 nm) for 2 min, the orifice diameter increased to 65 nm, possibly due to local heating effects, electrostatic pressure, and acid-catalyzed hydrolysis of silica[68]. The orifice turned to be stable at lower ESI voltage: another trial with ~42 nm showed unchanged orifice size after applying a potential of 0.9 kV. Potential mechanisms have been proposed to explain the increased ionization efficiency from ESI emitters with small tip sizes: sharper tips increase the droplets surface charge density and create ions of higher charge states. In addition, the nanotips have been demonstrated to be suitable for direct analysis of biological samples, despite the presence of salt effect. Sun *et al*. developed an electrokinetically pumped sheath–flow interface for CZE-ESI-MS/MS.[69] They inserted the CE capillary inside a pulled emitter with a tip i.d. of 6 μm. With 84 pg of *E.coli* digest loaded, they identified 162 ± 8 and 570 ± 11 peptides and proteins respectively. With 400 fg loadings, 9 peptides, corresponding to 4±1 proteins, were identified. The data from 400 fg sample were used to estimate the detection limit using ion signals of three peptides from the elongation factor Tu. A detection limit (S/N = 3) of 1 zmol or 600 molecules were determined for m/z in range of 270-290. Despite many efforts to perform ESI at low flow rates with small tip orifice, the pL-per-min flow rate region remained mostly unexplored. In 2014 Marginean *et al*.[70] demonstrated stable electrospray at flow rates as low as 400 pL·min$^{-1}$ with a chemically etched[71] 2-μm-i.d. capillary emitter.

They did not find any indication of analyte suppression effects or charge competition between the selected peptides. However, even at such a low flow rate, ionization efficiency of peptides appeared analyte-dependent, whereas uniform response (i.e. same signal at identical concentration) was not achieved. They discovered an exponentially increasing ion utilization efficiency with decreasing flow rates.

The first pL-per-min-level *n*OTLC-MS was achieved by Xiang *et al*.[12] In this study, a 2-µm-i.d. × 80-cm long *n*OTC was coupled with MS detection (Orbitrap Fusion Lumos Tribrid MS, system configuration is presented in Figure 5.3). The exit-end of the column was sharpened via HF etching to achieve high ESI efficiency at ~790 pL·min$^{-1}$. The chemically sharpened tip also helped to prevent tip clogging during ESI.[70] High voltage was then applied to the metal stopper on the flow splitter cross. To stabilize the spray, a nitrogen sheath flow was introduced by a Tee at the column tip. With only 75pg of *Shewanella oneidensis* tryptic digest loaded on the column, ~ 1000 proteins were profiled in 30 min, which represents a 10-to-100-fold increase in sensitivity compared to previously developed packed column LC[65, 72]. Despite these exciting achievements, more improvements are needed for coupling 2-µm-i.d. OTC with MS. In the 3-h high peak capacity separation, hundreds of peaks (peak width within seconds) were observed.[11] In contrast, the 30 min separation using *n*OTLC-MS setup has much shorter gradient time, generating narrower peaks. Many of the peaks are overlapped due to the low scanning frequency of a MS, because a MS has significantly lower scanning frequency than a LIF detector under operating conditions (operating at high scanning resolution, large m/z range and/or with MS/MS detection). Indeed, the MS, as a powerful second

dimension, identifies overlapped analytes in the *n*OTLC-MS study.[12] Improving the separation efficiency of *n*OTLC will potentially further increase the unique proteins identified by the MS. This could be addressed by optimizing the experiment condition such as using a longer gradient time.

# Chapter 2: Experimentally Validating Open Tubular Liquid Chromatography for a Peak Capacity of 2000 in 3 h

## 1. Abstract

The advancements in life science research mandate effective tools capable of analyzing large numbers of samples with low quantities and high complexities. As an essential analytical tool for this research, LC encounters an ever-increasing demand for enhanced resolving power, accelerated analysis speed, and reduced limit of detection. Although theoretical studies have indicated that OTCs can produce superior resolving power under comparable elution pressures and analysis times, ultrahigh resolution and ultrahigh speed OTLC separations have never been reported. Here we present experimental results to demonstrate the predicted potential of this technique. We use a 2-μm-i.d. × 75 cm long OTC coated with trimethoxyoctadecylsilane for separating pepsin/trypsin digested E. coli lysates and routinely produce exceptionally high peak capacities (e.g., 1900−2000 in 3−5 h). We reduce the column length to 2.7 cm and exhibit the capability of OTLC for ultrafast separations. Under an elution pressure of 227.5 bar, we complete the separation of six amino acids in ∼800 ms and resolve these compounds within ∼400 ms. In addition, we show that OTLC has low attomole limits of detection (LOD) and each separation requires samples of only a few picoliters. Importantly, no ultrahigh elution pressures are required. With the ultrahigh resolution, ultrahigh speed, low LOD, and low sample volume requirement, OTLC can potentially be a powerful tool for biotech research, especially single cell analysis.

# 1. Introduction

High-resolution and high-speed separation techniques have played pivotal roles in life science research such as human genome sequencing,[73-77] and more recently in proteomics[78-81] and metabolomics[82-85] research. As life science research advances, the samples are getting more complex and more samples are being analyzed. The demand for improved resolving power and enhanced analysis speed is ever-increasing. LC is a relatively high-resolution and high-speed analytical technique and has dominated chemical, biological, and especially pharmaceutical separations for decades, but approaches for increased resolution and accelerated speed are relentlessly explored. In fact, the evolution of LC is tied to the endeavor for continuously improving its resolution and speed.

A common approach to achieve enhanced resolution and speed is to pack a column with small and uniform particles. This has led to the transition from simple gravity-driven LC using columns packed with large and nonuniform particles to sophisticated HPLC using columns packed with a-few-micrometers-diameter and uniform particles. Toward the end of the last century, the highest separation efficiencies were obtained using columns packed with 5 μm particles.[86] Investigation of packing columns with less-than-2-μm-diameter particles was reported first by Jorgenson's group in 1997.[87] Due to the reduced particle size, high elution pressures were required, and this effort eventually led to the state-of-the-art separation technique, ultrahigh performance LC (UPLC). The primary goals of reducing the particle size and making the particles uniform are (i) to decrease the pore sizes among particles and hence shorten the mass transfer times in the mobile phase and (ii) to reduce eddy dispersions. Fun-

damentally speaking, an effective and straightforward path to achieve these goals is to utilize a *n*OTC.

An OTC is referred to as a hollow tube with a layer of stationary phase on its interior wall. OTCs were first used by Golay[88] in GC more than a half century ago. Because OTCs achieved increased efficiencies under similar elution pressures and within comparable analysis times, these columns quickly replaced packed columns in GC. Under optimized conditions, OTCs had inner diameters (i.d.) of around several hundred micrometers. High efficiencies were predicted for OTLC[5, 8, 13, 21, 89] since chromatographic theory made no distinction between gases and liquids as the mobile phase. However, because analyte diffusivities in liquid phases are generally 2−3 orders of magnitude smaller than those in gas phases, the column i.d. must be reduced by 100−1000 times compared to that used in GC to achieve the predicted high efficiencies.[90] The reduced column i.d. has caused challenges for preparing columns with adequate sample loadability and analyte retention; this has consequently impeded the OTLC advancement. Increasing the surface area was experimented to mitigate the low-loadability and low-retention issue. For example, Jorgenson *et al*.[91] used hydrochloric acid to remove the nonsilica components of a borosilicate glass capillary and created a thin layer of porous silica on the capillary inner wall. The authors claimed that they had increased the surface area by about thirty-fold compared to that of a geometrically smooth capillary. Ammonium hydrogen bifluoride was proved to be more effective toward creating porous silica having increased the surface areas by Pesek and Matyska,[92] and around 1000- fold surface-area enhancement was reported.[93] Etching the surfaces had indeed led to enhanced sample loadabili-

ties, but ultrahigh-resolution results were not obtained. Alternatively, a porous polymer stationary phase was created on the capillary wall to improve the sample loadability[94, 95], and these columns are now called porous layer open tubular (PLOT) columns. High efficiency separations were obtained using PLOT columns.[30, 39] For example, a poly(styrenedivinylbenzene) PLOT column was prepared by Yue *et al.*,[30] and a peak capacity of approximately 400 within a 3.5 h gradient was produced using this column for separating a tryptic digest mixture. Utilizing microfabrication technology, Desmet *et al.*[96] fabricated an array of radially elongated pillars in a microchannel and used all the surface to host a stationary phase. Because the pillars were accurately engineered and arranged so perfectly that the all gaps between the pillars had the same size and length, these channels (gaps between the pillars) were virtually a parallel-OT-column. Using such a device, these researchers obtained efficiencies of 160 000 theoretical plates for unretained analytes and 70 000 theoretical plates for a retained coumarin derivative. It is worth mentioning that these high-efficiency results were obtained three decades after the first OTLC separation was demonstrated for separating 3−6 aromatic compounds using a 60 μm i.d. column by Tsuda *et al.*[6] Ultrahigh efficiencies are possible for simple OTLC according to the theoretical investigations,[5, 8, 88, 91, 97] but these four decade old predictions have never been experimentally validated. Here we present experimental results to demonstrate the predicted potential of OTLC. We use a 2-μm-i.d. × 80 cm long (75 cm effective) OTC to separate pepsin/trypsin digested E. coli lysates and routinely produce exceptionally high peak capacities in the range of 1900−2000 in 3−5 h. Since the narrow bore is key to the high performances, we tentatively call the column *n*OTC and the

technique *n*OTLC. We also reduce the *n*OTC length to 6 cm (2.7 cm effective) to demonstrate *n*OTLC's capability of performing ultrafast (millisecond) separations. In addition, we show that a sample of only a few picoliters is required for each *n*OTLC separation, and the technique has low attomole LOD.

## 2. Experimental Section

### 2.1. Materials and Reagents

Fused-silica capillaries used for making the *n*OT columns (2 μm inner diameter, 150 μm outer diameter) were purchased from Polymicro Technologies, a subsidiary of Molex (Phoenix, AZ). Trypsin was purchased from Promega (Madison, WI). Pepsin was purchased from MP Biomedicals (Santa Ana, CA). Amino acids, sodium hydroxide, ammonia bicarbonate, acetonitrile, toluene, and trimethoxy- (octadecyl) silane were purchased from Sigma-Aldrich (St. Louis, MO). ATTO-TAG FQ Amine-Derivatization Kit was purchased from Thermo Fisher Scientific (Waltham, MA). All solutions were prepared with ultrapure water (Nanopure ultrapure water system, Barnstead, Dubuque, IA) and filtered through a 0.22 μm filter (VWR, TX), degassed before use.

### 2.2. Preparation of *n*OT Column

Columns were prepared as described previously.[41, 43] Briefly, after the polyimide coating at one end of a 2 μm i.d. capillary was removed for about 1 cm in length, this end of the capillary was inserted into a vial containing 50 μL of 1 M NaOH solution inside a pressure chamber. The other end (with polyimide coating) of the capillary was placed into a 0.5 mL sealed vial containing DDI water. Pressurized nitrogen at 35 bar was applied to wash the ca-

pillary with NaOH, DDI water, and then acetonitrile. Inside a dry glovebox, a trimethoxy(octadecyl) silane toluene solution was flushed through the capillary to coat the inner wall of the capillary.

### 2.3. Peptide Sample Preparation

One milliliter of E. coli lysate (~10 mg total protein·$mL^{-1}$) was mixed with 5 μL of 1 M NaAc/HAc buffer (pH = 4) and 1 μL of pepsin (1 μg·$mL^{-1}$), and the mixture was incubated at 37 °C for 1 h. A volume of 100 μL of the above solution was diluted with 900 μL of 25 mM $NH_4HCO_3$ and mixed with 1 μL of 1 M DTT at room temperature for at least 1 h. Then, 10 μL of 0.2 mg·$mL^{-1}$ trypsin solution was added into above mixture, and the mixture was incubated at 37 °C for 24 h.

### 2.4. Fluorescent Dye Labeling

Amino acid and peptide labeling was proceeded following the instruction provided with the ATTO-TAG FQ Amine-Derivatization Kit by Thermo Fisher Scientific. Briefly, a 10 mM ATTO-TAG FQ stock solution was prepared by dissolving 5.0 mg of ATTO-TAG FQ in 2.0 mL of methanol and stored in −20 °C. A 10 mM working KCN solution was prepared by diluting a 0.2 M KCN stock solution with 10 mM borax solution (pH 9.2). Amino acid stock solutions (each containing 1 mM of one amino acid) were prepared by dissolving individual amino acids in DDI water and filtered with a 0.22 μm filter. A volume of 1.0 μL of the amino acid stock solution was mixed with 10 μL of the 10 mM KCN working solution and 5 μL of the 10 mM FQ solution in a 0.25 mL vial. This mixture was maintained at room temperature for 1 h in dark before use. The FQ-labeled amino acid was diluted with 10 mM $NH_4HCO_3$ to

an appropriate concentration prior to analysis. To label the digested E. coli lysate, 10 μL of the peptide solution was mixed with 10 μL of 10 mM KCN and 10 μL of 10 mM FQ. After 1 h of reaction in the dark at ambient temperature, the peptides were ready for separation.

### 2.5. Apparatus

Figure 2.1 A presents a schematic diagram of the experimental apparatus used in this work. For ultrahigh resolution separations and LOD determinations, a gradient pump (Agilent 1200 quaternary pump, Santa Clara, CA) was used for driving a mobile phase through a six-port valve (VICI Valco, Houston, TX), via a flow splitter with a 20-μm i.d. and 20 cm long restriction capillary, to a *n*OTC. At 5 cm from the tip of the *n*OTC, polyimide coating was removed, forming a detection window. Figure 2.1 B presents a schematic diagram of the experimental apparatus used for ultrahigh-speed separations, a HPLC pump supplied mobile phase A (MA, 10 mM $NH_4HCO_3$) continuously. V1, along with a 20-μL loop, was employed for injecting a plug of MB (50% acetonitrile in 10 mM $NH_4HCO_3$) into the MA conduit for gradient (the so-called plug-gradient) generation. A plug of 900 pL of MB was injected into the *n*OTC. V2, along with a 2.6 μL loop, was utilized for sample injection. 120 pL of sample was injected into the *n*OTC. The detection end of the column was affixed to a capillary holder on an x−y−z translation stage so that the detection window could be aligned for the maximum fluorescent output. A confocal LIF detector, as described previously,[60] was employed to monitor the resolved analytes. Briefly, an argon ion laser (LaserPhysics, Salt Lake City, UT) generated a 488-nm laser beam. Then the laser beam was directed by a dichroic mirror (Q505LP, Chroma Technology, Rockingham, VT) and focused onto the detection windows of

the *n*OTC via an objective lens (20× and 0.5 NA, Rolyn Optics, Covina, CA). The emission of fluorescence was collimated by the same lens, and passed through the same dichroic mirror, an interference band-pass filter (532 nm, Carlsbad, CA) and a 1-mm pinhole, and finally were collected by a photosensor module (H5784-04, Hamamatsu). A data acquisition card USB-1208FS (Measurement Computing, Norton, MA) was used to measure the response from the photosensor module as voltage signal. The data were collected and analyzed by a home-made LabView program (National Instruments, Austin, TX).

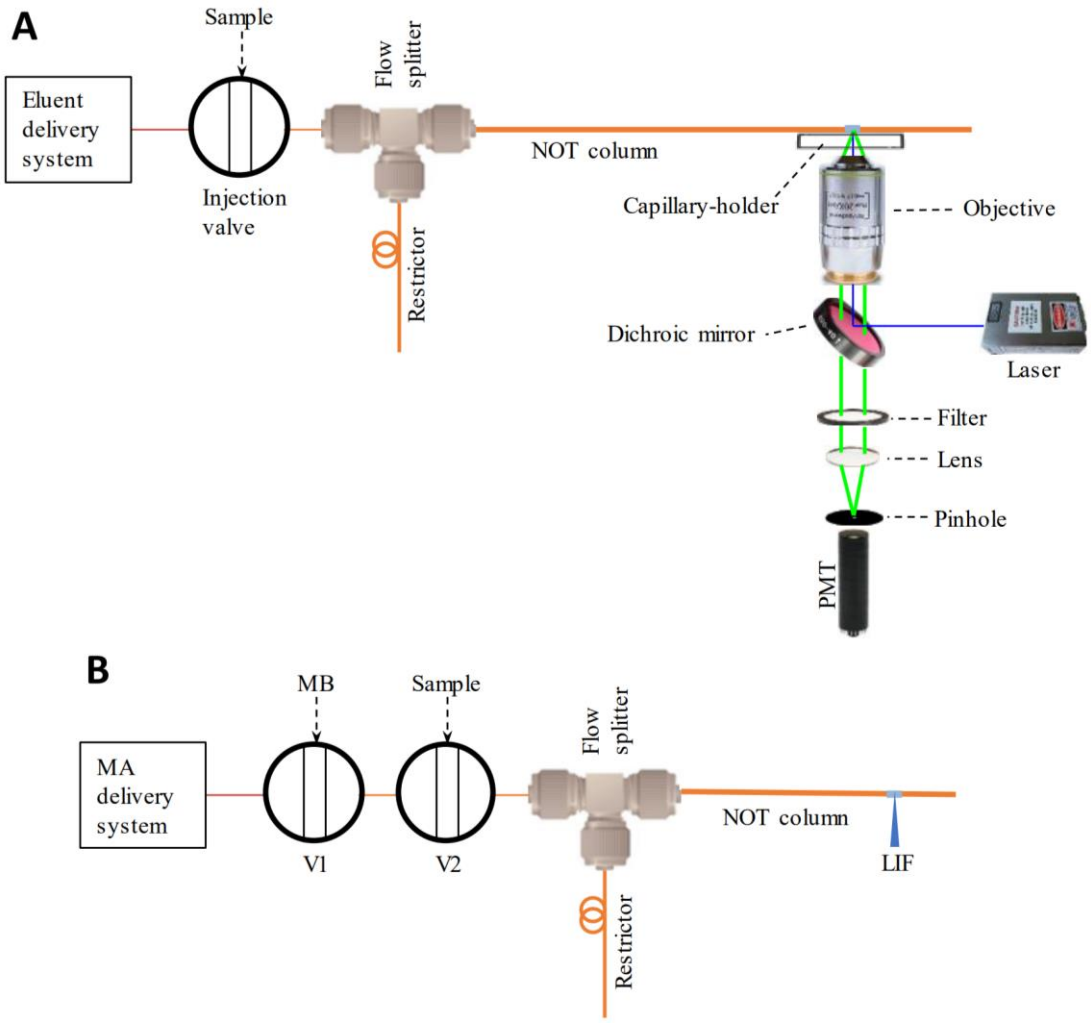


**Figure 2.1 Schematic diagrams of experimental apparatus for ultrahigh resolution and ultrafast separation**

(A) Apparatus used to perform ultra-high-resolution separations and LOD determinations. The *n*OTC had a 2-μm i.d. and was OTMS derivatized. The flow splitter was built using an Upchurch micro-T. A 10-cm-long and 20-μm-

i.d. capillary was used as a restrictor. A 200-μm i.d. and 360-μm-o.d. capillary was used to connect the injection valve and the micro-T. Inside the flow splitter, a small portion of the 2-μm-i.d. *n*OTC was inserted into a 200-μm i.d.and 360-μm o.d. connection capillary. A detection window was made at 5 cm away from the *n*OTC outlet by removing the polyimide coating. A LIF detector was used to detect the resolved analytes. (B) Apparatus to perform ultrafast separations. An HPLC pump was used to supply mobile phase A (10 mM $NH_4HCO_3$) continuously. V1 had a 20-μL loop and was employed for injecting a plug of mobile phase B (50% acetonitrile in 10 mM $NH_4HCO_3$) into the MA conduit for gradient generation. V2 had a 2.6-μL loop and was utilized for sample injection. The identical LIF detector was used in both A and B.

## 2.6. nOTLC Separation

To align the *n*OTC on the LIF detector, 10 μM fluorescein solution was pressurized through the column and the column was roughly aligned. The fluorescein solution was constantly flushed though the column until the alignment was done. Then, the LIF detector was turned on and fluorescein signal was monitored. By tunning the column position via the x-y-z transition stage until the maximum fluorescein output was obtained, the x, y and z positions of the stage were locked. The capillary was thoroughly rinsed with an eluent (e.g., 50% ACN with 10 mM $NH_4HCO_3$) before conducting a *n*OTLC separation.

In this work, we used 10 mM $NH_4HCO_3$ as the pH buffer for our mobile phase because that buffer was recommended for labeling amino acid or peptide with ATTO TAG FQ at a pH between 8.5 and 9.5. The pH of 10mM $NH_4HCO_3$ was measured to be 8.7. For the fast separation (Figure 2.8), 50% ACN was chosen because it allowed all amino acids to be eluted out fast and baseline resolved. If the ACN concentration was high (e.g. 80%), the amino acids could not be baseline resolved. If the ACN concentration was low (e.g. 20%), the elution was slow. Under the condition in the Figure 2.8 caption, the linear velocity of the mobile phase was 79 $mm \cdot s^{-1}$. This velocity was much higher than the optimum velocity for high resolution. In this experiment, we were pursing high separation speed.

The sample injection volume was estimated to be 120 pL. We used a couple of approaches to determine this volume. For the more common approach, we replaced the *n*OTC with an uncoated capillary having identical dimensions. Several windows at fixed locations on that capillary were made for LIF detection. An unretained analyte (e.g., 1 μM fluorescein) was injected into the column and fluorescent signal were measured at different windows. The different arrival time of the dye revealed the velocity of the mobile phase. The flow rate through the restriction capillary was measured directly by collecting fluid from the capillary. The splitting ratio was calculated by dividing the flow rate inside the restriction capillary by the flow rate in the *n*OTC. The sample injection volume was estimated by dividing the sample loop volume by the splitting ratio.

For ultrahigh resolution separations and LOD determinations, data acquisitions started immediately after sample injection. For ultrahigh speed separations, mobile phase was injected a couple of seconds after the sample injection, and data acquisitions started immediately after mobile phase B injection.

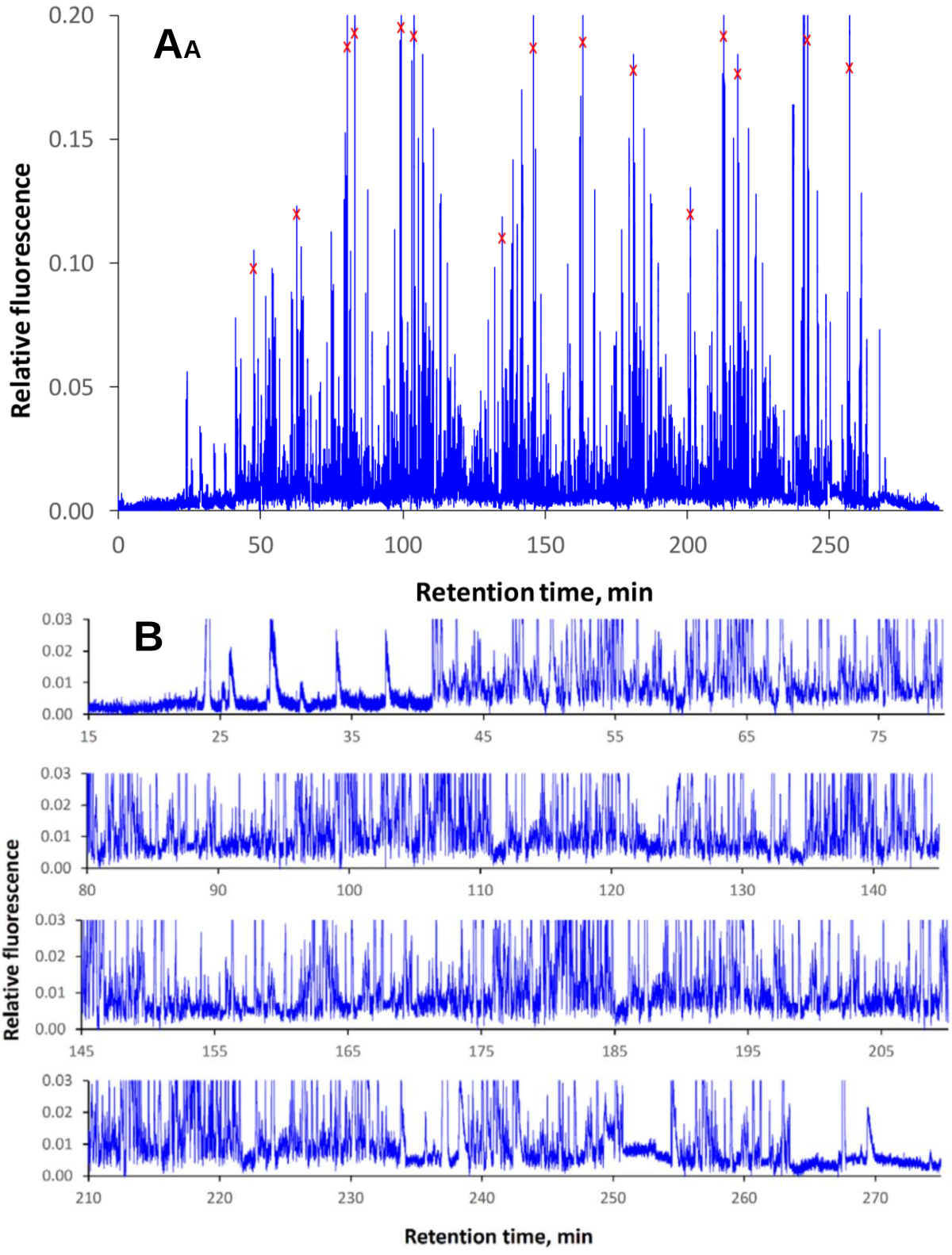


**Figure 2.2 Ultrahigh resolution *n*OTLC separation**

*n*OTC: 2-μm-i.d. × 80 cm (75 cm effective) capillary coated with C18; sample: *E. coli* lysates digested with pepsin/trypsin; mobile phase A: 10 mM $NH_4HCO_3$; mobile phase B: 80% acetonitrile in 10 mM $NH_4HCO_3$; injected volume: ~120 pL; elution pressure: ~35 bar; and gradient: mobile phase B increased from 5% to 100% in 300 min. (A) Single panel of the chromatogram. (B) Four panel display of the same separation.

# 3. Results and Discussion

## 3.1. Ultrahigh-Resolution *n*OTLC Separation

Figure 2.2 A presents an ultrahigh-resolution chromatogram for a pepsin and trypsin digested *E. coli* lysate. Hundreds of compounds are nicely resolved as seen in Figure 2.2 A, and many peaks are sharp [had full widths at half-maxima (FWHM) of 3−5 s]. The chromatogram is presented in four separate panels to exhibit the extraordinarily high resolutions. The single-panel chromatogram is presented in Figure 2.2 B. The peak widths of the 15 highest peaks across the chromatogram were measured, and the average FWHM value of these peaks was calculated to be 4.6 ± 0.5 s. Based on this value, the average full peak width ($4\sigma \approx 1.7 \times$ FWHM) was 7.9 s. The peak capacity of this separation was evaluated by dividing the time gap (245 min) between the first peak (the peak of an unretained analyte) and the last peak by the average full peak width, yielding a peak capacity of 1900. Although the 15 highest peaks were selected for peak capacity evaluation, there were many narrow low-intensity peaks. In fact, high-intensity peaks could have wider widths than low-intensity peaks because high-intensity peaks could be overloaded. Figure 2.3 exhibits four zoomed-in regions. Again, the average FWHM of the highest peaks (with cross) in these groups was 4.72, leading to a peak capacity of 1830. Nevertheless, the estimated peak capacity of 1830−1900 within 245 min is very impressive and a record for one dimensional LC separations. Importantly, the separation was carried out under an elution pressure of only ~35 bar.

High peak capacities had been reported for one-dimension separations,[98-101] but they were usually obtained at high elution pressures and in long separation times. Han *et al*.[98] em-

ployed a meter-long packed nano-LC column and generated a peak capacity of 800 under an elution pressure of 400 bar in more than 10 h. Shen *et al.*[100] obtained peak capacities of 1000−1500 using a 1379 bar RPLC-MS in greater than 12 h. To the best of our knowledge, one-dimension separation peak capacities of higher than 1900 within 3−5 h were never reported.

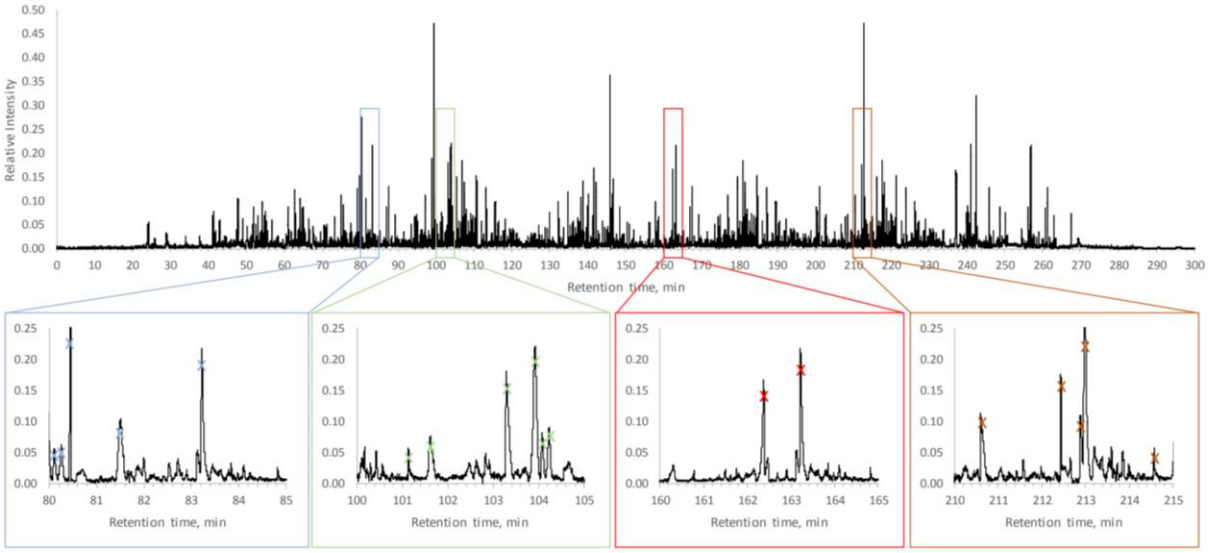


**Figure 2.3 Single panel exhibition of an ultrahigh resolution chromatogram showing four zoomed-in regions**

This chromatogram is identical to Figure 2.2. Peaks marked with crosses were used for peak capacity calculations.

The *n*OTC used in the above experiment was prepared first by activating an 80 cm long and 2 μm i.d. fused-silica capillary with NaOH and then the surface was coated with OTMS. Although 1 M NaOH was flushing through the capillary at 100 °C for 2 h to activate the surface in this work, we had no evidence that we had made the surface porous. We had tested flushing 1 M NaOH at 50 °C for 30 min and 75 °C for 1 h but did not observe any obvious column-performance differences. Figure 2.4 presents SEM images of the capillary i.d. before any treatment, after NaOH activating, and after OTMS coating. The capillary i.d. seemed to have increased slightly (by 190 nm) after NaOH activating, but this number was within the

capillary i.d. variations (capillary i.d. = 2 ± 0.5 μm according to Molex, Lisle, IL).

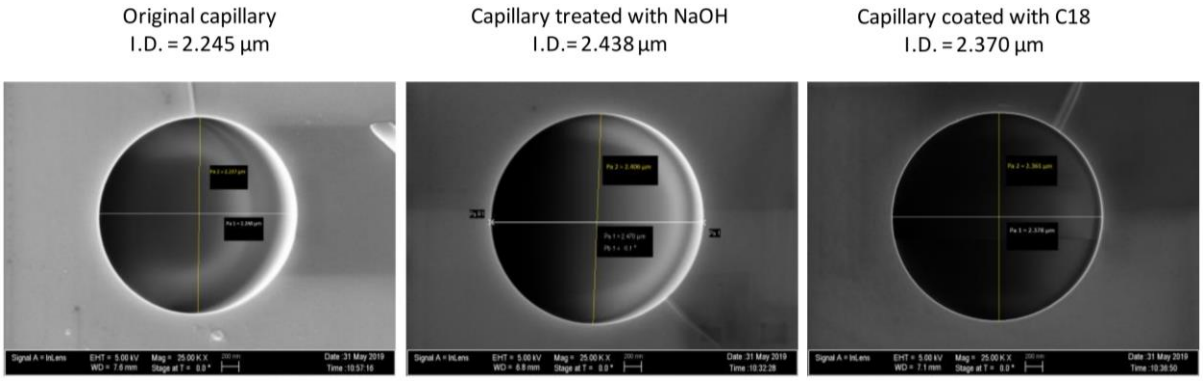


**Figure 2.4 SEM images of original 2-μm-i.d. capillary, after NaOH activation and after OTMS coating**

It should be noted that analytes in Figure 2.2 were labeled with ATTO-TAG FQ in order to use a LIF detector. Although excessive labeling dye was added to label all binding sites on each peptide, there could be unlabeled sites, leading to multiple labeling and hence multiple peaks for one peptide. Therefore, each peak in Figure 2.2 represents only a specific fluorescent molecule (i.e., a peptide labeled with a specific number of fluorescent dye molecules at specific binding sites).

In an attempt to further increase the peak capacity, we increased the *n*OTC length from 80 to 160 cm and separated similar samples under an elution pressure of ~35 bar and using a 3, 4, and 5 h gradient time (see results in Figure 2.5). Using the same approach to evaluate the peak capacity for these separations, we obtained peak capacities of 2000, 1900, and 1900 respectively for the 3, 4, and 5 h separations. These results indicated that, under the experimental conditions, merely increasing the gradient time could no longer enhance the peak capacity. This could be explained by recognizing the fact that the initial (5% mobile phase B and 95% mobile phase A) and the final (100% mobile phase B) compositions of the gradient solutions were the same. The increased gradient time reduced the slope of the gradient profile

(hence the gradient focusing) and consequently broadened the peaks. If we shortened the gradient time, the peak capacity did decrease with the gradient time as shown in Figure 2.6.

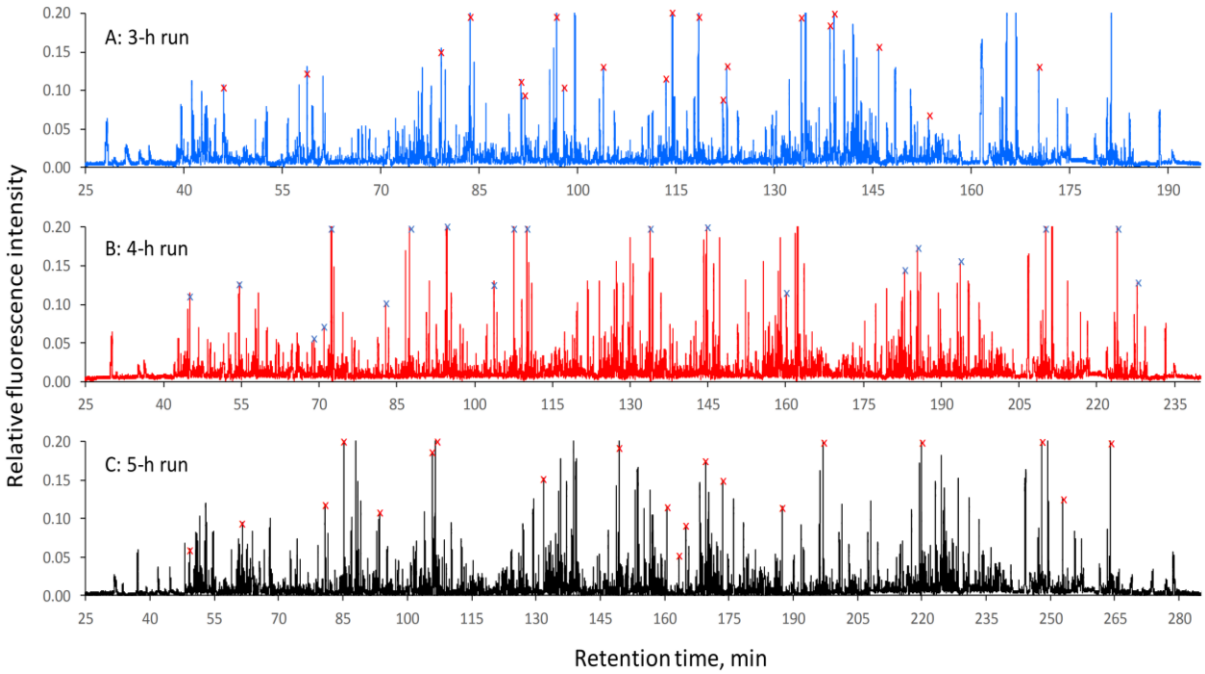


**Figure 2.5 Ultrahigh resolution chromatogram from 3h, 4h and 5h separations**

These chromatograms were obtained using a 160-cm-long (155 cm effective) × 2-μm-i.d. *n*OTC under an elution pressure of ~35 bar. Sample: E. coli lysate digested with pepsin/trypsin. Injected sample volume: ~120 pL. Gradient: MB from 5% to 100% in 180 min, 240 min and 300 min for top, middle and bottom respectively.

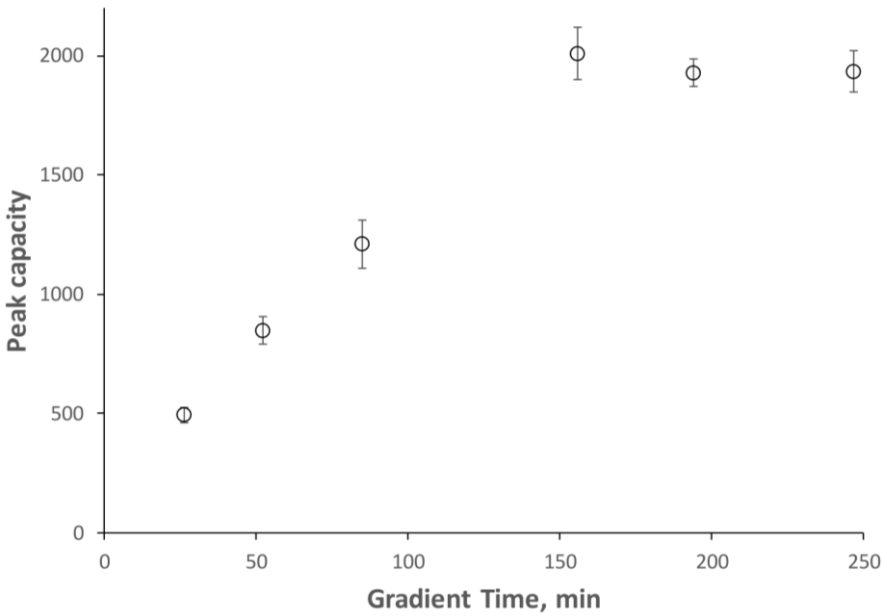


**Figure 2.6 Peak capacity vs gradient time in ultrahigh resolution separations**

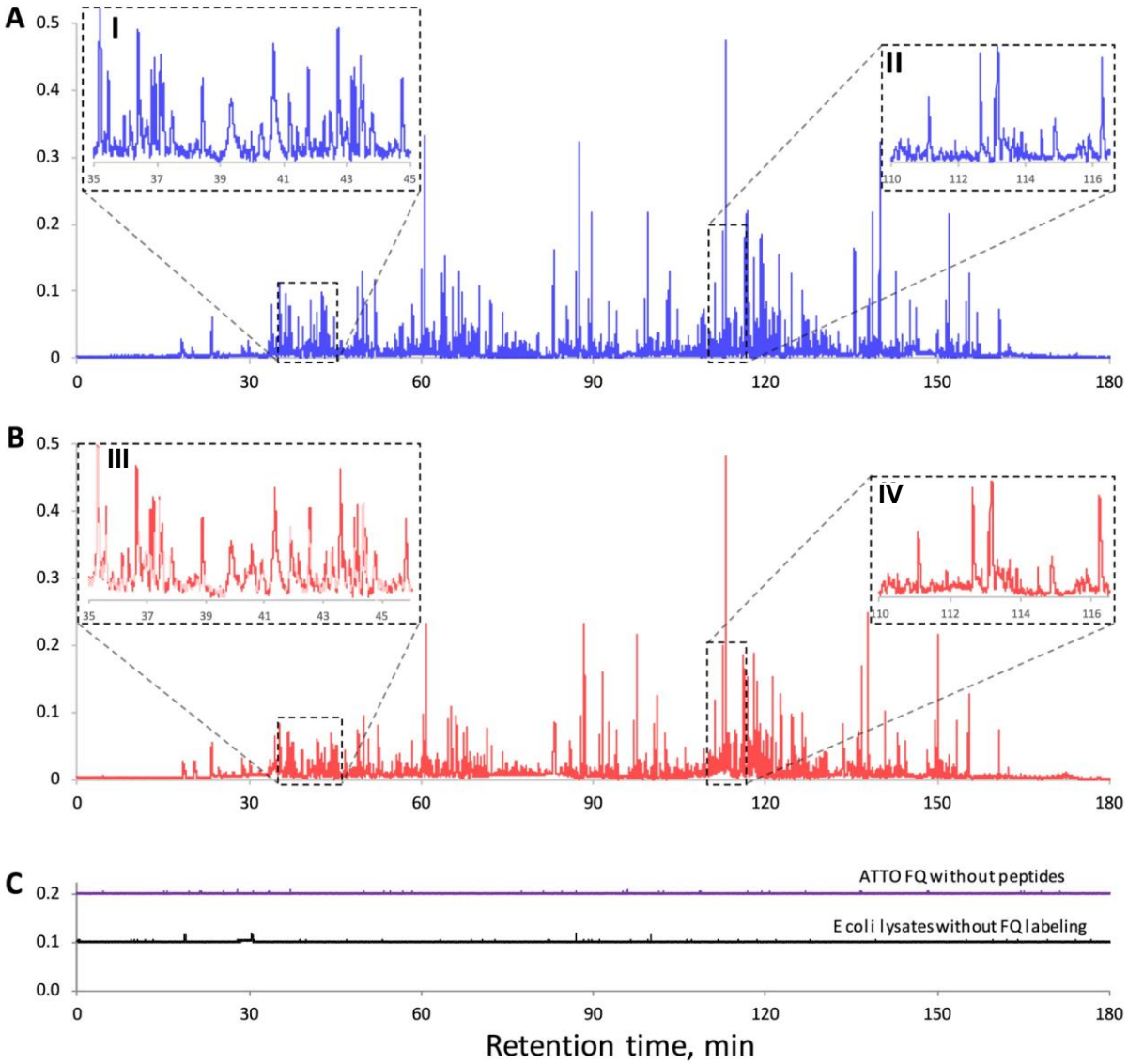


**Figure 2.7 Chromatograms for repeated peptide separations.**

*n*OTC: 2-μm-i.d. × 160 cm (155 cm effective) length; mobile phase A: 10 mM $NH_4HCO_3$; mobile phase B: 80% acetonitrile in 10 mM $NH_4HCO_3$; injected sample volume: ~120 pL; elution pressure: 64.8 bar; gradient: mobile phase B increasing from 5 to 100% in 180 min. In (A)−(C), the x-axes and y-axes have the same scales. Insets I and III/insets II and IV in (A)/(B) show expanded views of the same retention-time regions of the two chromatograms.

In this work, all *n*OTLC separations were performed under a constant pressure source. A common concern associated with such a system was the separation reproducibility. In one of our earlier reports,[43] we had shown the good repeatability results for amino acid separations. Figure 2.7 A and B presents chromatograms for two repeated peptide separations. Insets I and III and insets II and IV in Figure 2.7 A and B present expanded views of the same retention

time regions of the two chromatograms. Through peak pattern comparison, we can conclude that the separations were reproducible. To check if any artifact peaks were present in the above chromatograms, we carried out two "control" separations: one for the fluorescent labeling dye without peptides and the other for the pepsin/trypsin digested E. coli lysate without fluorescent dye labeling. The chromatograms are exhibited in Figure 2.7 C. The ATTO FQ chromatogram was raised by 0.2 and the E. coli lysate chromatogram was raised by 0.1 relative fluorescence intensity unit so that we could see the fluorescence signal variations. In general, the fluorescence signals were stable, and no high peaks were observed.

### 3.2. Ultrafast *n*OTLC Separation

Figure 2.8 presents an ultrafast separation using a 6 cm long (2.7 cm effective) *n*OTC. The sample contained six amino acids, and the separation was executed using a plug gradient (see Experimental Section for details) under an elution pressure of ~227.5 bar. The last analyte was eluted out in less than 800 ms, and all six amino acids were resolved within ~400 ms. In Figure 2.8, we might have set a speed record for that high resolution in LC. Setting the speed record was not our intention, because we could have increased the speed simply by shortening the column length and/or boosting the elution pressure after reducing the number of analytes. Figure 2.9 presents a comparison between our results and the fastest LC separation reported[102] using a short packed-column. Both separations were completed in less than 1 s, but our results exhibited much sharper peaks and higher resolutions.

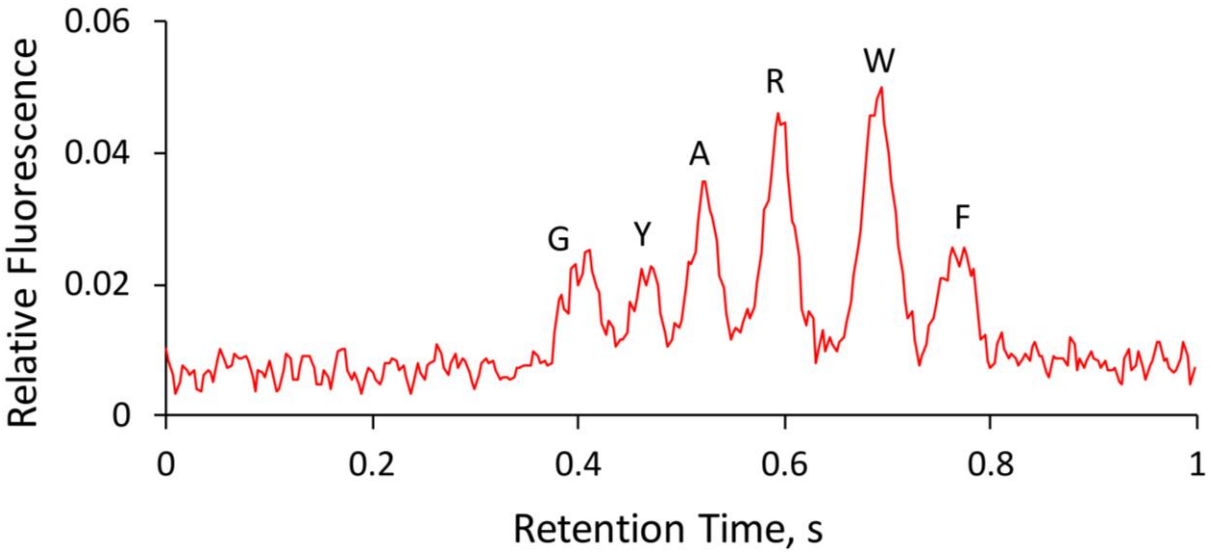


**Figure 2.8 Typical chromatograms for fast *n*OTLC separations**

*n*OTC: 2-μm-i.d. × 60 mm (27 mm effective) length capillary coated with C18; sample: mixture of glycine (1 μM), tyrosine (3 μM), alanine (3 μM), arginine (3 μM), tryptophan (10 μM), and phenylalanine (2.5 μM); sample volume injected: 120 pL; gradient created by injecting a plug (900 pL) of 50% acetonitrile in 10 mM $NH_4HCO_3$ into the *n*OTC; and elution pressure: 227.5 bar. Gradient delay time was subtracted from the retention time.

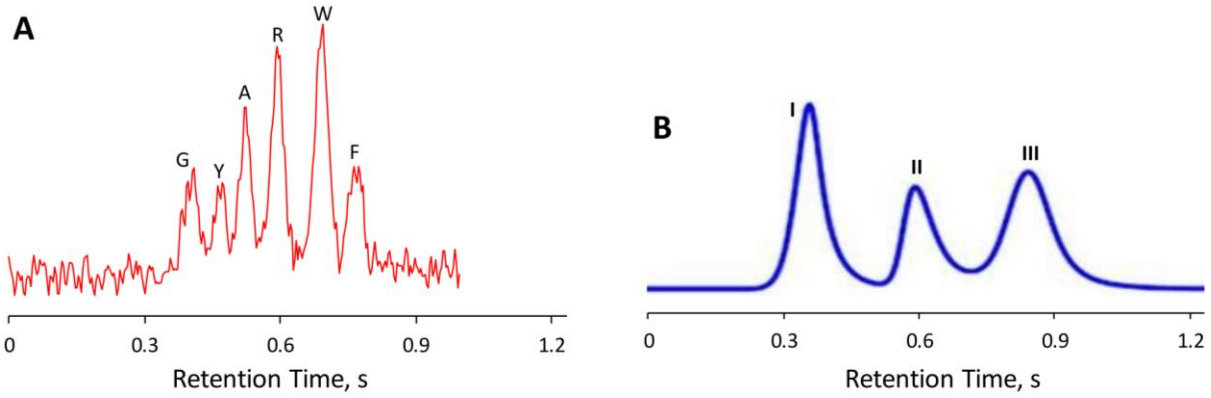


**Figure 2.9 Chromatogram comparison between ultrafast separations**

(A) Same chromatogram as Figure 2.8. (B) Chromatogram of an ultrafast HPLC separation. Separation was performed on an Agilent 1290 UHPLC with a diode array detector. The in-line filter was removed for high flow rate. The pump outlet was directly connected to a presaturator column (5 × 0.46 cm i.d.) filled with silica (M.S. Gel, D-50-120A, AGC SciTech Co., Ltd.) The column had a length of 0.5 cm and an i.d. of 0.46 cm. Rheodyne 7520 manual injector with an internal loop size of 1 μL was connected to the presaturator outlet and then the analyte column. The mobile phase (70:30 ACN:water) flow rate was 5mLmin-1. I: 4-formyl-benzene-1,3-disulfonic acid, II: N-acetyl-D-alanine, III: methyl benzenesulfonate. The three peaks in B were sharpened by raising Gaussian functions to power 3 to fit all these peaks.

### 3.3. *n*OTLC Limit of Detection

Figure 2.10 presents a chromatogram for three amino acids to evaluate the *n*OTLC's detection limits. The sample contained 0.04 μM Gly, 0.08 μM Ile, and 0.08 μM Leu in 10 mM $NH_4HCO_3$. After 157 pL of the sample was injected, the separation was carried out using a 2-μm-i.d. × 80 cm long (75 cm effective) *n*OTC under an elution pressure of ~65.5 bar. From Figure 2.10, a noise of 0.00069 was measured for the background signal, and net signals of 0.0195, 0.0161, and 0.0265 were measured, respectively, for 0.04 μM Gly, 0.08 μM Ile, and 0.08 μM Leu. Using a criterion of S/N = 3, the LODs for Gly, Ile, and Leu were 0.73, 1.8, and 1.1 aM, respectively. With the ultrahigh resolving power and ultrafast separation speed, combined with the low sample volume (pL) and low limit of detection (attomole), *n*OTLC has the potential to become a powerful tool for biotech research, especially for single cell analysis.

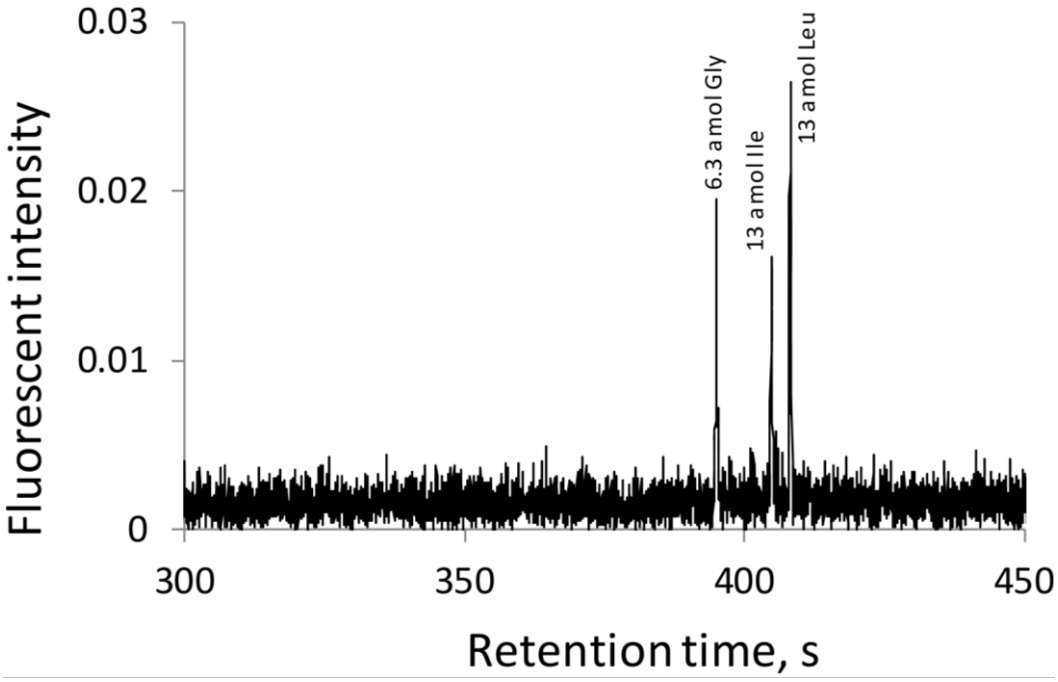


**Figure 2.10 LOD determination**

*n*OTC: 2-μm-i.d. × 80-cm length (75 cm effective) coated with C18; sample: 0.04 μM Gly, 0.08 μM Ile, and 0.08 μM Leu in 10 mM $NH_4HCO_3$; injection volume: ca. 157 pL; mobile phase: mixture of 4 parts of 10 mM $NH_4HCO_3$ and 1 part of acetonitrile; and elution pressure: 65.5 bar.

The materials in Chapter 2: are adapted with permission from **Xiang, Piliang, Yu Yang, Zhitao Zhao, Apeng Chen, and Shaorong Liu. "Experimentally validating open tubular liquid chromatography for a peak capacity of 2000 in 3 h."** ***Analytical chemistry*** **91, no. 16 (2019): 10518-10523**. Copyright © 2019, American Chemical Society. Ultrahigh resolution and LOD part credit to Dr. Yang Yu(🐑🐟)

# Chapter 3: Ultrafast Gradient Separation with Narrow Open Tubular Liquid Chromatography

## 1. Abstract

Separation speed and resolution are two important figures of merit in chromatography. Often, one gains the speed at the cost of the resolution, and vice versa. Scientists have employed short-packed columns for ultrafast separations but encountered challenges such as limited mobile phase velocity, extra-column effect caused band broadening, and column packing difficulty. We have recently demonstrated ultrahigh resolutions of *n*OTLC; this allows us to trade some of the resolution for speed. In this work, we explored *n*OTLC for ultrafast LC separations. We used a 2.7 cm (effective length) *n*OTC and showed a baseline separation of 6 amino acids in less than 700 ms. Ways to further increase the speed were discussed. Using short *n*OTC to perform ultrafast separation we overcame the challenges from using short, packed columns. To demonstrate the feasibility of using this ultrafast separation technique for practical applications, we separated complex protein digests; peptides were nicely resolved in ~1 min.

## 1. Introduction

High-throughput analysis plays an important role in many fields including identifying drug compound hits,[103] surveying diseases,[104] and analyzing controlled substances,[105] to name just a few. Ultrafast chromatography provides an effective means to achieve these high-throughput analyses. By current standards,[106] LC separations completed in sub minute may be considered ultrafast, while those completed in a few minutes are considered fast, although

separations completed in 30−60 min were once called fast half century ago.[107] The use of sub-2-μm particles has revolutionized ultrafast LC separations. The original idea of reducing particle sizes for packed columns was to enhance the separation efficiency and improve the resolution,[87] and this pioneering work eventually laid the foundation for the UPLC today. UPLC enabled us to perform fast and ultrafast separations,[108] because we could afford to trade some of increased resolution for speed. Using short UPLC columns, separation speeds within several seconds are common nowadays,[106, 109-119] and sub-second separations are also demonstrated.[106, 119, 120]

Armstrong's group is currently the front-runner in the effort to accelerate LC separations,[106, 109, 110, 113-115, 120] although millisecond[121] or even submillisecond[122] electrophoretic separations were reported more than two decades ago. [Note: electrophoretic separation is fundamentally a faster separation technique than LC, because the former occurs inside a single phase while the latter happens between two phases.] These researchers used short packed columns and high mobile phase velocity to demonstrate LC separations at speeds comparable or faster than sensor responses.[106, 120] They also developed an algorithm to make peaks unresolved out of the column nicely resolved mathematically. After being processed using this algorithm, 10 peaks could be baseline resolved in about a second.[120] These researchers also pointed out several challenges associated with the realization of these ultrafast separations. (1) The packing particles could not be too small, because elution pressure increased inversely with the square of the particle diameter and the pressure limit restricted the flow velocity and hence the separation speed. (2) Extra-column effects contributed consider-

ably to band broadening. (3) It was extremely difficult to pack a short column homogeneously.

We have recently experimentally validated the most efficient chromatography format−OTLC. Because the narrowness of the OTC was essential for achieving the ultrahigh performances, we called the column *n*OTC and the technique *n*OTLC. Using a 2-μm-i.d. *n*OTC we routinely obtained peak capacities of ∼2000 in ∼3 h[11] for separating pepsin/trypsin digested E. coli lysates. These peak capacities were actually higher than ever obtained for single-dimension LC separations. Like UPLC, *n*OTLC offers us a great means to perform ultrafast separations through compromising some of the resolutions.

Limited surface area/loading capacity has been perceived as an issue of *n*OTCs, and this perception has intimidated researchers from investigating *n*OTLC columns for high-resolution separations. With the detection technology advancement, we have demonstrated that the "limited surface area/loading capacity" is not an issue anymore. In an earlier paper,[11] we reported that we could trap 0.3 fmol analytes at the head of a *n*OTC and resolve and detect them nicely. In a separate test, we loaded 18 fmol ATTO-TAG FQ-labeled phenylalanine onto a 60 cm-long and 2-μm-i.d. *n*OTC, and a sharp peak (FWHM = 1 s) was eluted out, although the peak tailed badly (it took ∼100 s for the peak signal to get down to 10% level).

Importantly, employing a *n*OTC to perform ultrafast separation can avoid all three challenges[120] from utilizing short packed columns. A *n*OTC has much higher permeability than a fine-particle-packed column. *n*OTLC separations were usually carried out under a pressure of several hundred psi. This addresses the aforementioned challenge #1. A *n*OTC has a straight open pore therefore eliminates eddy flow. Using an on-column detection scheme such as a

LIF detector or a MS detector, flow-cell-caused band broadening can be avoided. This mitigates the aforementioned challenge #2. A *n*OTC has no packing. This eliminates the aforementioned challenge #3.

In this work, we explored the potential of using *n*OTLC for ultrafast LC separations. We used a short (2.7 cm effective) *n*OTC and presented baseline resolutions for 6 amino acids in less than 700 ms under an elution pressure of 20 MPa. The 6 amino acids were resolved within ~400 ms. These speeds could be further increased if we raised the elution pressure and/or shortened the column; approaches toward faster separations were discussed. To demonstrate the feasibility of this fast separation technique for practical uses, we used trypsin to digest a protein (cytochrome C). After the peptides were fluorescently labeled, we separated them using a 3.5 cm-long (2.7 cm effective) and 2-μm-i.d. *n*OTC. The peptide sample could be nicely resolved under an elution pressure of 0.36 MPa in ~1 min.

## 2. Experimental Section

### 2.1. Reagents

Fluorescein sodium salt, amino acids, cytochrome C, sodium hydroxide, ammonium bicarbonate, acetonitrile, toluene and octadecyltrimethoxysilane were obtained from Sigma-Aldrich (St. Louis, MO). ATTO-TAG FQ Amine-Derivatization Kit was obtained from Thermo Fisher Scientific (Waltham, MA). All solutions were prepared using ultrapure water (Nanopure ultrapure water system, Barnstead, Dubuque, IA) and filtered through a 0.22-μM filter (VWR, TX), degassed before use. Fused-silica capillaries having an inner diameter (i.d.) of 2 μm and an outer diameter (o.d.) of 150-μm were purchased from Polymicro Technologies, a

subsidiary of Molex (Phoenix, AZ).

### 2.2. *n*OT Column Preparation

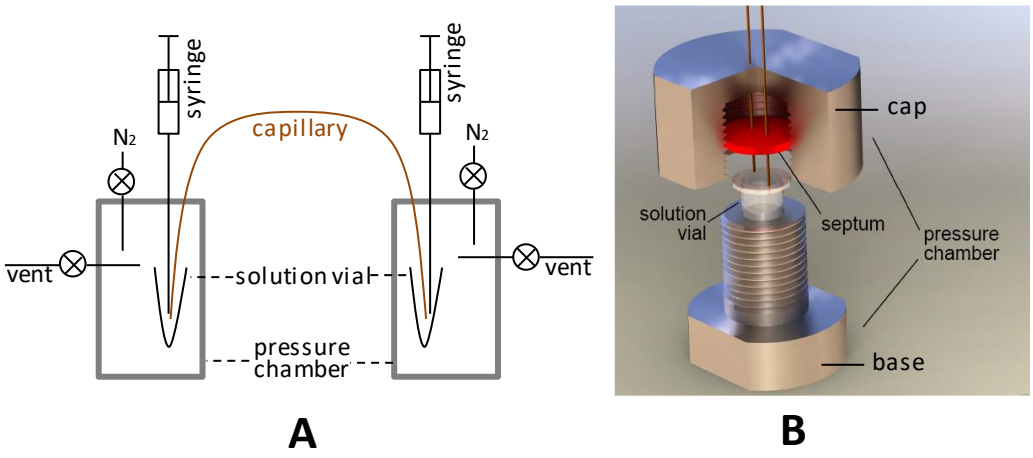


**Figure 3.1 Schematic diagram of experimental arrangement for coating capillaries.**

A: Schematic diagram of experimental arrangement. B: Configuration of pressure chamber.

Figure 3.1 presented a detailed configuration of the apparatus for *n*OTC preparation. One or two septa were placed between the stainless-steel pressure chamber base and cap to make the chamber airtight. To prepare a *n*OTC for fast separation, a 2-μm-i.d. × 60 cm-long capillary was cut, and about 1 cm of polyimide coating at one end of the capillary was removed. A 25 G × 7/8″ hypodermic needle was used as a guide to facilitate the insertion of this capillary through the septa into the reagent vial holding 100 μL of a 1 M NaOH solution. The other end (with polyimide coating) of the capillary was inserted into the waste container with DI water inside. High pressure (6.9 MPa or 1000 psi) nitrogen was applied to the reagent chamber to pressurize NaOH through the capillary at 75 °C for 1 h before being taken out of the oven. After the chamber cooled, the NaOH solution was replaced with DDI water to rinse the capillary for another hour. The whole setup was taken out of the oven, allowing it to cool to room

temperature. Then the DDI water vial was replaced with an empty vial. High pressure nitrogen (6.9 MPa or 1000 psi) was applied again to dry the capillary with nitrogen for 1 h.

The setup was then moved inside a dry glovebox. A mixture of 75 μL OTMS and 25 μL toluene was prepared in the dry glovebox and placed inside the reagent chamber. The polyimide-removed end of the capillary was inserted into the pressure chamber via a needle guide, pressurized nitrogen (6.9 MPa or 1000 psi) was applied to the chamber, and the setup was moved inside an oven at 75 °C. After 18 h, the coating reagent was replaced with an empty vial. The column was ready for use after being dried with nitrogen.

### 2.3. Cytochrome C Tryptic Digest Preparation

100 μL of 10 $mg \cdot mL^{-1}$ cytochrome C stock solution was diluted to 1 $mg \cdot mL^{-1}$ with 25 mM $NH_4HCO_3$, mixed with 1 μL of 1 M DTT and stayed at 37 °C for 1 h. Then the mixture was reacted with 10 μL of 0.2 $mg \cdot mL^{-1}$ trypsin solution at 37 °C for 24 h.

### 2.4. Analyte Fluorescence Labeling

Following the instruction provided with the ATTO-TAG FQ Amine-Derivatization Kit by the manufacturer. A 10 mM working KCN solution was prepared by diluting a 0.2 M KCN stock solution with 10 mM borax solution (pH 9.2). Amino acid stock solutions (5 mM for each amino acid) were prepared by dissolving individual amino acids in DDI water and filtered with 0.22-μm filter. A volume of 5.0 μL of the amino acid stock solution was mixed with 15 μL of the 10 mM KCN working solution and 5 μL of the 10 mM FQ solution in a 0.25 mL vial. The solution was ready for use after the mixture was maintained at room temperature for 1 h in the dark.

To label tryptic digests of cytochrome C, 5 μL of the peptide solution was mixed with 15 μL of 10 mM KCN working solution and 10 μL of the 10 mM FQ solution. After 1 h reaction in dark at room temperature, the peptides were ready for dilution/separation.

### 2.5. Apparatus

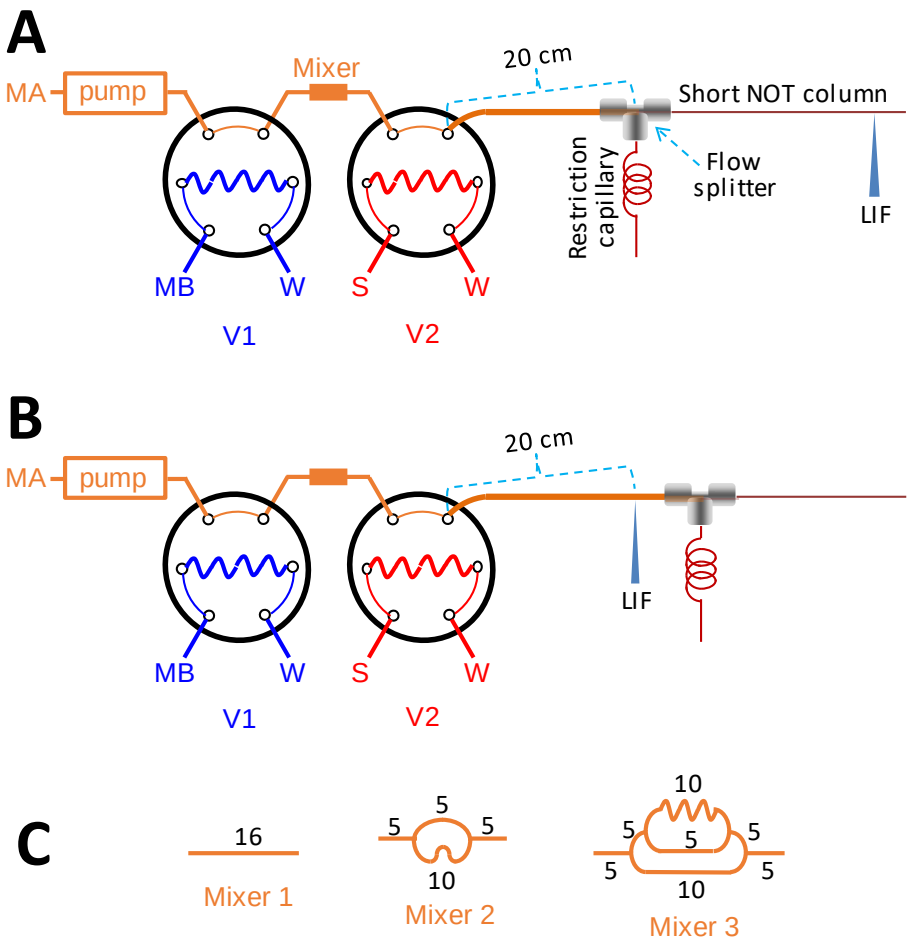


**Figure 3.2 Apparatus for ultrafast gradient *n*OTLC separation**

(A) Apparatus for ultrafast gradient *n*OTLC separation. (B) Apparatus for gradient delay measurements. (C) Schematic presentation of three mixers, all numbers are in cm.

Figure 3.2A presents the experimental apparatus used in this work. An HPLC pump (LC-30AD, Shimadzu, MD) was used to drive mobile phase A (MA, 10 mM $NH_4HCO_3$) through the entire system. The first 6-port valve (V1) (VICI Valco, Houston, TX) was attached with a 20-μL loop for Mobile phase B (MB, 50% acetonitrile with 10 mM $NH_4HCO_3$) injection,

while a second six-port valve (V2) was attached with a 2.6-μL loop for sample injection. V1 and V2 were electrically actuated, and their switching actions could be accurately detected. Between V1 and V2 there was a mixer (see Figure 3.2C) for smoothing the gradient profiles. A 20 cm capillary with 150-μm i.d. and 360-μm o.d. was used to connect V2 and the flow splitter. The *n*OTC had an effective length of 2.7 cm (from the column head to the LIF detector). About 1 mm of the polyimide coating was removed from the column head, and ~0.5 mm of the polyimide-removed end was inserted into the 20 cm connection capillary to minimize the injection dead-volume. The column was mounted on an x-y-z translation stage to allow for aligning with the LIF detector as described previously.[60] During a separation, the LIF detector constantly monitored all fluorescent analytes passing across it. The restriction capillary had a length of 68.5 cm and an i.d. of 50-μm. All other connection capillaries had an i.d. of 150 μm and an o.d. of 360 μm. Figure 3.2B presents the apparatus for gradient delay measurements. Basically, the 20-cm-long connection capillary in Figure 3.2A was replaced with a 30 cm capillary having the same 150-μm i.d. and 360-μm o.d. A detection window was created 20 cm away from the capillary inlet and aligned with the LIF detector. V2 was left at the injection position during all gradient delay measurements. Figure 3.2C presents various mixers used in this work for generating different gradient profiles.

### 2.6. Elution Pressure Measurement

Referring to Figure 3.2A, after a desired MA delivery rate was set (via the Shimadzu HPLC pump) and the system pressure became stabilized, the pressure rating on the pump was recorded as $P_{\mathrm{tot}}$. While the pump was on, the restriction capillary was removed, and the pres-

sure rating on the pump dropped and recorded as $P_{\mathrm{sys}}$. At this time, the flow inside the *n*OTC stopped. The elution pressure, $P_{\mathrm{elu}}$, across the *n*OTC under that specific pump rate was calculated by $P_{\mathrm{elu}} = P_{\mathrm{tot}} - P_{\mathrm{sys}}$.

### 2.7. *n*OT Column Alignment

The *n*OTC attached to the x-y-z translation stage was roughly aligned with the LIF detector. 1 μM fluorescein solution was injected into the system via V1 at a low constant flow rate (e.g., 0.01 mL·min$^{-1}$ on the HPLC pump). After the fluorescein solution passed across the detector (a fluorescence would start increasing after ~60 s and become stabilized after ~90 s). The column position was finely tuned using the x-y-z translation stage until the maximum fluorescence intensity was reached. After this alignment, at least 3 MB injections via V1 should be carried out to wash the system before any *n*OTLC separations.

### 2.8. Ultrafast *n*OTLC Separation

Referring to Figure 3.2A, the HPLC pump was set to a desired flow rate, MB was loaded to V1, and the sample was loaded to V2. The data acquisition sampling rate was set to be 1000 Hz. While the pump was running, V2 was switched to the injection position. About 3 s later, the data acquisition was started, and V1 was switched to the injection position. After all analytes were eluted out, the data acquisition was terminated. HPLC pump was kept running to rinse and equilibrate the column.

## 3. Results and Discussion

### 3.1. *n*OT Column Loadability

Limited surface area/loading capacity has been perceived as an issue of *n*OTCs, and this

perception has intimidated researchers from investigating *n*OTLC columns for high-resolution separations. With the detection technology advancement, we have demonstrated that the "limited surface area/loading capacity" is not an issue anymore. In an earlier paper,[11] we reported that we could trap 0.3 fmol analytes at the head of a *n*OTC and resolve and detect them nicely. In a separate test, we loaded 18 fmol ATTO-TAG FQ-labeled phenylalanine onto a 60 cm-long and 2-μm-i.d. *n*OTC, and a sharp peak (FWHM = ~1 s) was eluted out, although the peak tailed severely (it took ~100 s for the peak signal to get down to the baseline).

### 3.2. Elution Pressure

In this work we utilized a HPLC pump combined with a flow splitter to drive *n*OTLC separations. Each separation was therefore performed under a constant pressure mode. The elution pressure was controlled primarily by the overall pump rate and the dimensions of the restriction capillary. When the restriction capillary dimensions were fixed, the elution pressure was directly proportional to the overall pump rate (Figure 3.3, R2 = 0.9995).

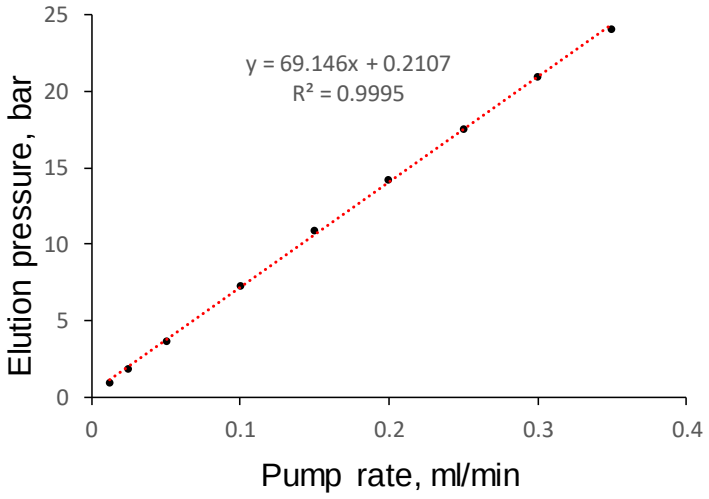


**Figure 3.3 Relationship between HPLC pump rate and elution pressure**

*n*OTC: 2-μm-i.d. × 6 cm (2.7 cm effective). Restriction capillary: 50-μm-i.d. × 68.5 cm.

### 3.3. Gradient Delay

Referring to Figure 3.2A, while the HPLC pump was constantly delivering MA, a segment of MB was injected via V1 into the stream of MA. The mixing zone at the front interface between MA and MB formed a zone with an increasing acetonitrile concentration, and this zone was the gradient we used for all our *n*OTLC separations in this paper.

During a *n*OTLC run, a sample was injected first via V2. As the injected sample was carried by MA to the *n*OTC, analytes were concentrated at the column head. MB was injected several seconds after the sample injection. As the gradient (the MA−MB interface) was driven through the column, the stacked analytes were resolved. In this work, we considered that a separation starting time to be the time when the gradient arrived at the head of the *n*OTC and that the time between such a starting time and a MB injection was a delay time.

The apparatus in Figure 3.2B was employed for measuring the gradient delay times. After the pump was set at a targeted flow rate and the system pressure became stabilized, 1 μM fluorescein solution was loaded to V1. V2 was kept at the injection position all the time throughout this gradient delay time measurement test. Then, the detector data acquisition was started, V1 was switched to the injection position, and V1 injection time was recorded as $t_{\mathrm{V1}}$. The data acquisition was terminated after the fluorescence signal passed across the detector and dropped to the background level. Typical gradient profiles are presented in Figure 3.4A. The gradient arrival time ($t_{\mathrm{gra}}$) was determined as fluorescein fluorescence signal rose to 5× the background noise (see inset of Figure 3.2A). The gradient delay time ($t_{\mathrm{del}}$) was calculated by $t_{\mathrm{del}} = t_{\mathrm{gra}} - t_{\mathrm{V1}}$. The reciprocal of the delay time had a good linear relationship (R2 =

0.9986) with the elution pressure (see Figure 3.4B).

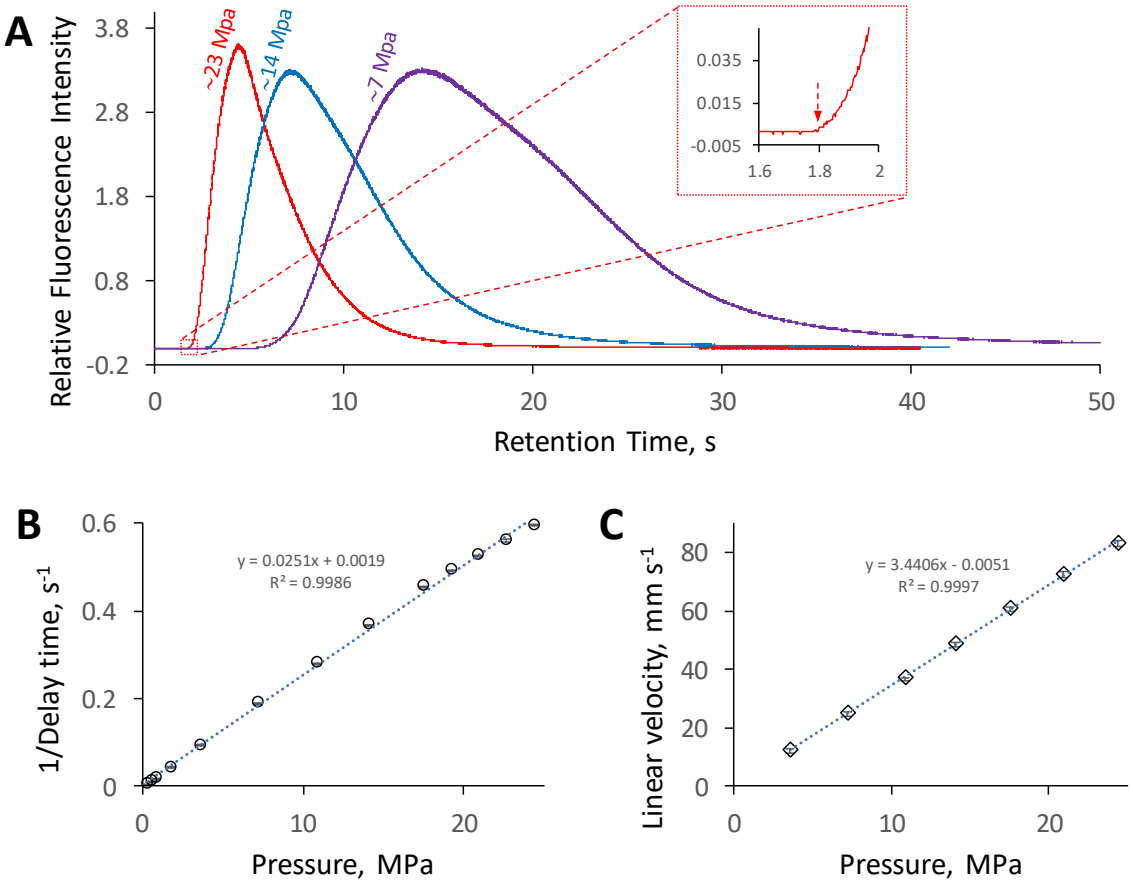


**Figure 3.4 Gradient delay measurement, gradient delay time vs. pressure and Linear flow velocity at different pump flow rates**

Inclusion of a mixer between the two valves presented a concept for smoothing the gradient profiles; a similar idea was described in literature.[123] Typical gradient profiles were presented in Figure 3.5 using the three mixers presented in Figure 3.2C; additional lines in the mixer did help smoothing the gradient profiles. If we use the time between 10% to 90% of MB as a measure for the gradient time, the gradient time increased by 55% from mixer 1 to mixer 2 and 88% from mixer 1 to mixer 3.

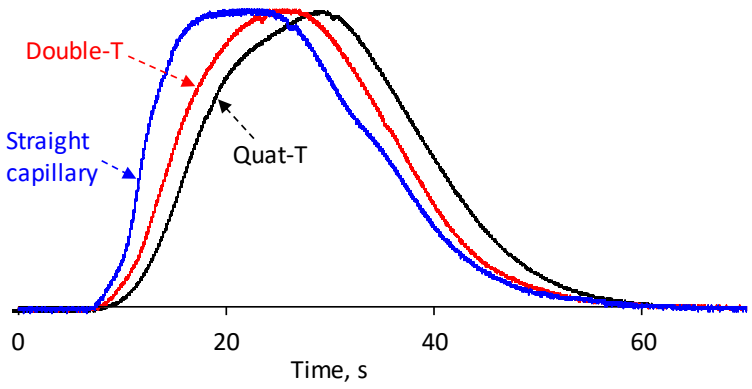


**Figure 3.5 Gradient profiles produced using different mixers**

The gradient profiles were normalized, and gradient arrival times were aligned for comparison purpose. HPLC pump rate: 0.05 mL·min$^{-1}$ (~3.6 MPa elution pressure).

### 3.4. Mobile Phase Linear Velocity

Mobile phase linear velocity is a key parameter for chromatographic separations. When 2-μm-i.d. *n*OTCs were used in this work, it was not straightforward how the linear velocity was measured. The following described an approach we used for the measurements.

Referring to Figure 3.2A, the *n*OTC was replaced with a 50 cm-long and 2-μm-i.d. uncoated capillary. Fluorescein was unretained inside an uncoated capillary under the experimental conditions; this was confirmed by the same retention time when fluorescein was eluted with eluents having different acetonitrile concentrations. A detection window was made 2.7 cm from the inlet-end of the capillary. The 2.7 cm distance was required for mounting the column on the x-y-z translation stage with adequate clearance for proper alignment. V1 was set at the loading position throughout this linear velocity measurement experiment. After the HPLC pump was set at a targeted rate, 1 μM fluorescein was loaded to V2. Then, the data acquisition was triggered, V2 was switched to the injection position, the switching time was recorded as $t_{V2}$, fluorescein peak was recorded, and the peak time was recorded as $t_{peak}$. The above test was repeated for a series of pump rates. Then, 5−10 cm of the uncoated

capillary was trimmed off from the outlet-end. The same tests were performed for the same series of pump rates. Then, another 5−10 cm of the uncoated capillary was trimmed off, and so on. The pump rates ($Q_i$) tested were 0.35, 0.325, 0.30, 0.25, 0.20, 0.15, 0.10, and 0.05 mL·min$^{-1}$, while the uncoated capillary lengths ($L_j$) tested were 50, 45, 40, 35, 30, 25, 20, 15, and 10 cm. For any given pump rate ($Q_i$), ($t_{\mathrm{peak}} - t_{\mathrm{V2}}$) was plotted against $L_{\mathrm{j}}$, and a good linear relation was obtained. The y-axis intercept was the time ($t_{Q_i}$)it took for the fluorescein to reach the inlet of the uncoated capillary. Because most of the flow went through the restriction capillary, $t_{Q_i}$ was dependent on $Q_i$ (but independent of $L_j$). The linear velocity ($u_{L_j}^{Q_i}$) under a given $Q_i$ (or elution pressure) and a total length of $L_j$ was calculated by $u_{L_j}^{Q_i}$ = $27/(t_{\mathrm{peak}} - t_{\mathrm{V2}} - t_{Q_i})$ (mm·s$^{-1}$). Figure 3.4C presents the relationship between linear velocity and elution pressure; a very good linear relationship ($R^2$ = 0.9997) was obtained. The same linear velocity was assumed inside a *n*OTC having the same dimensions as the uncoated capillary under the same conditions.

### 3.5. Ultrafast *n*OTLC Separation

Figure 3.6 presents three ultrafast *n*OTLC separations using short *n*OTCs. The separation for Figure 3.6A was completed in less than 800 ms, while 6 amino acids were baseline resolved within 400 ms. By shortening the *n*OTC total length (from 6 to 3.5 cm), a baseline separation of 6 different amino acids was completed in less than 700 ms (see Figure 3B). By increasing the elution pressure (from 20 to 25 MPa), a baseline separation of 3 amino acids was completed in less than 600 ms. Full widths at half-maximum (FWHM) for these separations were usually less than 50 ms, while the sharpest peaks had FWHM of ∼20 ms. It is

worth pointing out that the separation time did not include system initialization and that gradient delay was excluded as well.

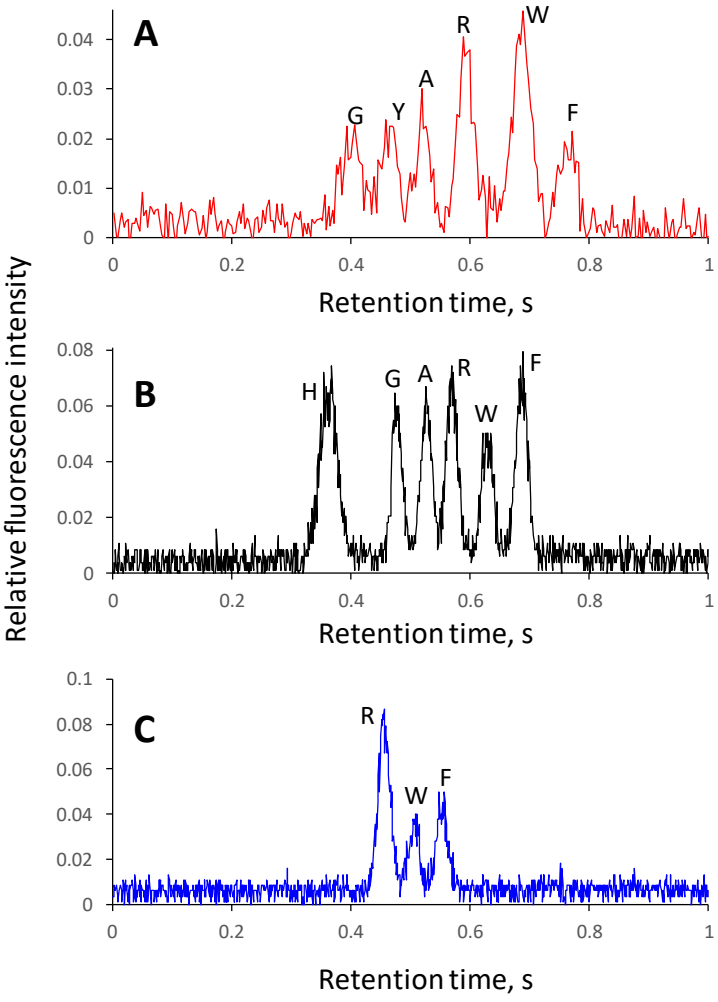


**Figure 3.6 Three typical ultrafast *n*OTLC separations**

(A) nOTC: 2-μm-i.d. × 6-cm-length (2.7 cm effective) coated with C18; MA: 10 mM NH4HCO3; MB: 50% acetonitrile in 10 mM $NH_4HCO_3$; Mixer: Mixer 2 in Figure 3.2C; Elution pressure: 23 MPa; Injected sample volume: ~120 pL. Sample: 1 μM gly, 3 μM tyr, 3 μM ala, 3 μM arg, 10 μM trp and 2.5 μM phe. (B) nOTC: 2-μm-i.d. × 3.5-cm-length (2.7 cm effective) coated with C18; MA: 10 mM $NH_4HCO_3$; MB: 50% acetonitrile in 10 mM NH4HCO3; Mixer: Mixer 1 in Figure 3.2C; Elution pressure: 20 MPa; Injected sample volume: ~200 pL. Sample: 9 μM his, 1.5 μM gly, 4.5 μM ala, 1.5 μM arg, 10 μM trp and 3 μM phe. (C) nOTC: 2-μm-i.d. × 3.5-cm-length (2.7 cm effective) coated with C18; MA: 10 mM $NH_4HCO_3$; MB: 50% acetonitrile in 10 mM $NH_4HCO_3$; Mixer: Mixer 1 in Figure 3.2C; Elution pressure: 24 MPa; Injected sample volume: ~200pL. Sample: 1.5 μM arg, 10 μM trp and 2.5 μM phe.

These speeds could be further increased by raising the elution pressure and/or shortening the *n*OTC. In this work, we employed a Shimadzu LC-30AD pump. It was not recommended to use this pump above 30 MPa, and we usually used it below 28 MPa. Currently high-

pressure UPLC pumps are often operated at 70−100 MPa. Obviously, replacing the Shimadzu LC-30AD pump with an UPLC pump will enable us to increase the separation speed.

With the current LIF arrangement we could not shorten the effective length of a *n*OTC to less than 2.7 cm due to clearance requirement for optical alignment. This issue can be alleviated by using a microfabricated T to assemble the flow splitter; the *n*OTC length can be shortened conveniently to less than 1 cm if such a splitter is utilized. A reduced column length will lead to faster separations.

It is also possible to increase the separation speed by increasing the steepness of the gradient or elevating the separation temperature, but these approaches will not be as effective as raising the elution pressure or shortening the column length.

**3.6. Effect of Sampling Frequency on Resolution.**

For ultrafast separations (FWHM of ∼20 ms), adequate sampling frequency is important for retaining separation resolutions. For a Gaussian peak, FWHM = 2.355σ, where 2σ is the variance. Often, the full width of a Gaussian peak equals 4σ. In general, 10 to 20 data points are sufficient to define a peak. For our ultrafast separations, the sharpest peak had a fwhm of ∼20 ms or a full width of 34 ms. Therefore, the sampling frequency needed to be 300 to 600 Hz. As presented in Figure 3.7, resolutions were mostly retained at a sampling frequency of 250 Hz.

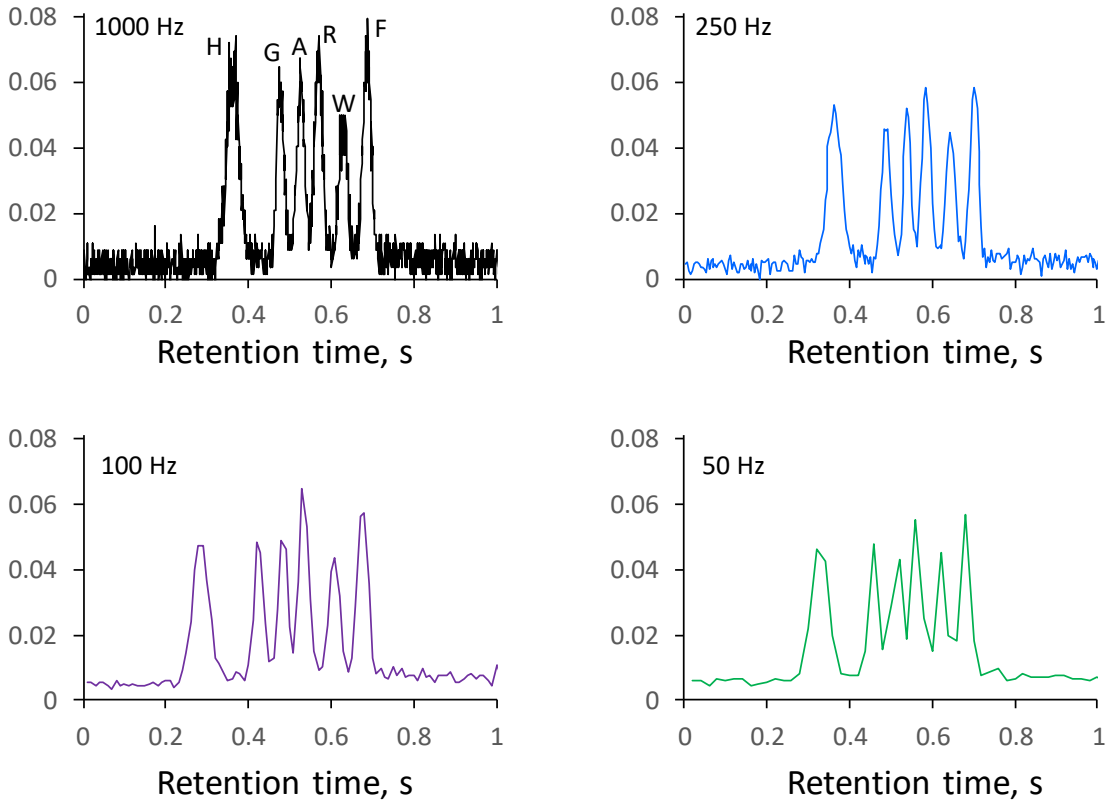


**Figure 3.7 Effect of sampling frequency on resolution**

*n*OTC: 2-µm-i.d. × 3.5-cm-length (2.7 cm effective). MA: 10 mM $NH_4HCO_3$. MB: 50% acetonitrile in 10 mM $NH_4HCO_3$. Mixer: Mixer 1 in Figure 3.2C. Elution pressure: 20 MPa. Injected sample volume: ~200 pL. Sample: 9 µM his, 1.5 µM gly, 4.5 µM ala, 1.5 µM arg, 10 µM trp and 3 µM phe.

The data acquisition program was developed in our lab more than a decade ago using LabView. The sampling frequency for the analog to digital converter (ADC) card was set at 1000 Hz, and a dialogue box was displayed on the screen so that a student could select a proper data output frequency (e.g., 1000, 500, 250, etc.) ≤ 1000. When a specific frequency was selected, for example 250 Hz, 4 data points from the card were averaged generating 1 data point for output. As can be seen in Figure 3.7, the baseline noise was reduced at lower data output frequency. In this ultrafast separation work, 1000 Hz was selected. If we wanted to reduce the noise, we could always average the data points afterward. However, it would be a good idea to select a reduced data output frequency to reduce the data file size for long sep-

aration runs.

### 3.7. Effect of Eluent Velocity on Resolution

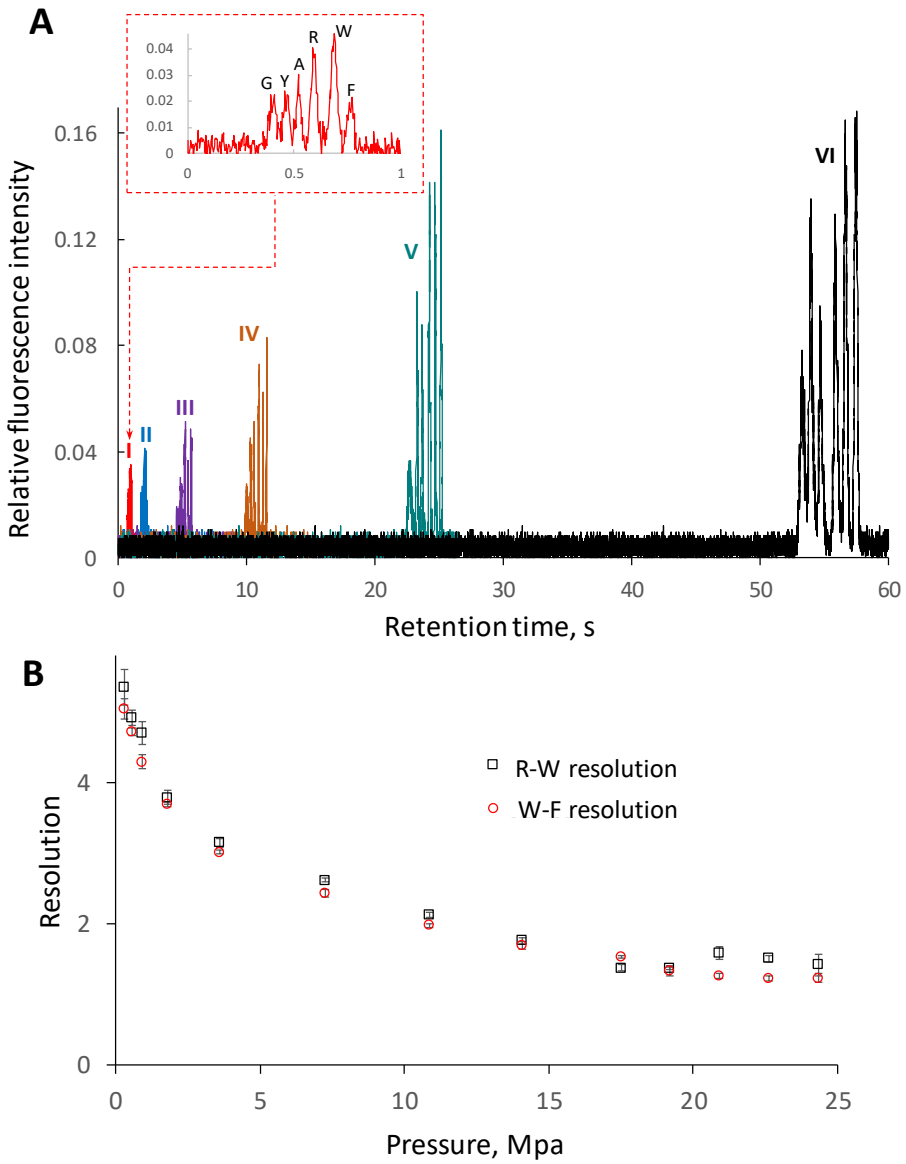


**Figure 3.8 Effect of elution pressure on resolution**

(A) Chromatograms of 6 separation runs under different elution pressures. *n*OTC: 2-μm-i.d. × 6-cm-length (2.7 cm effective) coated with C18; MA: 10 mM $NH_4HCO_3$; MB: 50% acetonitrile in 10 mM $NH_4HCO_3$; and Mixer: Mixer 2 in Figure 3.2C. From chromatogram I to chromatogram VI, the pump flow rates were 0.325, 0.20, 0.10, 0.05, 0.025 and 0.0125 mL·min$^{-1}$, corresponding to elution pressures of 23, 14, 7.2, 3.6, 1.8 and 0.9 MPa respectively. Gradient delay times were subtracted from the retention times. Injected sample volume: ~120 pL. Sample: 1 μM gly, 3 μM typ, 3 μM ala, 3 μM arg, 10 μM trp and 2.5 μM phe. (B) Effect of elution pressure on resolution. The resolutions were calculated from a series of the chromatograms, and only 6 of them were presented in (A).

A straightforward method to increase the separation speed is to increase the eluent ve-

locity or elution pressure. Figure 3.8A presents the chromatograms of 6 runs under different elution pressures: 23, 14, 7.2, 3.6, 1.8, and 0.9 MPa corresponding to 0.325, 0.20, 0.10, 0.050, 0.025, and 0.0125 mL·min$^{-1}$ of the HPLC pump rate, respectively. For these fast separations, the mobile phase velocity was relatively high (dozens mm·s$^{-1}$), and an increased speed usually came at a reduced resolution. Figure 3.8B presents the effect of elution pressure on resolutions, resolution declined with the elution pressure considerably.

### 3.8. Fast Separation for Trypsin-Digested Protein

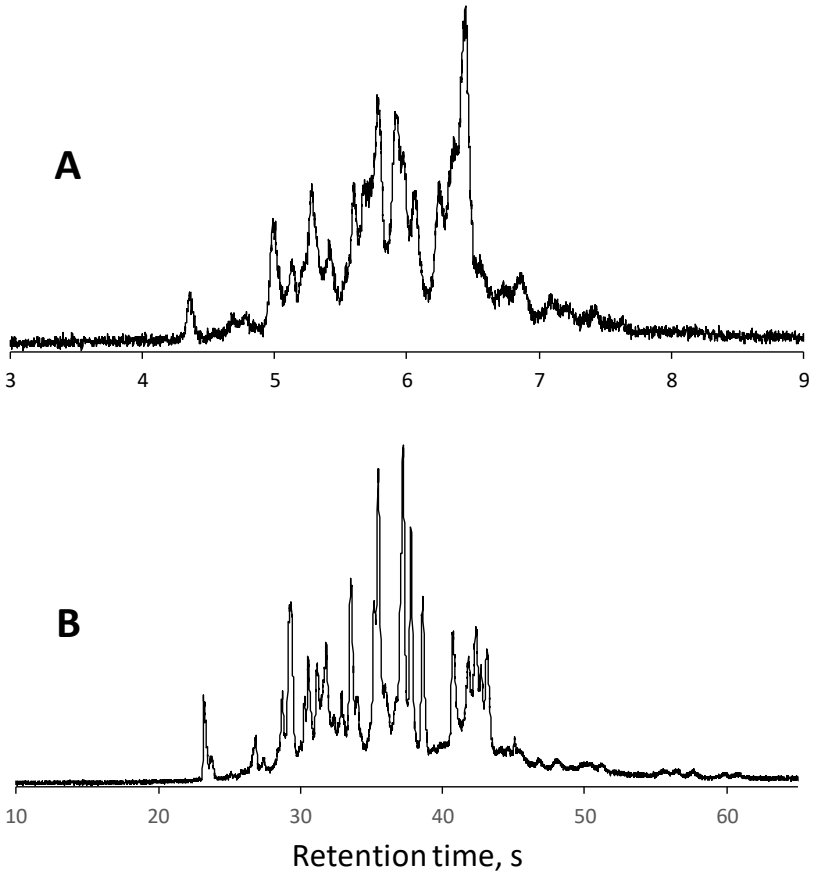


**Figure 3.9 Fast separation chromatograms for trypsin-digested cytochrome C**

(A) Chromatogram for separating trypsin-digested cytochrome C under an elution pressure of 1.4 MPa. *n*OTC: 2-μm-i.d. × 3.5-cm-length (2.7 cm effective) coated with C18; MA: 10 mM $NH_4HCO_3$; MB: 50% acetonitrile in 10 mM $NH_4HCO_3$; Mixer: Mixer 3 in Figure 3.2C; Sample: 10× diluted cytochrome C digests. Injected sample volume: ~200 pL. (B) Chromatogram for separating trypsin-digested cytochrome C under an elution pressure of 0.36 MPa. All other conditions were the same as in (B).

To demonstrate the potential of this ultrafast separation method for practical uses, we

used trypsin to digest a protein (cytochrome C). After the peptides were fluorescently labeled, they were separated using a 3.5 cm-long (2.7 cm effective) and 2-μm-i.d. *n*OTC, and the separation results were presented in Figure 3.9. Many peptides could be resolved under an elution pressure of 1.4 MPa, and the separation was completed in less than 10 s. Much better resolutions were obtained when the elution pressure was reduced to 0.36 MPa and the separation was completed in ~1 min. We also ran the separation under an elution pressure of 0.71 MPa, the resolutions were comparable to but slightly worse than that of Figure 3.9.

## 4. Conclusions

We have explored *n*OTLC for ultrafast LC separations and obtained sub-second separations routinely. We used a 2.7 cm (effective length) *n*OTC and baseline-resolved 6 amino acids in less than 700 ms. This speed could be further increased by raising the elution pressure and/or shortening the column length. To demonstrate the feasibility of this technique for practical applications, we separated a complex sample of protein digests; peptides were nicely resolved in ~1 min. Limited sample loadability has been a concern for *n*OTCs, but this issue seems to have been mitigated considerably with the detection technology advancement. Column lifetime has been examined for several hundred runs. To make *n*OTCs broadly accepted, the column lifetime needs to more than a thousand runs. Cautions must be taken to prevent *n*OTCs from clogging. A good feature of a *n*OTC is that clogging happens only at the column head and one can usually recover the column through back flushing. Once *n*OTLC is coupled with MS (we are working on it now), ultrafast *n*OTLC is expected to play an important role in high-speed and high-throughput analyses.

# Chapter 4: Performing Flow Injection Chromatography Using a Narrow Open Tubular Column

## 1. Abstract

Flow injection chromatography (FIC) or sequential injection chromatography (SIC) is a low-pressure LC technique that uses flow injection or sequential injection hardware. Due to the constraints of this hardware, the separation resolution is low; often no more than 3e5 components are resolved. We have recently demonstrated the excellent resolving power of *n*OTC for various biomolecules, and only moderate elution pressures are needed to carry out these separations. In this paper, we incorporate a *n*OTC with FIC and construct an FIC system using a pressure chamber and two injection valves to implement gradient elution. The resultant system not only improves the resolution but also reduces the system cost. When we use the system to separate peptides from trypsin-digested cytochrome C, we can resolve dozens of peptides (with resolutions of 0.5 or greater) at a speed of 12 samples per hour. When we use this system to separate a mixture containing 3 amino acids, we can base-line resolve these compounds at a speed of 1800 sample per hour.

## 1. Introduction

Flow Injection Analysis (FIA) is a technique for milli-to-micro scale solution manipulations in a controlled and automated fashion. The individual steps (e.g., sample/reagent metering, mixing, incubation, monitoring, conduit regeneration, etc.) are carried out in a liquid conduit network via various pumps and valves, and the pressures used to move the solutions within the conduits are usually no more than a few bars or a few dozen pounds per square

inch (PSI). With the first FIA paper published in 1975[124], it became an active research field in the analytical chemistry community during the 1980s and 1990s. Nowadays FIA is often abbreviated to FI to emphasize that it is a conceptual approach in addition to a means of performing analysis[125]. A sibling approach, Sequential Injection (SI) analysis, which uses bidirectional and stop flows to process samples and reagents on an intermittent and programmable flow, was introduced in 1990[126]. However, both FI and SI approaches share a common drawback – the incapability of performing chemical separation (e.g., multi-analyte separation or separation of an analyte from its interfering matrix) before chemical analysis.

Separations of complex samples are often achieved via using sophisticated instruments such as LC including HPLC, UPLC, CE, etc. Because HPLC or UPLC uses high-pressure pumps and conduits capable of sustaining these pressures, and because CE uses high voltage power supplies, these systems are generally incompatible with FI or SI manifolds. Satinsky *et al.*[127] for the first time incorporated a monolithic column with an SI manifold to perform chemical separations in an FI/SI system since a monolithic column required only a moderate-high pressure (a few MPa) to conduct the separations. These authors had since termed this SI and LC combination the Sequential Injection Chromatography (SIC). In the same year, Srisawang *et al.*[128] coupled FI with a diethylaminoethyl Sephadex column for hemoglobin (Hb) typing, and this approach was called FIC.

FIC/SIC is basically a low-pressure LC technique[129]. While isocratic elution has been utilized dominantly, gradient elution has been demonstrated[130] feasible. FIC/SIC has been applied for analyzing various samples including analytes of interests in beverages[129] and

pharmaceuticals[131]. Several papers[132-134] have been published reviewing the progress of this technique. FIC/SIC instruments have been commercially available and capable of handling pressures up to ~5.2 MPa. Although short monolithic columns (e.g., 25 mm × 4.6 mm) have been commonly used in order not to create high elution pressures, longer (e.g., 50 and 100 mm) and narrower (e.g., 2 – 3 mm)[135-137] monolithic columns, especially columns packed with 2.7 mm core-shell particle[137] are also proved feasible. However, FIC/SIC's separation speed, selectivity and efficiency cannot compete with HPLC or CE. In most cases, FIC/SIC systems have been used for separation of mixtures of not more than 3 – 5 components[133].

We have recently experimented OTLC using very small-inner-diameter OTCs and obtained ultrahigh resolutions and ultrahigh analysis speed for small molecules such as fluorescent dyes[33] and amino acids[10, 41, 42], to complex peptide mixtures[10, 42], and to large molecules such as proteins[37] and DNA[32, 34-36, 46, 58, 138]. The columns usually had inner diameters (i.d.) of around 1 – 5 μm and lengths of 0.5 – 1 m. The separations were frequently completed in a few seconds to a few minutes, while millisecond separations were demonstrated[10, 11]. Importantly, most separations were carried out under moderate elution pressures (a few MPa or lower). In this work, we report our initial progress of incorporating a *n*OTC with an FI setup to perform high-resolution and fast FIC. Compared with traditional FIC/SIC systems, the described system improved resolution and increased separation speed under a regular FIC/SIC pressure (a few MPa). We constructed a single-valve FIC system to perform isocratic elution and a dual-valve FIC system to perform gradient elution. We replaced the relatively expensive syringe pump in a traditional FIC/SIC system with a pressure chamber to reduce the cost.

Using the dual-valve FIC system, we separated mixtures containing 3 – 6 amino acids to mixtures containing dozens of peptides. Multiple analytes in a sample could be continuously monitored, and analysis speeds of up to 1800 sample per hour could be achieved for repetitive injections. For analyzing dozens of peptides or DNA fragments in complex mixtures, the analysis speed decreased, but still dozens of samples per hour were conveniently achieved. FIC/SIC with a *n*OTC is a promising candidate for high-throughput analyses.

## 2. Materials and methods

### 2.1. Reagents and materials

GeneRuler™ 1-kb plus DNA ladder (SM1331) was purchased from Fermentas Life Sciences Inc. (Glen Burnie, MD), and YOYO-1 was from Molecular Probes (Eugene, OR). Fluorescein sodium salt, amino acids, sodium hydroxide, ammonium bicarbonate, acetonitrile, toluene and tri-methoxy(octadecyl) silane were obtained from Sigma-Aldrich (St. Louis, MO). ATTO-TAG™ FQ Amine-Derivatization Kit, tris(hydroxymethyl)aminomethane (Tris), ammonium acetate, concentrated hydrochloric acid, and ethylenediaminetetraacetic acid (EDTA) was obtained from Thermo Fisher Scientific (Waltham, MA). All solutions were prepared using ultrapure water (Nanopure ultrapure water system, Barn-stead, Dubuque, IA) and filtered through a 0.22-mM filter (VWR, TX), degassed before use. 2-μm inner diameter (i.d.), 150-μm outer diameter (o.d.) fused-silica capillaries were purchased from Polymicro Technologies, a subsidiary of Molex (Phoenix, AZ).

### 2.2. *narrow* OT column preparation

The preparation procedure has been described previously[42]. Briefly, after 10 mm polyi-

mide coating at one end of a 2-mm-i.d. and 60 cm long capillary was removed, a 25 G × 7/8″ hypodermic needle was used as a guide to facilitate the insertion of the capillary through a septum into a pressure chamber holding a vial containing 100 mL 1 M NaOH solution. The other end (with polyimide coating) of the capillary was inserted into a waste container with DI water inside. Seven MPa was applied to the pressure chamber via a pressurized nitrogen line to push NaOH solution through the capillary. This process lasted for 1 h in an oven at 75 °C. The NaOH solution vial was then replaced with a DDI water vial to rinse the capillary at room temperature and under a pressure of 7 MPa for 1 h. The DDI water vial was replaced with an empty vial, and 7 MPa was applied again for 1 h to dry the capillary.

The coating setup was then moved inside a dry glove box. The coating reagent, a mixture of 75 mL OTMS and 25 mL toluene was prepared in the dry glove box and placed inside the pressure chamber. The polyimide-removed end of the capillary was inserted in the pressure chamber with the tip sub-merged in the coating reagent. Seven MPa nitrogen was then applied to the pressure chamber, and the whole setup was moved to an oven at 75 °C. After 18 h, the coating reagent was replaced with an empty vial and 7 MPa nitrogen was applied again for 1 h.

### 2.3. Preparation of Eluent and Standard DNA Samples

Ten mM Tris-EDTA (TE) buffer, composed of 10 mM Tris-HCl and 1.0 mM $Na_2EDTA$ at pH 8.0, was prepared using DDI water from a NANO pure infinity ultrapure water system. Before being used, the solution was filtered through a 0.22-μm filter (VWR, TX) and vacuum-degassed. This solution was used as the eluent as well. The stock solution of 100 $ng \cdot \mu L^{-1}$

1-kb plus DNA ladder was prepared by mixing 39 μL 10 mM TE buffer, 10 μL 500 ng·μL$^{-1}$ DNA, and 1 μL YOYO-1. All working DNA solutions were made by diluting the stock solution with DDI water. Eluent and DNA samples were stored at 4 ℃.

**2.4. Preparation of DNA Tandem Repeats**

Bioethanol Saccharomyces cerevisiae strains, CAT-1 and BG-1, were kindly supplied by Drs. Ana Teresa B. F. Antonangelo and Debora Colombi at San Paulo State University in Brazil. We first grew these strains in 10 mL yeast peptone dextrose (YPD) medium for 12 – 16 h at 30 ℃ until A600 of culture reach to 0.6 – 0.8. DNA of yeast cultures were extracted using Yeast Genomic DNA Purification Kit (AMRESCO, LLC, Solon, OH). The amplification of tandem DNA marker, G4, was conducted following the method as described in the literature[139]. Briefly, 50 μL polymerase chain reaction (PCR) solution contained 100 ng genomic DNA, 10 μL of 5 × Reaction Buffer, 800 μM *d*NTP mix (200 μM each), 0.2 μM of each forward and reverse primer for locus G4 (forward primer: 5′-AACCCATT-GACCTCG-TTACTATCGT-3 ′; reverse primer: 5′-TTCGATGGCTCTGA-TAACTCCATTC-3′), 5 units of *Tfi* DNA polymerase (Invitrogen, Carlsbad, CA), and 1.5 mM of $MgCl_2$. PCR reaction was proceeded by denaturing at 94 ℃ for 5 min, cycling temperatures for 14 cycles from 94 ℃ for 15 s, to 60 ℃ for 30 s (this temperature was decreased by 1 ℃ for every cycle), and to 72 ℃ for 30 s, cycling temperatures for 25 cycles from 94 ℃ for 15 s, to 48 ℃ for 30 s, and to 72 ℃ for 30 s, and maintaining the temperature at 72 ℃ for 5 min. The amplified products were confirmed by slab gel electrophoresis.

### 2.5. Peptide Sample Preparation

To prepare tryptic digests of cytochrome C, 100 μL of 10 $mg \cdot mL^{-1}$ cytochrome C stock solution was diluted to 1 $mg \cdot mL^{-1}$ with 25 mM $NH_4HCO_3$, mixed with 1 mL of 1 M DTT and stayed at room temperature for 1 h. Then the mixture was reacted with 10 μL of 0.2 $mg \cdot mL^{-1}$ trypsin solution at 37 ℃ for 24 h.

### 2.6. Amino Acid and Peptide Fluorescence Labelling

Following the instruction provided with the ATTO-TAG™ FQ Amine Derivatization Kit by the manufacturer, a 10 mM working KCN solution was first prepared by diluting a 0.2 M KCN stock solution with 10 mM borax solution (pH 9.2). Amino acid stock solutions (each containing 5 mM of one amino acid) were prepared by dissolving individual amino acids in DDI water and filtered with 0.22-mm filter. A volume of 5.0 mL of the amino acid stock solution was mixed with 15 μL of the 10 mM KCN working solution and 5 μL of the 10 mM FQ solution in a 0.25-mL vial. This mixture was maintained at room temperature for 1 h in dark before separation. To label tryptic digests of cytochrome C, 5 μL of the peptide solution was mixed with 15 μL of 10 mM KCN working solution and 10 μL of the 10 mM FQ solution. After 1-h reaction in dark at room temperature, the peptides were ready for dilution (with 10 mM $NH_4HCO_3$) and separation.

## 2.7. Apparatus

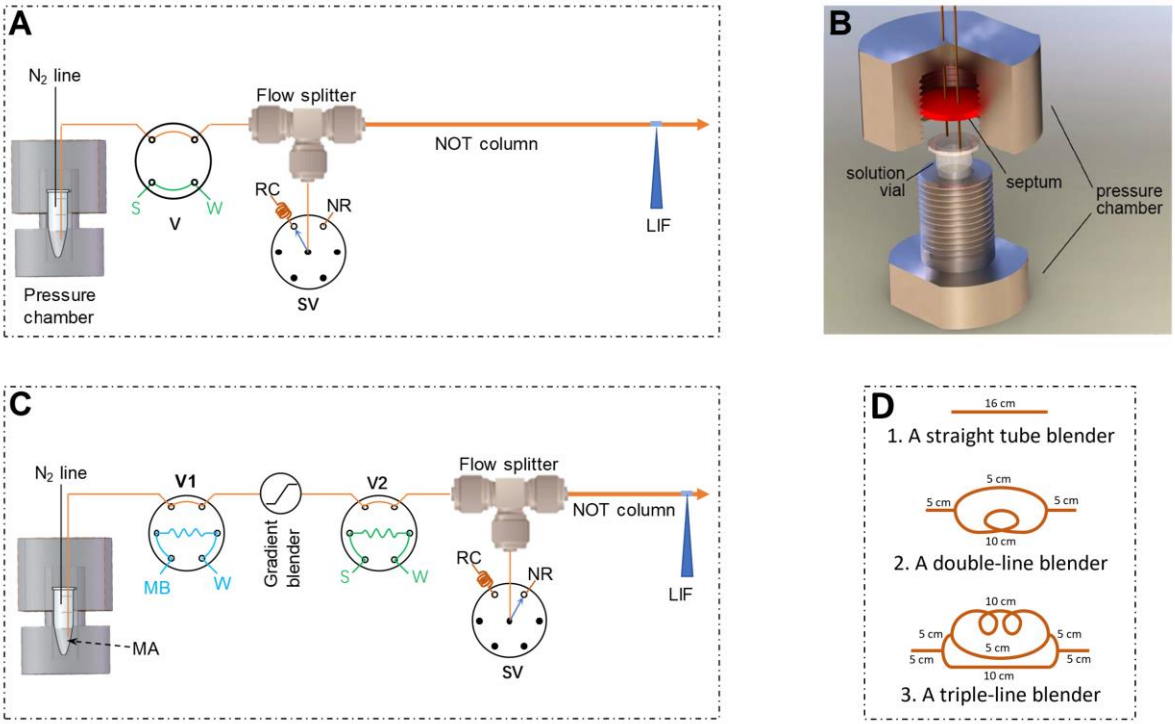


**Figure 4.1 FIC apparatus schematic configurations**

The *n*OTC had an i.d. of 2 μm and a length of 47 cm (41 cm effective). V was a 60-nL injection valve. The capillary connecting V and the flow splitter had an i.d. of 75 μm and a length of 6 cm. The flow splitter was connected to the restriction capillary (RC) via a selection valve. RC had an i.d. of 20 μm and a length of 6.5 cm, while NR (no restriction) had an i.d. of 200 μm and a length of 1 cm. The selection valve (SV) could be switched between RC and NR (no restriction). When the selection valve was connected to RC, a portion of the solution from V2 could flow through the *n*OTC, while no solution would enter the column if the selection valve was connected to NR. The carrier solution was 10 mM tris-EDTA buffer at pH 8.0. An elution pressure 2.5 MPa was applied for the separation. (B) Schematic rendering of pressure chamber. (C) Apparatus for gradient elution. The *n*OTC had an i.d. of 2 μm and a length of 3.5 cm (2.7 cm effective) coated with C18. MA was 10 mM $NH_4HCO_3$. Two injection valves (V1 and V2) were included in this system; V1 was used for mobile phase B (MB, 50% acetonitrile in 10 mM $NH_4HCO_3$) injection and V2 for sample injection. The external loop on V1 had a volume of 20 μL, while loop on V2 had a volume of 2.7 μL. A blender was inserted between V1 and V2 to smooth the gradient profile. Other parameters and conditions are provided in relevant figure legends. (D) Schematic designs of three gradient blenders.

Two apparatus configurations were used in this work. Figure 4.1A presents the apparatus used for isocratic elution. A pressure chamber was used to drive a mobile phase through a 6-port sample injection valve (V) (VICI Valco, Houston, TX), via a flow splitter, to a *n*OTC. Figure 4.1B presents a detailed structure of the pressure chamber. The detection end of the

column was affixed to a capillary holder on an x-y-z translation stage (not shown) so that the detection window could be aligned with the LIF detector for maximum fluorescence output. Figure 4.1C presents the apparatus used for gradient elution. An additional injection valve was included in this setup to produce a gradient eluent. Various gradient blenders (Figure 4.1D) were tested to achieve desired gradient profiles for improved resolutions. A confocal LIF detector, as described previously[60], was employed to monitor the resolved analytes. Briefly, an argon ion laser (Laser-Physics, Salt Lake City, UT) generated a 488-nm laser beam. The laser beam was directed by a dichroic mirror (Q505LP, Chroma Technology, Rockingham VT) and focused onto the detection window of the *n*OTC via an objective lens (20 × and 0.5 NA, Rolyn Optics, Covina, CA). The emission of fluorescence was collimated by the same lens, passed through the same dichroic mirror, an interference band-pass filter (532 nm, Carlsbad, CA) and a 1-mm pinhole, and finally collected by a photosensor module (H5784-04, Hamamatsu). A data acquisition card USB-1208FS (Measurement Computing, Norton, MA) was used to measure the response from the photosensor module as voltage signal. The data were collected and analyzed by a home-made LabView program (National Instruments, Austin, TX).

**2.8. FIC operation**

Referring to Figure 4.1A, it was straightforward for performing isocratic FIC. After the system was initialized, a carrier solution was pressurized into the system through the pressure chamber. It could take a few minutes for the background signal to be stabilized. A sample was then loaded in V while V was set at the position as shown in Figure 4.1A (the “Load” posi-

tion), and the sample was injected into the carrier stream by switching V to the other (the "Inject") position. The 60 nL sample was defined by the internal groove on the valve rotor; there was no external loop in this valve. One minute after the injection, V was switched back to the "Load" position to load another sample. After a preset period (4.5 min in this work) following the previous injection, another sample was injected for FIC. If the *n*OTC was clogged (rarely occurred in this work), we could set the selection valve to NR position, increase the chamber pressure and/or backflush the column.

| | Step # (Time in s) | Operation parameter or event | | | |
|---|---|---|---|---|---|
| | | Chamber pressure, MPa | V1 position | V2 position | SV position |
| For trypsin-digested cytochrome C FIC | Step 1 (0) | 7 | Load | Load | NR |
| | Step 2 (10) | $7 \rightarrow 2^a$ | Load | Load | NR |
| | Step 3 (45) | 2 | Load | Load | RC |
| | Step 4 (50) | 2 | Inject | Inject | RC |
| | Step 5 (150) | Go back to Step 1 | | | |
| For six amino acid FIC | Step 1 (0) | 20 | Load | Load | RC |
| | Step 2 (6) | 20 | Inject | Inject | RC |
| | Step 3 (8) | Go back to Step 1 | | | |
| For three amino acid FIC | Step 1 (0) | 24 | Load | Load | RC |
| | Step 2 (1) | 24 | Inject | Inject | RC |
| | Step 3 (2) | Go back to Step 1 | | | |

**Table 1 List of operation parameters or events during FIC**

Gradient FIC was performed on the apparatus shown in Figure 4.1C. A controller was used to control the activation of both V1 and V2. Mobile phase B (MB, 50% acetonitrile in 10 mM $NH_4HCO_3$) and sample solutions were loaded by pressurizing these solutions into the injection loops under ~0.4 MPa. For FIC separations of the three-amino-acid mixture, RC had an i.d. of 50 μm and a length of 70 cm, and the straight-tube blender was used. For FIC separations of the six-amino-acid mixture, RC had an i.d. of 50 μm and a length of 70 cm, and the triple-line blender was utilized. For FIC separations of trypsin-digest cytochrome C, RC had

an i.d. of 50 μm and a length of 140 cm, and the triple-line blender was utilized. Other parameters and experimental conditions were provided in relevant figure legends. Table 1 lists the operation parameters or events for repetitive FIC analyses after the system initialization.

## 3. Results and discussion

### 3.1. Isocratic FIC

Fig. 2 presents a typical FIC trace for DNA fragment separation, and this experiment was carried out using the apparatus shown in Figure 4.1A. For DNA separations, the *n*OTC was uncoated because the separation mechanism was hydrodynamic chromatography (HDC)[32, 46, 58]. The 1-kb plus DNA ladder consisted of 15 fragments (20, 10, 7, 5, 4, 3, 2, 1.5, 1, 0.7, 0.5, 0.4, 0.3, 0.2, and 0.075 kilo base pairs, with relative concentrations of 4, 4, 4, 15, 4, 4, 4, 16, 5, 5, 15, 5, 5, 5, and 5%, respectively). A super good thing about HDC was that the column did not require regeneration. Therefore, the FI carrier stream could be used conveniently as a mobile phase. A large number of samples could be analyzed continuously, as long as the chromatogram data could be properly stored. For the chromatogram in Figure 4.2, the first five peak groups were from injections of five DNA ladder solutions having increasing total-DNA-concentrations from 5 to 100 ng·μL$^{-1}$; the peaks in the first group were expanded and displayed in the inset and the number near each peak indicated the size of the fragment in base pairs (bp). The three peak groups after these standards were for two genomic samples (two injections of locus G4 CAT-1 and one injection of BG-1 of *S. cerevisiae* strain); expanded peaks were exhibited in the insets. The last peak group was from a reinjection of the 10 ng·μL$^{-1}$ DNA ladder.

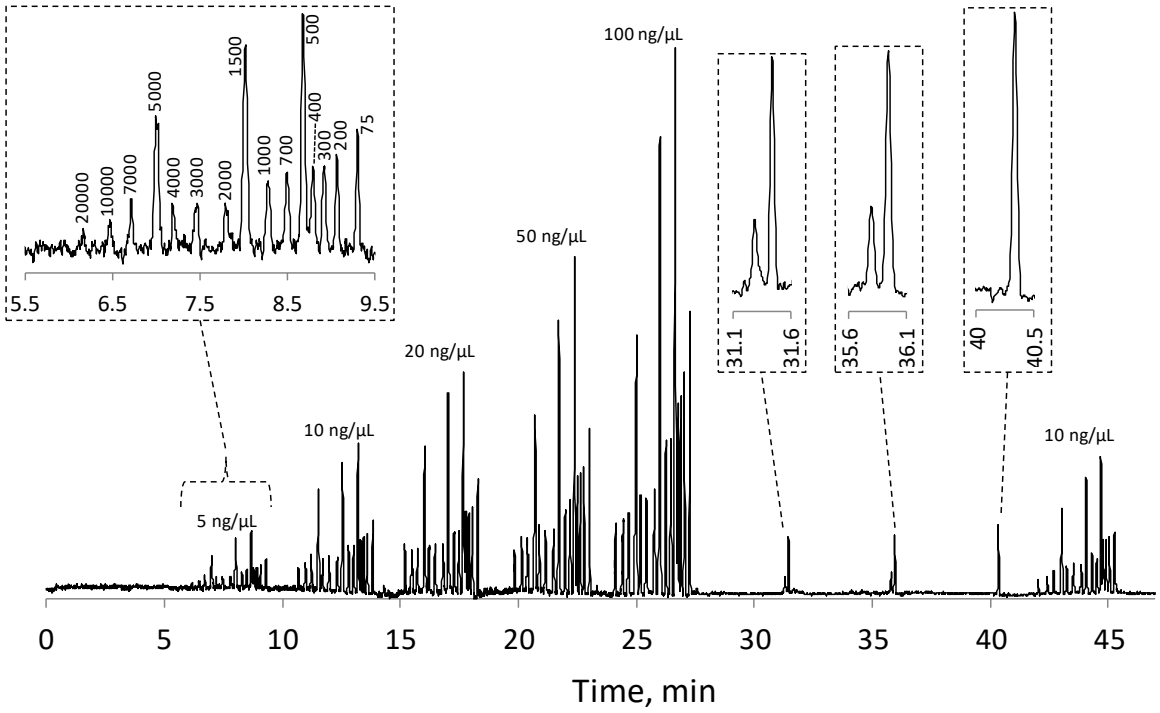


**Figure 4.2 Typical FIC trace for DNA separation**

*n*OTC was an uncoated capillary with an i.d. of 2 µm, an o.d. of 200 µm, and a total length of 47 cm (41-cm effective length). The restriction capillary had an i.d. of 20 µm with a length of 3.5 cm. The sample volume injected into the *n*OTC for each separation was ~0.85 pL. The eluent was 10 mM Tris-EDTA buffer at pH 8.0. An elution pressure of 2.5 MPa was applied to execute the separation. Solutions of a DNA ladder at five different concentrations were successively injected to produce the first five peak groups. The total DNA concentration was indicated on the top of each peak group. The peaks after these ladder standards were for two genomic samples (locus G4 CAT-1 and BG-1 of S. cerevisiae strain). The last peak group was from a reinjection of 10 ng·µL$^{-1}$ DNA ladder. The sample injection/measurement frequency was one injection/measurement every ~4.5 min. The peak heights in the insets were all magnified by a factor of ~4.

As can be seen from the inset of the DNA ladder separation, the time between the first peak (20,000 bp) and the last peak (75 bp) is ~3.5 min. That means that we must wait for more than 3.5 min between injections, otherwise the last peak from the previous injection would overlap with the first peak from the next injection. We selected a waiting period of 4.5 min (the sensor response time) between injections, leaving at least 1 min gap between peak groups. This gap was wider when a sample contained DNA fragments having a narrower size range than the ladder.

Two kinds of calibration curves will be generated from the data in Figure 4.2: DNA size

vs retention time and fluorescence intensity (peak area) vs DNA concentration. DNA size is a function of retention time but not a linear relationship[32, 34, 35]. The theoretical study of this relationship was published previously[32]; the retention time of a DNA fragment in the *n*th injection = the peak time - 4.5 × (n-1). The relationship between fluorescence intensity and DNA concentration was validated using standard DNA fragment solutions[138]. Using the two calibration curves from first five FIC peak groups, the lengths and concentrations of the two fragments in the heterozygotes were estimated to be respectively 0.26 ± 0.02 and 0.38 ± 0.02 kbp and 0.15 ± 0.04 and 0.55 ± 0.06 ng·μL$^{-1}$, and the length and concentration of the fragment in the homozygote were estimated to be 0.36 ± 0.01 kbp and 0.73 ± 0.07 ng·μL$^{-1}$.

### 3.2. Gradient FIC

To achieve the best performances, LC separations are usually performed under gradient elution conditions, and gradient conditions are especially desired for separating complex biological samples[140]. Gradient FIC/SIC have been implemented using a syringe pump combined with a selection valve or multiple-pump systems[130, 141-143]. Here we present an economic approach (Figure 4.1C) to perform gradient FIC. In this system we employed an MB injection valve and a sample injection valve. When sample and MB were injected at the same time, the sample plug moved in front of the MB plug. Because the sample was carried forward by MA (the carrier solution, 10 mM $NH_4HCO_3$), analytes were stacked at the head of the *n*OTC. As the MB plug moved forward, the MA-MB mixing at the interface formed a gradient. As this gradient reached the *n*OTC, it eluted the analytes forward and analytes were resolved based on a reversed-phase LC mechanism. Adding a blender between V1 and V2 could tune the

MA-MB mixing and hence vary the gradient profile. Figure 4.3 presents three gradient profiles using the blenders as shown in Figure 4.2D.

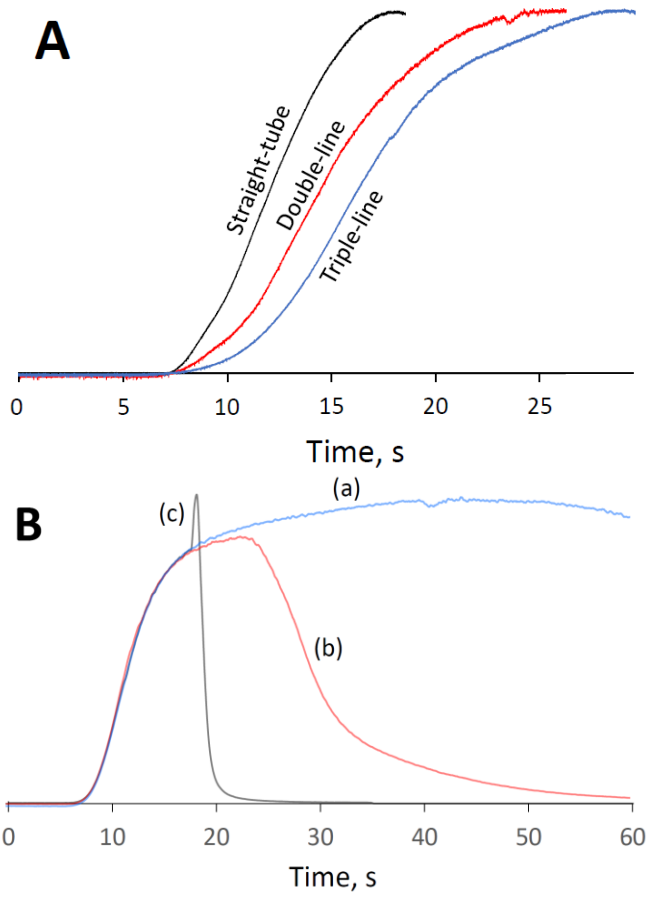


**Figure 4.3 Gradient profiles with different blenders and different valve/pump operations**

(A) Gradient profiles produced using three different blenders. This test was performed on the apparatus as shown in Figure 4.1C. While SV was connected to RC (50 μm × 70 cm), 10 mM $NH_4HCO_3$ was driven forward under a chamber pressure of ~7 MPa. After 1 μM fluorescein was injected into the system via V1, a fluorescence signal profile was produced; three profiles were produced using the three blenders as exhibited in Figure 4.1D. The three profiles were normalized and the traces after the maxima were eliminated. (B) Gradient profiles produced by changing the operations or varying the operation parameters. This test was performed using a straight-tube blender. Curve (a) was obtained by loading 1 μM fluorescein in the external loop on V1, injecting the fluorescein into the system, and recording the fluorescence signal on the *n*OTC; curve (b) was obtained by loading 1 μM fluorescein in the external loop on V1, switching V1 to inject the fluorescein into the system and quickly (10 s later) switching V1 back to the loading position, and recording the fluorescence signal on the *n*OTC; curve (c) was obtained by loading 1 μM fluorescein in the external loop on V1, switching V1 to inject the fluorescein into the system and quickly (10 s later) switching V1 back to the loading position, increasing the pump rate (from 25 μL·min$^{-1}$ to 250 μL·min$^{-1}$) immediately after V1 was switched to the loading position, and recording the fluorescence signal on the *n*OTC. All other conditions were the same as in (A).

To avoid interferences from residual MB, we must drive MB out of the column (to re-

equilibrate the column) between injections. Curve (a) in Figure 4.3B presents the MB concentration as a function of time if a simply inject MB and leave V1 at the injection position; it took several minutes for the gradient to go back to the injection conditions, and the analysis time could not be shorter than that. There were two approaches to suppress the interferences of residual MB. The first approach was to switch V1 back quickly after MB injection. As shown in Figure 4.3B curve (b), V1 was switched back 10 s after MB injection; MB concentration went down to near zero in ~1 min. The second approach was to do the same as the first one while increasing the pump rate and switching SV to NR position simultaneously after V1 was switched back to loading position. As exhibited in Figure 4.3B curve (c), MB concentration could go down to the sample injection conditions in a couple of seconds. There was a signal intensity surge after the pump rate was increased, presumably due to the reduced photobleaching.

To increase the resolution and measurement speed for gradient FIC, we used a 3.5-cm (2.7-cm effective) *n*OTC, 1.5 MPa chamber pressure (or elution pressure) and a triple-line blender for separating an enzyme-digested protein sample – a representative sample for bioanalysis. Figure 4.4A presents the FIC results for 4 repetitive injections. In this test, we used relatively low chamber pressure (1.5 MPa) to execute the separation to achieve good resolutions. Under this low pressure, the MB gradient (especially its tailing portion) moved slowly in the system. Therefore, the chamber pressure was elevated to 7 MPa to rinse the system with MA before the next injection was executed. The red trace in Figure 4.4A presents the gradient profile, which was measured separately using a procedure as described previously[10].

The final measurement/injection frequency was one sample every 2.5 min or 12 samples·h$^{-1}$. Figure 4.4B and C present the expanded traces for the second and the fourth injections. These separations were reproducible, and each measurement resolved more than two dozen peptides.

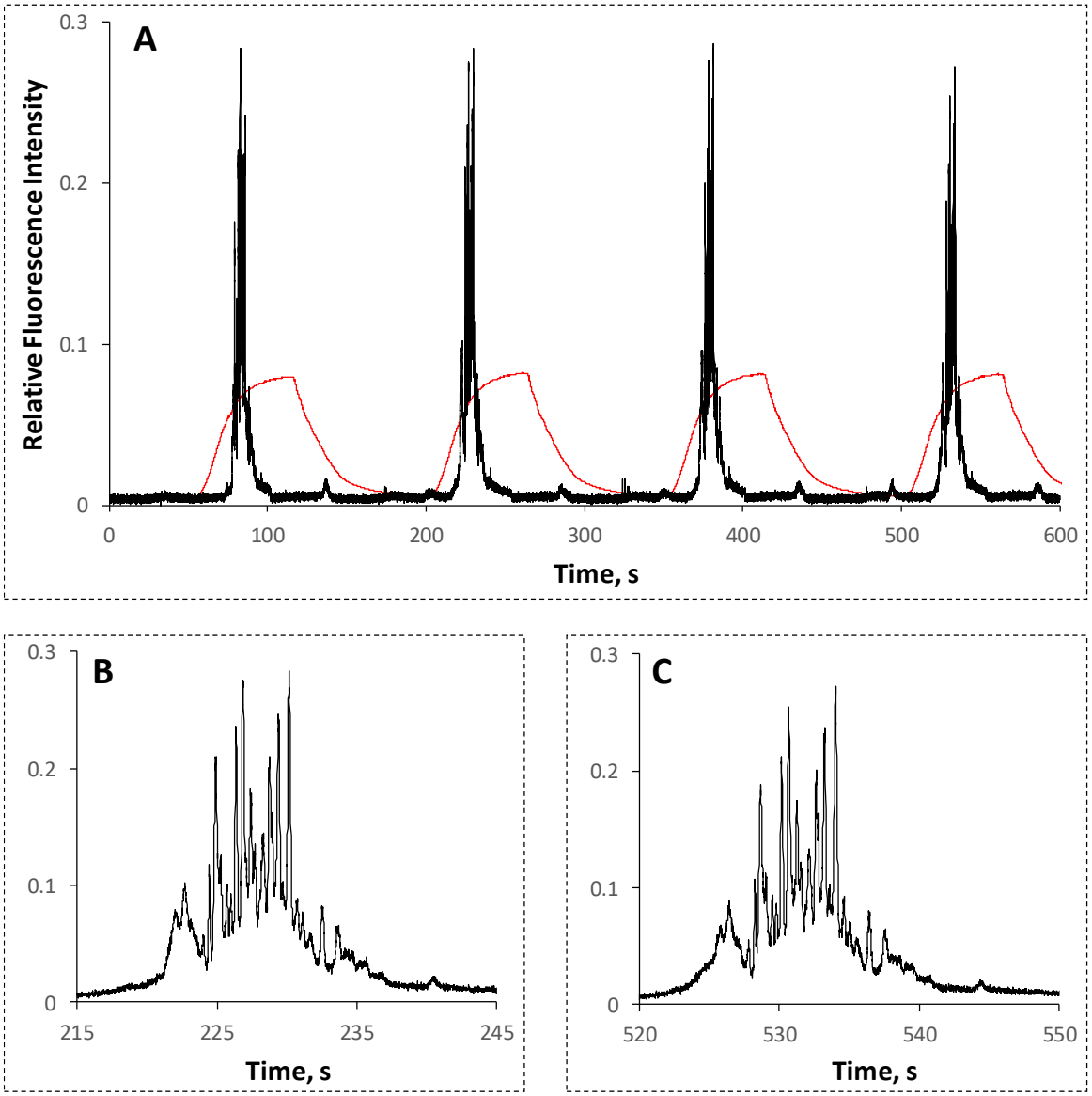


**Figure 4.4 A FIC trace with four repetitive injections and two zoomed-in chromatograms**

The *n*OTC coated with C18 had an i.d. of 2 μm and a length of 3.5 cm (2.7 cm effective). RC had an i.d. of 50 μm and a length of 140 cm, and the triple-line blender was utilized. MA was 10 mM $NH_4HCO_3$, MB was 50% acetonitrile in 10 mM $NH_4HCO_3$, and the red trace indicated the gradient profile. The peptide (trypsin-digested Cytochrome C) sample was diluted 40 times for this test; the final solution contained 4.2 ng·mL$^{-1}$ cytochrome C. The volume of sample injected to the *n*OTC was estimated to be ~400 pL. The FIC operations were presented in Table 1. Other parameters and conditions were provided in the Experimental Section.

### 3.3. Fast FIC separation

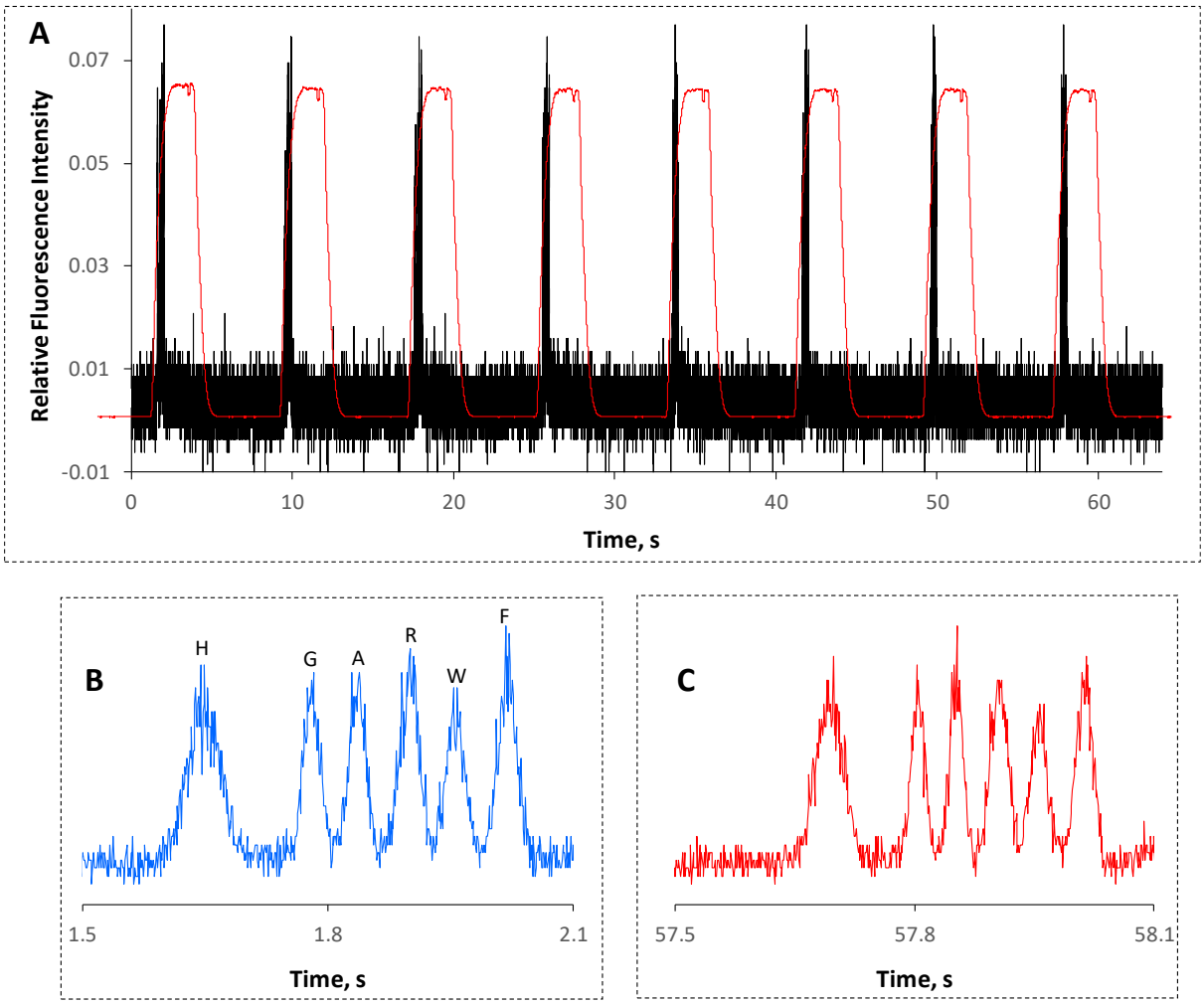


**Figure 4.5 FIC trace for six-amino-acid mixture**

RC had an i.d. of 50 μm and a length of 70 cm. The sample contained 9 μM his, 1.5 μM gly, 4.5 μM ala, 1.5 μM arg, 10 μM trp and 3 μM phe. Volume of sample injected to the *n*OTC was estimated to be ~200 pL. The chamber pressure was 20 MPa. The red trace indicated the gradient profile. The FIC operations were presented in Table 1. All other conditions were the same as in Figure 4.4.

To demonstrate fast FIC, we flowed a mixture of six amino acids through V2 continuously and analyzed the mixture once every 8 s under a chamber pressure of 20 MPa. Figure 4.5A presents the results. Peak groups were nicely separated. However, the triple-line blender made the gradient tailing significantly. If we increased the measurement frequency to one sample every 6 s, the histidine could not be properly stacked at the head of the *n*OTC due to the residual MB in the carrier stream. Figure 4.5B and C present the first and the last peak

groups, exhibiting baseline-resolution for all six amino acids. These separations were reproducible; the relative standard deviation of the retention times was <3%, while the relative standard deviation of the peak areas was ~5%.

To further increase FIC's measurement speed, we replaced the triple-line blender with a straight tube blender (see Figure 4.1) and removed H, A and W from the sample in Figure 4.5B. Fig. 6 presents the results; a measurement frequency of one sample every 2 s or a sampling throughput of 1800 samples·$h^{-1}$ was achieved.

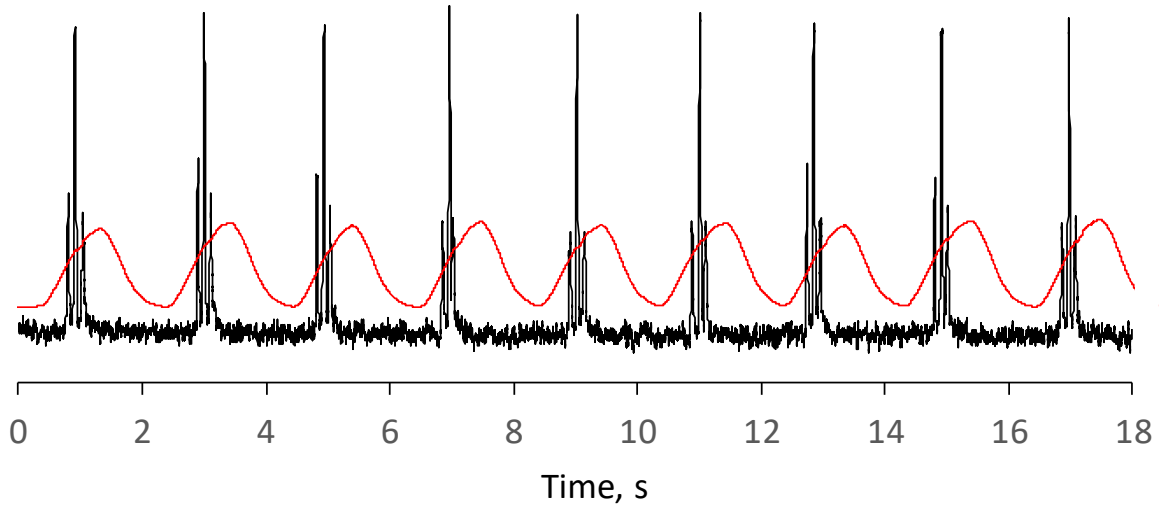


**Figure 4.6 FIC trace for three-amino-acid mixture**

A straight-tube blender was installed between V1 and V2. The sample contained 2 μM gly, 6 μM arg, and 6 μM phe. The chamber pressure was 24 MPa. The red trace indicated the gradient profile. The FIC operations were presented in Table 1. All other conditions were the same as in Figure 4.5.

## 4. Conclusion

We have incorporated a *n*OTC with a FIC setup and demonstrated the improvements in both resolution and measurement speed. In particular, we have constructed a dual-valve FIC system to perform fast gradient separation. For samples containing 3 – 6 amino acids, all amino acids can be resolved in sub-second. For separating dozens of peptides or DNA fragments in complex mixtures, the measurement speed was commonly several to dozens of sam-

ples per hour. A major challenge toward making FIC/SIC practically useful is to develop a miniaturized universal detector; electrochemical or miniaturized MS detectors are promising candidates. Once FIC/SIC is integrated with these detectors it will have great impact on high-throughput drug screening and pharmaceutical analysis. It will also facilitate 2D LC separations; its high speed and low sample consumption make it an excellent candidate for the 2nd-D separation.

# Chapter 5: Picoflow Liquid Chromatography−Mass Spectrometry for Ultrasensitive Bottom-Up Proteomics Using 2-μm-i.d. Open Tubular Columns

## 1. Abstract

In many areas of application, key objectives of chemical separation and analysis are to minimize the sample quantity while maximizing the chemical information obtained. Increasing measurement sensitivity is especially critical for proteomics research, especially when processing trace samples and where multiple measurements are desired. A rich collection of technologies has been developed, but the resulting sensitivity remains insufficient for achieving in-depth coverage of proteomic samples as small as single cells. Here, we combine picoliter-scale liquid chromatography (picoLC) with MS to address this issue. The picoLC employs a 2-μm-i.d. OTC to reduce the sample input needed to greatly increase the sensitivity achieved using ESI with MS. With this picoLC-MS system, we show that we can identify ∼1000 proteins reliably using only 75 pg of tryptic peptides, representing a 10−100-fold sensitivity improvement compared with the state-of-the-art LC or CE-MS methods. PicoLC-MS extends the limit of separation science and is expected to be a powerful tool for single cell proteomics.

## 1. Introduction

Proteomics typically aim to, as broadly as possible, identify and quantify expressed proteins (and often their post-translational modifications) in a biological sample and is increasingly transforming biological and medical research.[144, 145] In a typical shotgun proteomics

workflow, proteins are extracted from tissues and digested into peptides by trypsin. These peptides are separated by high-resolution LC and sequenced by tandem MS (i.e., MS/MS).[146] Advances in nanoflow LC and MS have significantly improved both the sensitivity and the throughput of proteomic measurements;[147] often >10,000 proteins can be reliably identified and quantified in common proteomics laboratories with reasonable time and cost.[148] However, significant sample quantities are required for such studies (typically >1 μg), precluding the analysis of trace samples (e.g., single cells). Unlike genomics and transcriptomics with amplification methods available, proteomic measurements largely depend on the efficiency of the sample processing workflow and the LC-MS platform sensitivity.

The rapid progress of LC-MS platforms and sample preparation approaches have made single cell proteomics feasible. The increased efficiency of ESI at decreasing flow rates combined with the advances in MS instrumentation (e.g., Orbitrap[149] based), and incorporating the ion funnel and related technologies, have served to significantly improve the sensitivity of mass analyzers.[149] Advanced ESI sources, such as nanospray and sub-ambient-pressure ionization source,[150] have allowed for >50% of analytes initially in solution phase to be transmitted to the MS detector. The flow rate and separation efficiency of LC are dominant factors determining the overall sensitivity of LC-MS. Shen *et al.*[65] observed the minimization of packing column i.d. from 75 to 15 μm, corresponding to reducing flow rates from 300 $nL \cdot min^{-1}$ to 20 $nL \cdot min^{-1}$, significantly increasing peptide detection sensitivity, allowing detection of 10 zmol (~6000 molecules) from a protein digest.[65] We previously demonstrated that the use of a 30-μm-i.d. column can increase protein identification by 95% for 0.5 ng tryptic

digest equivalent to ~3 mammalian cells, compared with a 75-μm-i.d. column.[72] Similarly, Ivanov and co-workers[151] developed porous-layer OTCs with an i.d. of 10 μm and an operation flow rate of 20 nL·min$^{-1}$ that enabled identification of 1800 proteins from diluted samples equivalent to 50 MCF-7 cells. In addition to low flow rates, Stadlmann *et al.*[152] showed that the use of microfabricated pillar array columns can greatly improve separation efficiency and provide increased proteome coverage for low-input samples. Regarding proteomic sample preparation, efforts have increasingly focused on reducing adsorptive sample losses while maintaining compatibility with the downstream LC-MS analysis. For example, we developed a microfluidic platform, termed nanoPOTS (Nanodroplet Processing in One pot for Trace Samples),[153, 154] for low-input (e.g., single cell) proteomics by downscaling sample preparation in microfabricated nanowells to total volumes of <200 nL. We demonstrated that nanoPOTS allowed >3000 proteins to be quantitatively profiled from as few as 10 HeLa cells[153] and >600 proteins from a single HeLa cell.[154] Despite these advances, the single cell proteomics coverage is still insufficient (~5% of the total proteome), and most biologically interesting proteins of low-to-moderate abundance are not detected, highlighting the necessity to further improve sensitivity after sample preparation (i.e., in the LC-MS analysis).

As it is technically difficult to pack small i.d. capillary columns, several groups have focused on developing OTLC columns with i.d. < 10 μm. Hara *et al*. developed[95] 5-μm-i.d. OTLC columns with sol−gel coated mesoporous silica layers. High separation efficiency with plate height of ~3 μm was obtained. Based on previous theoretical studies,[5] the inner diameter (i.d.) of the OTC should be in the range of 1−2 μm to achieve ultrahigh efficiency. How-

ever, due to various challenges in utilizing such *n*OTCs (e.g., column preparation, low sample loading capacity, sensitive detection, etc.), the ultrahigh efficiency was not obtained in the intervening ~4 decades. With technological advances and efforts, we have now overcome these challenges and validated the theoretical predictions by developing *n*OTLC with 2-μm-i.d. columns.[41, 43] We have recently demonstrated that *n*OTLC can yield ultrahigh peak capacities (>2000 in 3 h) and ultrahigh sensitivities (sub-attomole limit of detection) using fluorescence detection.[11]

In this paper, we report our progress toward significantly increasing proteomic sensitivity using a picoflow liquid chromatography mass spectrometry (picoLC-MS) system. A *n*OTC[5, 11] with 2 μm i.d. was employed for high-resolution separations at a flow rate of ~790 pL·min$^{-1}$. By coupling the picoLC with an Orbitrap MS, we show that ~1000 proteins can be reliably identified using only 75 pg tryptic peptides, representing over 10−100-fold improvement in sensitivity compared with previously developed 15 or 30-μm-i.d. packed-column LC[65, 72] and CE-MS systems.[69]

## 2. Experimental Section

### 2.1. Materials and Reagents

Fused-silica capillaries used for making the *n*OTCs (2-μm inner diameter, 150-μm outer diameter) were purchased from Polymicro Technologies, a subsidiary of Molex (Phoenix, AZ). Trypsin was purchased from Promega (Madison, WI). Sodium hydroxide, ammonia bicarbonate, acetonitrile, toluene and trimethoxy(octadecyl) silane were purchased from Sigma-Aldrich (St. Louis, MO). All solutions were prepared via ultrapure water (Nanopure ultrapure

water system, Barnstead, Dubuque, IA) and filtered through a 0.22-μm filter (VWR, TX), de-gassed before use.

### 2.2. *narrow* OT Column Preparation

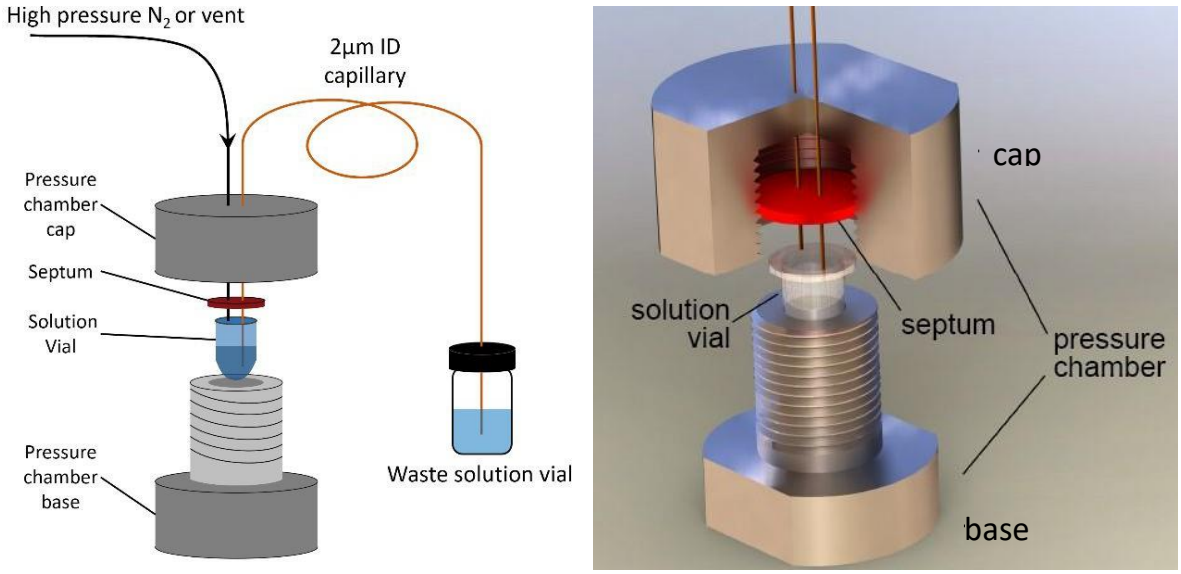


**Figure 5.1 Apparatus for coating the *n*OT column for *n*OTLC-MS**

(A) The whole setup for *n*OTC coating. (B) The rendered 3D diagram for the pressure chamber.

Figure 5.1 presents the apparatus configuration for *n*OTC preparation. Two septa were placed between the stainless-steel pressure chamber cap and base to make the chamber air-tight. To prepare a *n*OTC, an 85-cm-long, 2-μm-i.d. capillary (Polymicro Technologies) was cut. The polyimide coating on the beginning of the capillary was removed. A 25 G X 7/8" hypodermic needle was used as a guide to facilitate the insertion of this capillary through the septa into the reagent solution vial in the pressure chamber. First, a vial with piranha solution (3 parts of concentrated $H_2SO_4$ and 1 part of 30% $H_2O_2$) and 6.9 MPa $N_2$ was applied. The end of the capillary was inserted into a waste vial with DI water. The whole setup was then moved into an oven @ 75 ℃. After an hour, the piranha solution vial was replaced with a DDI water vial with 6.9 MPa $N_2$ applied. The setup was reinserted in the oven for 30 min. Then the setup was removed from the oven to cool to room temperature. An empty vial was

then placed inside the chamber with 6.9 MPa $N_2$ applied at room temperature. This procedure lasted for an hour to dry the inside of the capillary.

A syringe delivered a mixture of premixed 15 µL OTMS (Sigma-Aldrich (St. Louis, MO)) and 5 µL toluene (Sigma-Aldrich (St. Louis, MO)) into the reagent vial. The capillary inlet was inserted into the pressure chamber via a needle guide and 6.9 MPa $N_2$ was then applied to the chamber. The water waste vial was replaced with another vial with isopropanol. The whole setup was moved inside an oven at 75 °C. After 18 h, the coating reagent vial was replaced with an empty vial with 6.9 MPa $N_2$ in the pressure chamber to remove the coating reagent inside of the capillary.

### 2.3. Spray Tip Fabrication

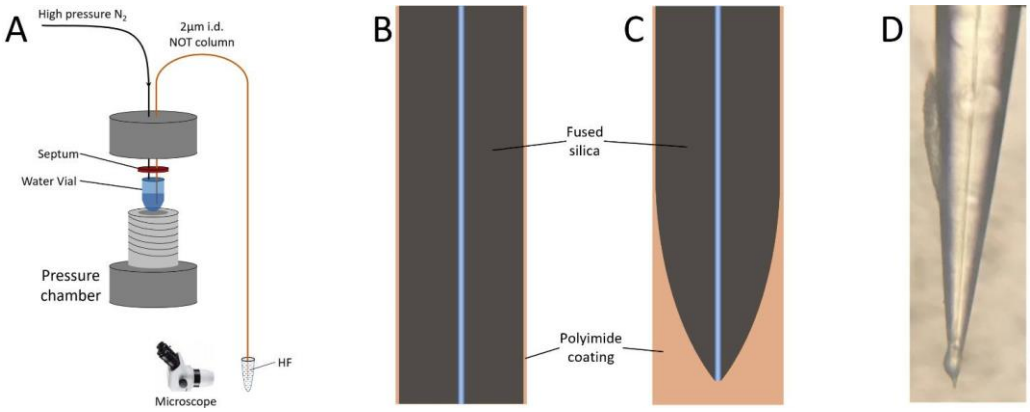


**Figure 5.2 Experimental setup and procedures for the fabrication of externally tapered electrospray emitter tip on the *n*OT column**

(A) One end of the *n*OTC was inserted into HF solution (49%) while flushing water from the capillary to prevent the etching of the inner capillary. (B) Illustration of the capillary end before (B) and after (C) HF etching. (D) A photograph of the etched emitter tip after removing the polyamide coating using heated sulfuric acid.

Figure 5.2 presents the setup for making the emitter. The uncoated end was inserted into a pressure chamber with a water vial inside. 6.9 MPa $N_2$ was applied to flush the capillary with water to prevent etching inside the channel. The end with polyimide coating was dipped

inside 49% HF for 90 min. The polyimide coating outside of the tip was then removed with hot $H_2SO_4$.

### 2.4. Cell Culture and Proteomic Sample Preparation

*Shewanella oneidensis* MR-1 was cultured under fed-batch mode using a Bioflow 3000 fermentor (New Brunswick Scientific, Enfield, NC) as described previously.[72] The horse blood agar (HBa) culture media was supplemented with 0.5 $mL \cdot L^{-1}$ of 100 mM ferric NTA, 1 $mL \cdot L^{-1}$ of 1mM $Na_2SeO_4$, and 1 $mL \cdot L^{-1}$ of 3 M $MgCl_2 \cdot 6H_2O$ as well as vitamins and amino acids. For proteomic preparation, bacterial cells were lysed by homogenizing with 0.1 mm zirconia/silica beads in a Bullet Blender (Next Advance, Averill Park, NY) at speed 8,000 rpm for 3 min. Proteins were denatured with 8 M urea and reduced with 10 mM DTT. The denatured proteins were digested with trypsin at a protein/trypsin ratio of 50:1 and incubated at 37 °C for 3 hours. The digested peptides were purified by C18 solid-phase extraction column and aliquoted at a concentration of 100 $ng \cdot \mu L^{-1}$ for long-term storage.

### 2.5. LC-MS/MS Analysis

A Dionex NCP3200RS UPLC gradient pump (Thermo Fisher) was employed for both sample injection and reversed-phase separation. Mobile Phase A (Fisher Scientific, Hampton, NH) consists of 0.1% (v/v) formic acid in water and Mobile phase B (Fisher Scientific, Hampton, NH) consists of 0.1% formic acid in acetonitrile. For sample injection, the VICI 6-port valve was switched to loading position. Protein digests were diluted using Mobile Phase A and manually injected into a 2.65-µL sample loop. The sample was loaded into the column head by infusing the sample at a flow rate of 700 $nL \cdot min^{-1}$ for 5 min with a 10-µm-i.d., 25-

cm-long restriction capillary. After sample loading, the 6-port valve was switched to separation position. A flow rate of 700 nL·min$^{-1}$ and a linear 40-min gradient from 5–35% mobile phase B were used for LC separation. The column was washed by increasing to 60% mobile phase B for 12 min and finally equilibrated with 5% mobile phase B for 15 min before the next injection.

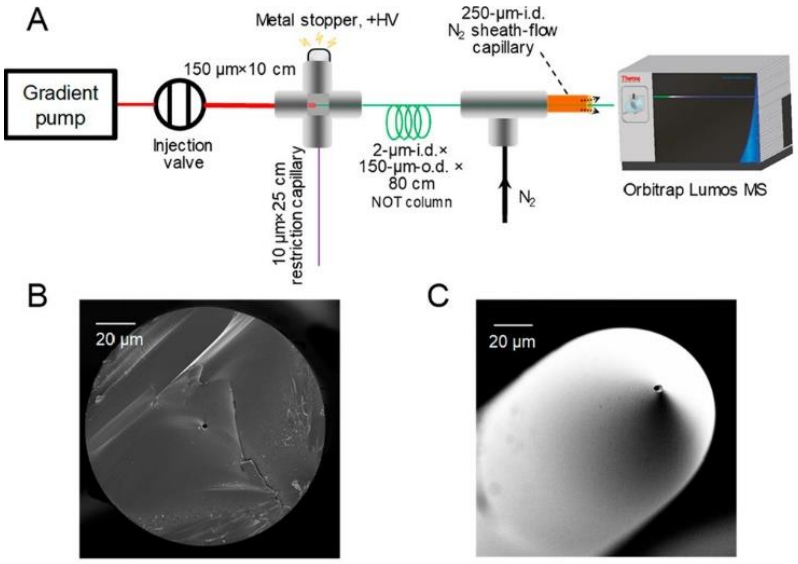


**Figure 5.3 Schematic diagram of experimental setup of *n*OTLC-MS and SEM images of *n*OT column**

(A) Schematic illustration of the experimental setup of the picoLC-MS system. (B) SEM images of the cross section of a *n*OTC and (C) the HF-etched electrospray emitter tip.

For ESI, a potential of 2 kV was applied to the capillary tip via the cross union-based flow splitter as shown in Figure 5.3. A nitrogen sheath flow maintained at 0.34 MPa was employed to stabilize the picoliter-scale electrospray. An Orbitrap Fusion Lumos Tribrid MS (Thermo Fisher, San Jose, CA) was employed for data acquisition under data dependent acquisition mode with a cycle time of 1.2 s. The ion transfer tube was set at 150 °C for desolvation and RF lens level was set at 30%. For MS1 acquisition, a mass range of 375 to 1575, a scan resolution of 120 k, an AGC target of 1E6, and a maximum injection time of 100 ms were employed. Precursor ions with charges of +2 to +7 and intensities >8,000 were selected

for MS/MS fragmentation in ion trap. Selected precursor ions were isolated with a m/z window of 2 Da and fragmented by collision induced dissociation (CID) at an energy level of 35% and an activation time of 10 ms. Rapid ion trap scan rate and an AGC target of 10,000 were used for MS/MS scan. For 0.75 pg and 7.5 pg peptide loading samples, a maximum injection time of 300 ms was used. For the highest 75 pg peptide loading samples, a maximum injection time of 80 ms was used.

**2.6. System Configuration**

The picoLC-MS system arrangement is illustrated in Figure 5.3A. Briefly, a 2-μm-i.d., 150-μm-o.d., 80-cm-long fused silica capillary (cross section shown in Figure 5.3B) with a layer of C18 stationary phase on the inner capillary surface serve as the *n*OTC. The capillary end was chemically etched by putting the capillary in 49% HF solution while flowing water continuously through the capillary (Figure 5.2).[5] The HF etching produced an externally tapered emitter tip (Figure 5.3C) for efficient ESI at the low picoliter-range flow rate. The externally tapered tip also minimized tip clogging problems during peptide separation,[70] compared with pulled tips having both internally and externally tapered structures. An Upchurch microcross was used to construct a flow splitter. A 10-cm-long × 150-μm-i.d. × 360-μm-o.d. capillary was used to connect the injection valve and the flow splitter. Inside the flow splitter, the *n*OTC head was inserted (1 mm deep) into this connection capillary. A metal stopper was used to apply ESI voltage, and a restriction capillary (RC) was used to control the splitting ratio.

A Dionex NCP3200RS UPLC gradient pump (Thermo-Fisher) operating at 700 $nL \cdot min^{-1}$

was employed for both sample injection and reversed-phase *n*OTLC separation. Using a 25-cm-long RC, the flow rate inside the *n*OTC was calculated to be around 790 $pL \cdot min^{-1}$. A high voltage was also applied through the cross to initiate ESI. To improve electrospray stability at picoliter-per-minute flow rates, a nitrogen sheath flow (0.34 MPa or 50 psi) was applied at the emitter through a Tee junction. Surprisingly, we cannot obtain evident peptide signals without the sheath gas, highlighting that more studies on the picoliter-scale electrospray are required to understand this phenomenon. The ionized peptides were collected by an Orbitrap Fusion Lumos Tribrid MS for data acquisition under data-dependent acquisition mode. To achieve optimal detection sensitivity, the precursor scans (MS1 scan) were performed at a scan resolution of 120K and a maximal injection time of 100 ms.[155] The tandem MS (MS2) scans were performed at ion trap with maximal injection times of 80 and 300 ms for highest peptide loading (75 pg) and lower peptide loadings (control, 0.75 pg, and 7.5 pg), respectively.

**2.7. Data Analysis**

All protein identification and quantification were performed using MaxQuant (version 1.6.2.6).[156] MS/MS spectra were searched against a UniProtKB/Swiss-Prot human database for *Shewanella oneidensis* MR-1 (Downloaded in 2/23/2017 and containing 645 reviewed and 3426 unreviewed sequences). Methionine oxidation and N-terminal acetylation were selected as variable modification. The minimal and maximal peptide lengths were set as 6 and 25, respectively. The maximal missed cleavage was set as 2. Both peptides and proteins were filtered with a maximum FDR of 0.01. Match between run (MBR) algorithm was activated with an alignment time window of 20 min and a match time window of 0.5 min. Note MBR

identifications were only used for protein quantification studies as shown in Figure 5.8.

# 3. Result and Discussion

## 3.1. Flow rate and splitting ratio

As an initial proof-of-concept, we injected serially diluted tryptic peptide samples from *Shewanella oneidensis* and eluted them using a 30 min LC gradient. To calculate the splitting ratio during the sample loading process, we injected a diluted peptide mixture, loaded it onto the *n*OTC, and then eluted it out using peptides at an isobaric condition of 35% Buffer B (0.1% formic acid in acetonitrile). We calculated the mobile-phase flow rate on the *n*OTC as ~790 $pL \cdot min^{-1}$ by measuring the dead time of unretained peptides (Figure 5.4, Figure 5.5). Using the resulting flow splitting ratio (1/886) and the total injected peptides in the sample loop (0.66 ng, 6.63 ng, and 66.3 ng), the on-column peptide amounts are calculated as 0.75 pg, 7.5 pg, and 75 pg, respectively. We observed feature-rich chromatograms for all peptide loadings.

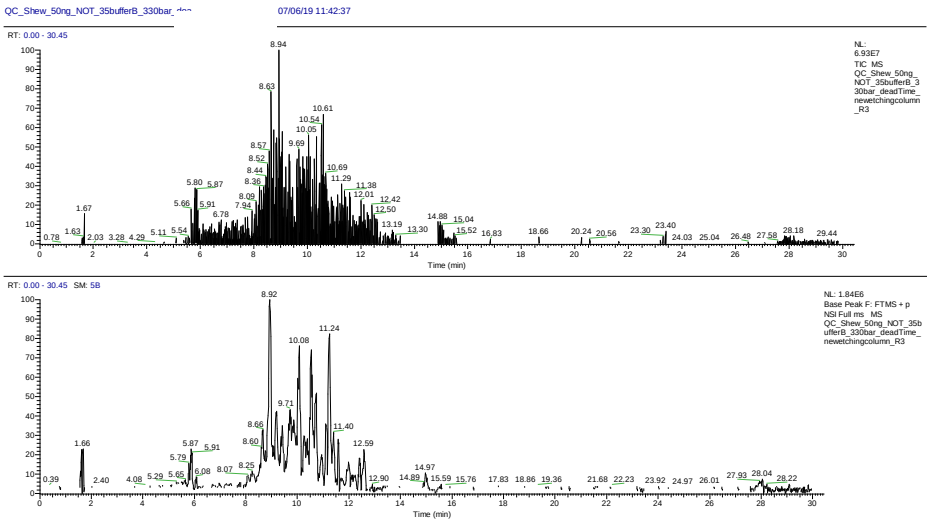


**Figure 5.4 The base-peak and TIC chromatograms showing the dead time of the *n*OT column by eluting the peptide mixtures with 35% Buffer B.**

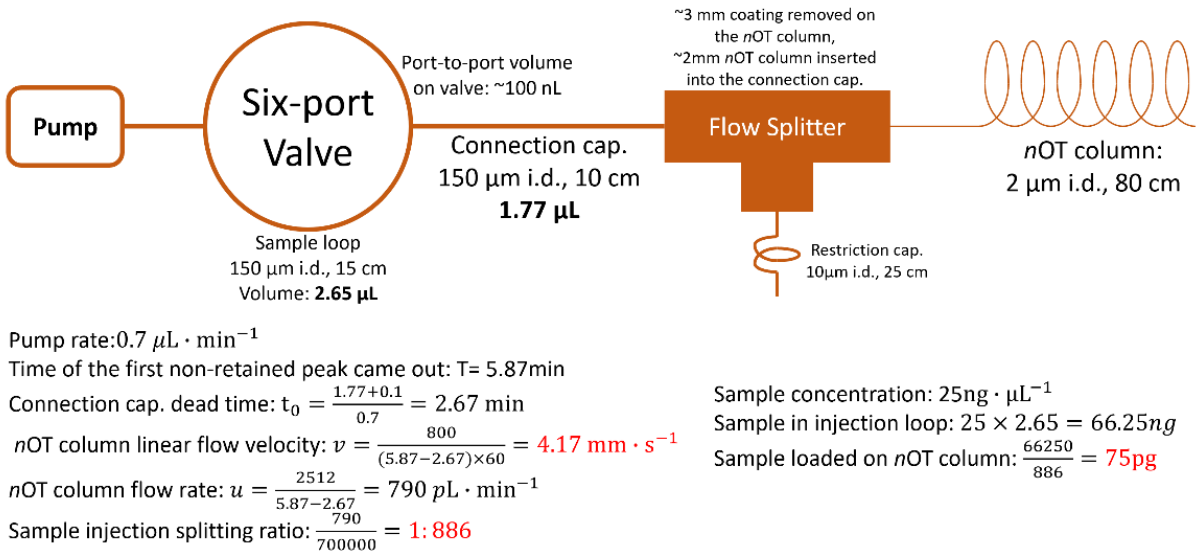


**Figure 5.5 Step-by-step calculation of the splitting ratio and on-column peptide amounts.**

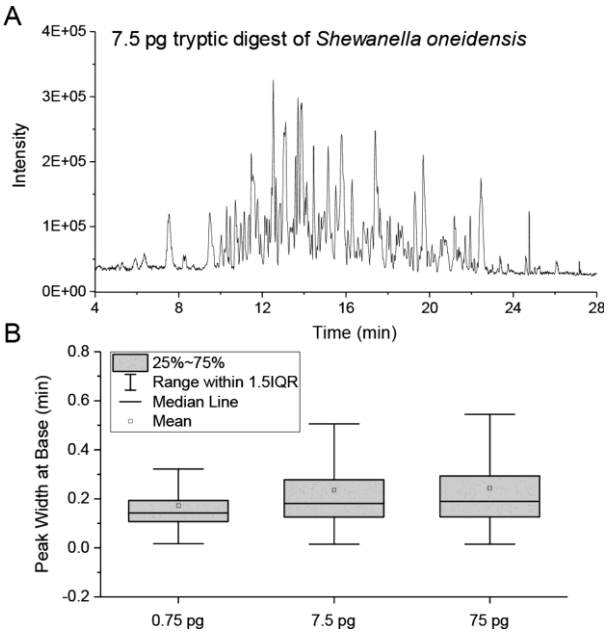


**Figure 5.6 Base peak chromatogram of 7.5 pg *S. oneidensis* and box plots of identified peptides' base peak widths**

(A) PicoLC-MS base peak chromatogram of 7.5 pg *S. oneidensis* tryptic digest. (B) Box plots of peak widths at base for the identified peptide peaks from peptide loadings of 0.75 pg, 7.5 pg, and 75 pg and a separation gradient of 30 min.

A typical base peak chromatogram of 7.5 pg peptide loading is shown in Figure 5.6. Most peptide peaks have intensities from $1 \times 10^4$ to $3 \times 10^5$. Notably, the background signal is surprisingly low with an average total ion current (TIC) of $3 \times 10^5$, which we ascribe to

minimal contamination from solvent and ambient air at picoliter-scale flow rates. By comparison, we generally observe a background TIC signal in the range of $5 \times 10^6$ to $2 \times 10^7$ from conventional nanoLC systems having flow rates of 150−300 $nL \cdot min^{-1}$ (data not shown). The low background signals are not likely due to the use of sheath gas, because we observed similar background signals with and without sheath gas. Next, we evaluated the separation efficiency of the *n*OTC using the peak widths provided by MaxQuant. As shown in Figure 5.6B, the median peak widths are 0.14, 0.18, and 0.19 min for 0.75 pg, 7.5 pg, and 75 pg peptides, respectively, separated using 30 min gradients. Although only a thin-layer C18 coating was used in the *n*OTC, it still provided good separation efficiency for the complex peptide digest. No significant peak broadening was observed when the peptide amount was increased from 7.5 pg to 75 pg.

### 3.2. Qualitative Analysis

To evaluate the sensitivity of the picoLC-MS system, the proteome coverage for the three peptide loading samples together with a control blank sample (an injection of Buffer A – 0.1% formic acid in water) were extracted. Only two peptides and proteins were identified in blank samples. In comparison to blank samples, the average peptide identifications based on MS/MS spectra range from 175 to 4000 and the corresponding protein identifications are from 78 to 949 for duplicate loadings of 0.75 pg, 7.5 pg, and 75 pg peptides, respectively (Figure 5.7 A, B). As expected, most proteins identified for lower loading samples were present with higher loadings (Figure 3C), indicating LC-MS coverage was not limited by MS/MS peptide identification/sequencing speed. The ability to profile ~1000 proteins from

only 75 pg total peptides represented over 10−100-fold improvement in sensitivity compared with previously developed 15 or 30-μm-i.d. packed column LC[65, 72] and CE-MS systems.[69] We attribute the improvement to three unique aspects of the picoLC-MS system: (1) At picoflow rates, the ESI efficiency is greatly increased;[65] (2) sample losses to stationary-phase surfaces are minimized compared to conventional nanoflow LC; and (3) the reduced flow rates combined with a nitrogen sheath gas minimize chemical background from LC solvents and ambient air, which improve both ion accumulation and detection of low-abundance peptide species in the MS detector.

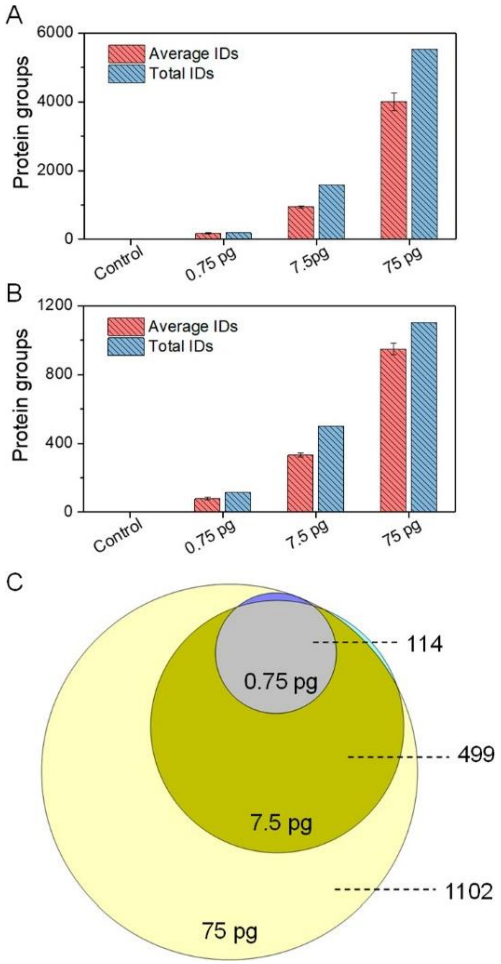


**Figure 5.7 Unique peptides/proteins identifications from different sample loaded and overlap of total protein identification from three peptide loadings**

(A) Unique peptide and (B) protein group identifications (IDs) from duplicate injections of 0.75 pg, 7.5 pg, and 75 pg tryptic digests of *Shewanella oneidensis* using the picoLC-MS system. (C) Overlap of total protein iden-

tifications from the three peptide loadings. All peptides and proteins were identified based on MS/MS spectra using Andromeda of MaxQuant at 1% False Discovery Rate (FDR) at both peptide and protein levels.

### 3.3. Quantitative Analysis

In addition to protein identification, we next evaluate the feasibility of the picoLC-MS system for quantitative analysis. We extracted the LFQ intensities of identified proteins and performed the pairwise correlations between samples containing the same loading amounts. To increase the number of quantified proteins, we used the Match Between Runs (MBR) algorithm of MaxQuant, where peptides were identified based on accurate masses and LC retention times. To maintain high rigor and robustness, "LFQ min ratio count of 2" and "Require MS/MS for LFQ comparisons" were selected as quantification criteria. As shown in Figure 5.8, the picoLC-MS system was able to quantify 41, 165, and 605 proteins from 0.75, 7.5, and 75 pg samples. Pairwise correlation coefficients with $R^2$ of 0.94, 0.86, and 0.90 were obtained between the three protein loadings (Figure 5.8A−C). The slight decrease of $R^2$ with the increase of protein loading is not well understood. We suspect the picoliter-scale electrospray was operated at suboptimal conditions. Thus, the signal stability could be further improved though the use of liquid sheath flow or pulled emitters.[67] We then calculated the linear correlation coefficients between loading amounts and protein LFQ intensities for all the common 41 proteins across all the samples. High linear correlation coefficients, with a median $R^2$ of 0.98, were obtained (Figure 5.8F). $R^2$ values exceeding 0.96 were observed for both high- (Peroxiredoxin TsaA) (Figure 5.8D) and relatively low-abundance (50S ribosomal protein L1) (Figure 5.8E) proteins. Together, although only picogram proteins were injected in each analysis, the picoLC-MS still provided decent quantification performance.

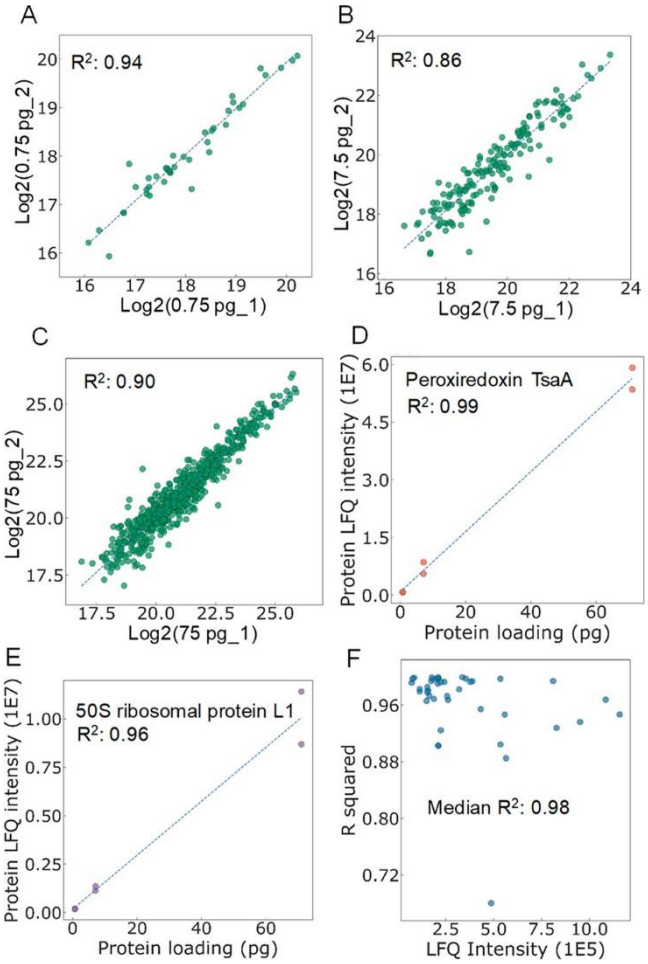


**Figure 5.8 Pairwise correlation of protein LFQ intensities between samples, linear correlations between protein loading amount and protein LFQ intensities and distribution of $R^2$ for the commonly identified 41 proteins as a function of protein LFQ**

Pairwise correlation of protein LFQ intensities between samples containing the same loading amounts, including (A) 0.75 pg, (B) 7.5 pg, and (C) 75 pg tryptic digests of *S. oneidensis*. Linear correlations between protein loading amount and protein LFQ intensities for (D) a high-abundance protein (Peroxiredoxin TsaA) and (E) a low-abundance protein (50S ribosomal protein L1). (F) Distribution of $R^2$ for the commonly identified 41 proteins as a function of protein LFQ.

## 3.4. Conclusion

In summary, we have demonstrated that the sensitivity of LC-MS for bottom-up proteomics can be significantly improved by reducing the flow rates using a 2-µm-i.d. *n*OTC. To the best of our knowledge, the capability of identifying ~1000 protein groups represented the highest proteomic coverage for low picogram samples (75 pg). Given that 100−500 pg of total protein is typically contained in single mammalian cells, the picoLC-MS system provides

the basis for greatly increasing proteome coverage from single cells, and even enabling fractionation or multiple measurements from a single cell to obtain valuable statistical information from technical replicates. We envision that coupling of picoLC-MS with a high-recovery sample processing platform (e.g., nanoPOTS) and loss-less injection will significantly advance single-cell proteomics. The capability of identifying ~80 proteins from sub-picogram samples also opens the door for proteomic studies of much smaller single microbes or subcellular organelle in single cells.

To make the picoLC-MS practically applicable to single cells, new developments are clearly required. Loss-less sample injection approaches are desired to avoid using the split flow setup. Sample filtering and desalting technologies should be developed to prevent column clogging by cell debris and precipitates. To improve the stability and robustness of picoliter electrospray, a liquid sheath flow[69] could be incorporated to wash away crystallized/precipitated materials from the tip and increase the overall flow rate to low $nL \cdot min^{-1}$ range. In addition, it should be noted that there is enormous room to further improve the analytical performance. The benefits of *n*OTLC's ultrafast[10] and ultrahigh-resolution potential are not completely capitalized due to the suboptimal separation conditions and constrained MS sampling frequency (number of MS spectra per second), which will be included in our future development.

# Chapter 6: The Future of *narrow* OTLC

Theoretical studies suggest that to achieve the optimal performance of OTLC, the i.d. of the OTC should be 1 ~ 2 μm. Guided by this prediction, instrumental improvements in the past decades enabled us to develop *n*OTLC with such small i.d.s. We have made significant progress in the field since our first publication of 2-μm-i.d. OTMS-coated *n*OTCs (e.g., reduced column preparation time and dramatically improved performance). With improved columns, we demonstrated ultrahigh resolution separations, ultrafast separations, and ultrasensitive *n*OTLC-MS separations. We only explored *n*OTCs with C18 stationary phase, but different stationary phases (e.g. shorter hydrocarbon chains, aromatic hydrocarbons, fluorocarbon chains, etc) can be chosen for specific separation purposes.

LIF detectors are generally employed to analyze ultralow amounts of samples eluted from *n*OTCs. While LIF detectors are great for proof-of-concept studies and evaluation and optimization of column performance, the prerequisite for fluorogenic samples and the requirement for precise optical alignment make them less practical in real-world applications. To develop *n*OTLC technique for real-world applications (e.g., portable *n*OTLC devices), major improvements must be made such as miniaturized, universal, and sensitive detectors (e.g. an electrochemical detector or a portable MS).

To accommodate the ultralow flow rates of *n*OTC, flow splitters are routinely used to split excessive eluent from the pump. While mobile phase is abundant, the analytes are not always so. Even with the lowest splitting ratio we ever used, only ~ $\frac{1}{886}$ of sample in the sample loop was loaded on the *n*OTC. To use *n*OTCs for ultrasensitive separation (e.g., single-

cell proteomics), lossless injection methods must be developed.

Every coin has two sides. What impedes the development of *n*OTLC is perhaps its greatest advantage. Equipped with proper lossless sample delivery devices, *n*OTLC provides new opportunities for single-cell or even sub-cellular analysis. In addition, with a flow-splitter-free system, a *n*OTLC-MS system can be potentially developed for applications requiring long-term, robust analysis with ultralow consumption of eluent and samples such as analytical instruments in a celestial body lander/rover. For example, in an ideal condition with no splitting flow, 2 L eluent can last for $5 \times 10^9$ min or 9513 years with a continuous flow rate at 400 $pL \cdot min^{-1}$. Indeed, not all eluent can be used for separations, this simple calculation indicates that with proper *n*OTCs and management, *n*OTCs could outlast other spacecraft instruments for analyzing samples with small amount of eluents.

I believe, for *n*OTLC, the best is yet to come. I am looking forward to future developments of *n*OTLC by all the great minds.

1. Karger, B. L., HPLC: Early and recent perspectives. *Journal of chemical education* **1997,** *74* (1), 45.
2. Horvath, C. G.; Lipsky, S., Use of liquid ion exchange chromatography for the separation of organic compounds. *Nature* **1966,** *211* (5050), 748-749.
3. Snyder, L. R.; Kirkland, J. J.; Dolan, J. W., *Introduction to modern liquid chromatography*. John Wiley & Sons: 2011.
4. Karger, B. L.; Berry, L. V., Rapid liquid-chromatographic separation of steroids on columns heavily loaded with stationary phase. *Clin Chem* **1971,** *17* (8), 757-64.
5. Jorgenson, J. W.; Guthrie, E. J., Liquid chromatography in open-tubular columns: theory of column optimization with limited pressure and analysis time, and fabrication of chemically bonded reversed-phase columns on etched borosilicate glass capillaries. *Journal of Chromatography A* **1983,** *255*, 335-348.
6. Tsuda, T.; Hibi, K.; Nakanishi, T.; Takeuchi, T.; Ishii, D., Studies of open-tubular micro-capillary liquid chromatography: II. Chemically bonded octadecylsilane stationary phase. *Journal of Chromatography A* **1978,** *158*, 227-232.
7. Guiochon, G., Conventional packed columns vs. packed or open tubular microcolumns in liquid chromatography. *Analytical Chemistry* **1981,** *53* (9), 1318-1325.
8. Knox, J. H., Theoretical aspects of LC with packed and open small-bore columns. *Journal of Chromatographic Science* **1980,** *18* (9), 453-461.
9. Knox, J. H.; Gilbert, M. T., Kinetic optimization of straight open-tubular liquid chromatography. *Journal of Chromatography A* **1979,** *186*, 405-418.
10. Xiang, P.; Yang, Y.; Zhao, Z.; Chen, M.; Liu, S., Ultrafast Gradient Separation with Narrow Open Tubular Liquid Chromatography. *Anal Chem* **2019,** *91* (16), 10738-10743.
11. Xiang, P.; Yang, Y.; Zhao, Z.; Chen, A.; Liu, S., Experimentally Validating Open Tubular Liquid Chromatography for a Peak Capacity of 2000 in 3 h. *Anal Chem* **2019,** *91* (16), 10518-10523.
12. Xiang, P.; Zhu, Y.; Yang, Y.; Zhao, Z.; Williams, S. M.; Moore, R. J.; Kelly, R. T.; Smith, R. D.; Liu, S., Picoflow Liquid Chromatography–Mass Spectrometry for Ultrasensitive Bottom-Up Proteomics Using 2-μm-id Open Tubular Columns. *Analytical chemistry* **2020,** *92* (7), 4711-4715.
13. Crego, A. L.; Diez-Masa, J. C.; Dabrio, M. V., Preparation of open tubular columns for reversed-phase high-performance liquid chromatography. *Analytical Chemistry* **1993,** *65* (11), 1615-1621.
14. Yang, F. J., Open tubular column LC: Theory and practice. *Journal of Chromatographic Science* **1982,** *20* (6), 241-251.
15. Hibi, K.; Ishii, D.; Fujishima, I.; Takeuchi, T.; Nakanishi, T., Studies of open tubular micro capillary liquid chromatography. 1. The development of open tubular micro capillary liquid chromatography. *Journal of High Resolution Chromatography* **1978,** *1* (1), 21-27.
16. Hibi, K.; Ishii, D.; Tsuda, T., Alumina and support-coated open-tubular columns in open-tubular micro-capillary liquid chromatography. *Journal of Chromatography A* **1980,** *189* (2), 179-185.

17. Ishii, D.; Takeuchi, T., Open tubular capillary LC. *Journal of Chromatographic Science* **1980,** *18* (9), 462-472.
18. Ishii, D.; Tsuda, T.; Hibi, K.; Takeuchi, T.; Nakanishi, T., Study of open-tubular micro-capillary liquid chromatography. *Journal of High Resolution Chromatography* **1979,** *2* (6), 371-377.
19. Tsuda, T.; Nakagawa, G., Open-tubular liquid chromatography with 5–10-μm I.D. Columns. *Journal of Chromatography A* **1983,** *268*, 369-374.
20. Vliet, H. V.; Poppe, H., The performance of some cell designs for laser-induced fluorescence detection in open-tubular liquid chromatography. *Journal of Chromatography A* **1985,** *346*, 149-160.
21. Tock, P. P. H.; Stegeman, G.; Peerboom, R.; Poppe, H.; Kraak, J. C.; Unger, K. K., The application of porous silica layers in open tubular columns for liquid chromatography. *Chromatographia* **1987,** *24* (1), 617-624.
22. Berkel, O. V.; Poppe, H.; Kraak, J. C., The application of immobilized liquids for open tubular liquid chromatography. *Chromatographia* **1987,** *24*, 739-744.
23. Manz, A.; Miyahara, Y.; Miura, J.; Watanabe, Y.; Miyagi, H.; Sato, K., Design of an open-tubular column liquid chromatograph using silicon chip technology. *Sensors and Actuators B-chemical* **1990,** *1*, 249-255.
24. Beale, S. C.; Hsieh, Y. Z.; Savage, J. C.; Wiesler, D.; Novotny, M., 3-benzoyl-2-quinolinecarboxaldehyde: A novel fluorogenic reagent for the high-sensitivity chromatographic analysis of primary amines. *Talanta* **1989,** *36* (1-2), 321-5.
25. Beale, S. C.; Hsieh, Y.-Z.; Wiesler, D.; Novotny, M., Application of 3-(2-furoyl) quinoline-2-carbaldehyde as a fluorogenic reagent for the analysis of primary amines by liquid chromatography with laser-induced fluorescence detection. *Journal of Chromatography A* **1990,** *499*, 579-587.
26. Göhlin, K.; Larsson, M., Narrow (5-50-μm id) open tubular columns in liquid chromatography using immobilized polymethyloctadecylsiloxane as stationary phase. *Journal of Microcolumn Separations* **1991,** *3* (6), 547-556.
27. Swart, R.; Kraak, J. C.; Poppe, H., Preparation and evaluation of polyacrylate-coated fused-silica capillaries for reversed-phase open-tubular liquid chromatography. *journal of chromatography a* **1994,** *670* (1-2), 25-38.
28. Swart, R.; Kraak, J. C.; Poppe, H., Highly efficient separations on 5 μm internal diameter open tubular capillaries coated with thick polyacrylate stationary phases. *chromatographia* **1995,** *40* (9), 587-593.
29. Luo, Q.; Yue, G.; Valaskovic, G.; Gu, Y.; Wu, S.-l.; Karger, B., On-line 1D and 2D porous layer open tubular/LC-ESI-MS using 10-microm-i.d. poly(styrene-divinylbenzene) columns for ultrasensitive proteomic analysis. *Analytical chemistry* **2007,** *79 16*, 6174-81.
30. Yue, G.; Luo, Q.; Zhang, J.; Wu, S. L.; Karger, B. L., Ultratrace LC/MS proteomic analysis using 10-microm-i.d. Porous layer open tubular poly(styrene-divinylbenzene) capillary columns. *Anal Chem* **2007,** *79* (3), 938-46.

31. Wang, X.; Wang, S.; Veerappan, V.; Byun, C. K.; Nguyen, H.; Gendhar, B.; Allen, R.; Liu, S., Bare nanocapillary for DNA separation and genotyping analysis in gel-free solutions without application of external electric field. *Analytical chemistry* **2008,** *80 14*, 5583-9.
32. Wang, X.; Liu, L.; Pu, Q.; Zhu, Z.; Guo, G.; Zhong, H.; Liu, S., Pressure-induced transport of DNA confined in narrow capillary channels. *J Am Chem Soc* **2012,** *134* (17), 7400-5.
33. Wang, X.; Kang, J.; Wang, S.; Lu, J. J.; Liu, S., Chromatographic separations in a nanocapillary under pressure-driven conditions. *J Chromatogr A* **2008,** *1200* (2), 108-13.
34. Wang, X.; Veerappan, V.; Cheng, C.; Jiang, X.; Allen, R. D.; Dasgupta, P. K.; Liu, S., Free solution hydrodynamic separation of DNA fragments from 75 to 106,000 base pairs in a single run. *J Am Chem Soc* **2010,** *132* (1), 40-1.
35. Wang, X.; Liu, L.; Guo, G.; Wang, W.; Liu, S.; Pu, Q.; Dasgupta, P. K., Resolving DNA in free solution. *TrAC Trends in Analytical Chemistry* **2012,** *35*, 122-134.
36. Chen, H.; Zhu, Z.; Lu, J. J.; Liu, S., Charging YOYO-1 on capillary wall for online DNA intercalation and integrating this approach with multiplex PCR and bare narrow capillary-hydrodynamic chromatography for online DNA analysis. *Anal Chem* **2015,** *87* (3), 1518-22.
37. Wang, X.; Cheng, C.; Wang, S.; Zhao, M.; Dasgupta, P. K.; Liu, S., Nanocapillaries for open tubular chromatographic separations of proteins in femtoliter to picoliter samples. *Anal Chem* **2009,** *81* (17), 7428-35.
38. Luo, Q.; Rejtar, T.; Wu, S. L.; Karger, B. L., Hydrophilic interaction 10 microm I.D. porous layer open tubular columns for ultratrace glycan analysis by liquid chromatography-mass spectrometry. *J Chromatogr A* **2009,** *1216* (8), 1223-31.
39. Rogeberg, M.; Wilson, S. R.; Greibrokk, T.; Lundanes, E., Separation of intact proteins on porous layer open tubular (PLOT) columns. *J Chromatogr A* **2010,** *1217* (17), 2782-6.
40. Li, R.-n.; Shao, Y.; Yu, Y.; Wang, X.; Guo, G.-s., Pico-HPLC system integrating an equal inner diameter femtopipette into a 900 nm I.D. porous layer open tubular column. *Chemical communications* **2017,** *53 29*, 4104-4107.
41. Chen, H.; Yang, Y.; Qiao, Z.; Xiang, P.; Ren, J.; Meng, Y.; Zhang, K.; Juan Lu, J.; Liu, S., A narrow open tubular column for high efficiency liquid chromatographic separation. *Analyst* **2018,** *143* (9), 2008-2011.
42. Yang, Y.; Xiang, P.; Chen, H.; Zhao, Z.; Zhu, Z.; Liu, S., On-column and gradient focusing-induced high-resolution separation in narrow open tubular liquid chromatography and a simple and economic approach for pico-gradient separation. *Anal Chim Acta* **2019,** *1072*, 95-101.
43. Yang, Y.; Chen, H.; Beckner, M. A.; Xiang, P.; Lu, J.; Cao, C.; Liu, S., Narrow, Open, Tubular Column for Ultrahigh-Efficiency Liquid-Chromatographic Separation under Elution Pressure of Less than 50 bar. *Analytical chemistry* **2018,** *90 18*, 10676-10680.
44. Yang, Y.; Xiang, P.; Chen, A.; Liu, S., Liquid Chromatographic Separation Using a 2 μm i.d. Open Tubular Column at Elevated Temperature. *analytical chemistry* **2021,** *93* (10), 4361-4364.

45. Small, H., Hydrodynamic chromatography a technique for size analysis of colloidal particles. In *Joint International Conference on Information Sciences*, 1974; Vol. 48, pp 147-161.
46. Zhu, Z.; Liu, L.; Wang, W.; Lu, J. J.; Wang, X.; Liu, S., Resolving DNA at efficiencies of more than a million plates per meter using bare narrow open capillaries without sieving matrices. *Chem Commun (Camb)* **2013,** *49* (28), 2897-9.
47. Folestad, S.; Josefsson, B.; Larsson, M., Performance and preparation of immobilized polysiloxane stationary phases in 5–55 μm I.D. open-tubular fused silica columns for liquid chromatography☆. *journal of chromatography a* **1987,** *391* (2), 347-372.
48. Tock, P. P. H.; Boshoven, C.; Poppe, H.; Kraak, J. C.; Unger, K. K., Performance of porous silica layers in open-tubular columns for liquid chromatography. *journal of chromatography a* **1989,** *477* (1), 95-106.
49. Unger, K.; Schick-Kalb, J.; Krebs, K.-F., Preparation of porous silica spheres for column liquid. *journal of chromatography a* **1973,** *83*, 5-9.
50. Swart, R.; Kraak, J. C.; Poppe, H., Recent progress in open tubular liquid chromatography. *TrAC Trends in Analytical Chemistry* **1997,** *16* (6), 332-342.
51. Kazarian, A. A.; Rodriguez, E. S.; Deverell, J. A.; McCord, J. P.; Muddiman, D.; Paull, B., Wall modified photonic crystal fibre capillaries as porous layer open tubular columns for in-capillary micro-extraction and capillary chromatography. *Analytica chimica acta* **2016,** *905*, 1-7.
52. da Silva, M. R.; Brandtzaeg, O. K.; Vehus, T.; Lancas, F. M.; Wilson, S. R.; Lundanes, E., An automated and self-cleaning nano liquid chromatography mass spectrometry platform featuring an open tubular multi-hole crystal fiber solid phase extraction column and an open tubular separation column. *J Chromatogr A* **2017,** *1518*, 104-110.
53. Li, R.-n.; Wang, Y.; Peng, M.; Wang, X.; Guo, G.-s., Preparation and Application of Porous Layer Open Tubular Capillary Columns with Narrow Bore in Liquid Chromatography. *Chinese Journal of Analytical Chemistry* **2017,** *45*, 1865-1873.
54. Hara, T.; Izumi, Y.; Nakao, M.; Hata, K.; Baron, G.; Bamba, T.; Desmet, G., Silica-based hybrid porous layers to enhance the retention and efficiency of open tubular capillary columns with a 5#¼m inner diame9ter. *Journal of chromatography. A* **2018,** *1580*, 63-71.
55. Vehus, T.; Roberg-Larsen, H.; Waaler, J.; Aslaksen, S.; Krauss, S.; Wilson, S. R.; Lundanes, E., Versatile, sensitive liquid chromatography mass spectrometry - Implementation of 10 mum OT columns suitable for small molecules, peptides and proteins. *Sci Rep* **2016,** *6*, 37507.
56. Xiang, P.; Yang, Y.; Zhao, Z.; Wang, J.; Chen, M.; Chen, A.; Liu, S., Performing flow injection chromatography using a narrow open tubular column. *Analytica chimica acta* **2020,** *1109*, 19-26.
57. Yang, Y.; Liu, S., Non-porous Thin Dense Layer Coating: Key to Achieving Ultrahigh Peak Capacities Using Narrow Open Tubular Columns. 2020; Vol. 1.
58. Zhu, Z.; Chen, H.; Wang, W.; Morgan, A.; Gu, C.; He, C.; Lu, J. J.; Liu, S., Integrated bare narrow capillary-hydrodynamic chromatographic system for free-solution DNA separation at the single-molecule level. *Angew Chem Int Ed Engl* **2013,** *52* (21), 5612-6.

59. Swart, R.; Kraak, J. C.; Poppe, H., Performance of an ethoxyethylacrylate stationary phase for open-tubular liquid chromatography. *journal of chromatography a* **1995,** *689* (2), 177-187.
60. Weaver, M. T.; Lynch, K. B.; Zhu, Z.; Chen, H.; Lu, J. J.; Pu, Q.; Liu, S., Confocal laser-induced fluorescence detector for narrow capillary system with yoctomole limit of detection. *talanta* **2017,** *165*, 240-244.
61. Zhang, W.; Liu, L.; Zhang, Q.; Zhang, D.; Hu, Q.; Wang, Y.; Wang, X.; Pu, Q.; Guo, G., Visual and real-time imaging focusing for highly sensitive laser-induced fluorescence detection at yoctomole levels in nanocapillaries. *chemical communications* **2020,** *56* (16), 2423-2426.
62. Wahl, J.; Goodlett, D.; Udseth, H.; Smith, R. D., Attomole level capillary electrophoresis-mass spectrometric protein analysis using 5 .mu.m i.d. capillaries. *Analytical Chemistry* **1992,** *64*, 3194-3196.
63. Gale, D.; Smith, R., Small volume and low flow-rate electrospray lonization mass spectrometry of aqueous samples. *Rapid Communications in Mass Spectrometry* **1993,** *7*, 1017-1021.
64. Emmett, M. R.; Caprioli, R. M., Micro-electrospray mass spectrometry: Ultra-high-sensitivity analysis of peptides and proteins. *J Am Soc Mass Spectrom* **1994,** *5* (7), 605-13.
65. Shen, Y.; Tolic, N.; Masselon, C.; Pasa-Tolic, L.; Camp, D. G., 2nd; Hixson, K. K.; Zhao, R.; Anderson, G. A.; Smith, R. D., Ultrasensitive proteomics using high-efficiency on-line micro-SPE-nanoLC-nanoESI MS and MS/MS. *Anal Chem* **2004,** *76* (1), 144-54.
66. Heemskerk, A. A. M.; Busnel, J.-M.; Schoenmaker, B.; Derks, R. J. E.; Klychnikov, O.; Hensbergen, P. J.; Deelder, A. M.; Mayboroda, O. A., Ultra-low flow electrospray ionization-mass spectrometry for improved ionization efficiency in phosphoproteomics. *analytical chemistry* **2012,** *84* (10), 4552-4559.
67. Yuill, E. M.; Sa, N.; Ray, S. J.; Hieftje, G. M.; Baker, L. A., Electrospray ionization from nanopipette emitters with tip diameters of less than 100 nm. *Anal Chem* **2013,** *85* (18), 8498-502.
68. Lynch, W. T., Calculation of electric field breakdown in quartz as determined by dielectric dispersion analysis. *journal of applied physics* **1972,** *43* (8), 3274-3278.
69. Sun, L.; Zhu, G.; Zhao, Y.; Yan, X.; Mou, S.; Dovichi, N. J., Ultrasensitive and fast bottom-up analysis of femtogram amounts of complex proteome digests. *Angew Chem Int Ed Engl* **2013,** *52* (51), 13661-4.
70. Marginean, I.; Tang, K.; Smith, R. D.; Kelly, R. T., Picoelectrospray ionization mass spectrometry using narrow-bore chemically etched emitters. *J Am Soc Mass Spectrom* **2014,** *25* (1), 30-6.
71. Kelly, R. T.; Page, J. S.; Luo, Q.; Moore, R. J.; Orton, D. J.; Tang, K.; Smith, R. D., Chemically etched open tubular and monolithic emitters for nanoelectrospray ionization mass spectrometry. *Anal Chem* **2006,** *78* (22), 7796-801.
72. Zhu, Y.; Zhao, R.; Piehowski, P. D.; Moore, R. J.; Lim, S.; Orphan, V. J.; Pasa-Tolic, L.; Qian, W. J.; Smith, R. D.; Kelly, R. T., Subnanogram proteomics: impact of LC column

selection, MS instrumentation and data analysis strategy on proteome coverage for trace samples. *Int J Mass Spectrom* **2018,** *427*, 4-10.
73. Zubritsky, E., How analytical chemists saved the human genome project...or at least gave it a helping hand. *Analytical chemistry* **2002,** *74 1*, 23A-26A.
74. Mathies, R.; Huang, X. C., Capillary array electrophoresis: an approach to high-speed, high-throughput DNA sequencing. *Nature* **1992,** *359*, 167-169.
75. Dovichi, N.; Zhang, J., How Capillary Electrophoresis Sequenced the Human Genome. *ChemInform* **2001,** *32*.
76. Ruiz-Martinez, M. C.; Berka, J.; Belenkii, A.; Foret, F.; Miller, A. W.; Karger, B. L., DNA sequencing by capillary electrophoresis with replaceable linear polyacrylamide and laser-induced fluorescence detection. *Anal Chem* **1993,** *65* (20), 2851-8.
77. Kambara, H.; Takahashi, S., Multiple-sheathflow capillary array DNA analyser. *Nature* **1993,** *361* (6412), 565-6.
78. Washburn, M. P.; Wolters, D.; Yates, J. R., 3rd, Large-scale analysis of the yeast proteome by multidimensional protein identification technology. *Nat Biotechnol* **2001,** *19* (3), 242-7.
79. Plumb, R. S.; Johnson, K. A.; Rainville, P.; Smith, B. W.; Wilson, I. D.; Castro-Perez, J. M.; Nicholson, J. K., UPLC/MS(E); a new approach for generating molecular fragment information for biomarker structure elucidation. *Rapid Commun Mass Spectrom* **2006,** *20* (13), 1989-94.
80. Chait, B. T., Chemistry. Mass spectrometry: bottom-up or top-down? *Science* **2006,** *314* (5796), 65-6.
81. Aebersold, R.; Mann, M., Mass spectrometry-based proteomics. *Nature* **2003,** *422* (6928), 198-207.
82. Nassar, A. F.; Wu, T.; Nassar, S. F.; Wisnewski, A. V., UPLC-MS for metabolomics: a giant step forward in support of pharmaceutical research. *Drug Discov Today* **2017,** *22* (2), 463-470.
83. Vos, R. D.; Moco, S.; Lommen, A.; Keurentjes, J.; Bino, R.; Hall, R. D., Untargeted large-scale plant metabolomics using liquid chromatography coupled to mass spectrometry. *Nature Protocols* **2007,** *2*, 778-791.
84. Wilson, I. D.; Plumb, R.; Granger, J.; Major, H.; Williams, R.; Lenz, E. M., HPLC-MS-based methods for the study of metabonomics. *J Chromatogr B Analyt Technol Biomed Life Sci* **2005,** *817* (1), 67-76.
85. Jones, D. R.; Wu, Z.; Chauhan, D.; Anderson, K. C.; Peng, J., A nano ultra-performance liquid chromatography-high resolution mass spectrometry approach for global metabolomic profiling and case study on drug-resistant multiple myeloma. *Anal Chem* **2014,** *86* (7), 3667-75.
86. Jorgenson, J., Capillary liquid chromatography at ultrahigh pressures. *Annual review of analytical chemistry* **2010,** *3*, 129-50.
87. MacNair, J. E.; Lewis, K. C.; Jorgenson, J. W., Ultrahigh-pressure reversed-phase liquid chromatography in packed capillary columns. *Anal Chem* **1997,** *69* (6), 983-9.

88. Golay, M. J. E. In *Gas Chromatography 1957 (Lansing Symposium) ed VJ Coates, HJ Noebels, IS Fagerson.*, Academic Press: New York: 1958; p 1−13.
89. Guo, Y.; Colon, L. A., A stationary phase for open tubular liquid chromatography and electrochromatography using sol-gel technology. *Analytical Chemistry* **1995,** *67* (15), 2511-2516.
90. Collins, D. A.; Nesterenko, E. P.; Paull, B., Porous layer open tubular columns in capillary liquid chromatography. *analyst* **2014,** *139* (6), 1292-1302.
91. Jorgenson, J. W.; Kennedy, R. T.; St. Claire, I. R. L.; White, J. G.; Dluzneski, P. R.; de Wit, J. S. M., Open tubular liquid-chromatography and the analysis of single neurons. *Journal of Research of the National Bureau of Standards* **1988,** *93* (3), 403-406.
92. Pesek, J. J.; Matyska, M. T., Electrochromatography in chemically modified etched fused-silica capillaries. *journal of chromatography a* **1996,** *736*, 255-264.
93. Onuska, F. I.; Comba, M. E.; Bistricki, T.; Wilkinson, R. J., Preparation of surface-modified wide-bore wall-coated open-tubular columns. *Journal of Chromatography A* **1977,** *142*, 117-125.
94. Kennedy, R. T.; Oates, M. D.; Cooper, B. R.; Nickerson, B.; Jorgenson, J. W., Microcolumn separations and the analysis of single cells. *Science* **1989,** *246* (4926), 57-63.
95. Hara, T.; Futagami, S.; Eeltink, S.; De Malsche, W.; Baron, G. V.; Desmet, G., Very High Efficiency Porous Silica Layer Open-Tubular Capillary Columns Produced via in-Column Sol-Gel Processing. *Anal Chem* **2016,** *88* (20), 10158-10166.
96. Desmet, G.; Callewaert, M.; Ottevaere, H.; De Malsche, W., Merging Open-Tubular and Packed Bed Liquid Chromatography. *Anal Chem* **2015,** *87* (14), 7382-8.
97. Desmet, G.; Eeltink, S., Fundamentals for LC miniaturization. *analytical chemistry* **2013,** *85* (2), 543-556.
98. Han, J.; Ye, L.; Xu, L.; Zhou, Z.; Gao, F.; Xiao, Z.; Wang, Q.; Zhang, B., Towards high peak capacity separations in normal pressure nanoflow liquid chromatography using meter long packed capillary columns. *analytica chimica acta* **2014,** *852*, 267-273.
99. Luo, Q.; Shen, Y.; Hixson, K. K.; Zhao, R.; Yang, F.; Moore, R. J.; Mottaz, H. M.; Smith, R. D., Preparation of 20-microm-i.d. silica-based monolithic columns and their performance for proteomics analyses. *Anal Chem* **2005,** *77* (15), 5028-35.
100. Shen, Y.; Zhang, R.; Moore, R. J.; Kim, J.; Metz, T. O.; Hixson, K. K.; Zhao, R.; Livesay, E. A.; Udseth, H. R.; Smith, R. D., Automated 20 kpsi RPLC-MS and MS/MS with chromatographic peak capacities of 1000-1500 and capabilities in proteomics and metabolomics. *Anal Chem* **2005,** *77* (10), 3090-100.
101. Zhou, F.; Lu, Y.; Ficarro, S. B.; Webber, J. T.; Marto, J. A., Nanoflow low pressure high peak capacity single dimension LC-MS/MS platform for high-throughput, in-depth analysis of mammalian proteomes. *analytical chemistry* **2012,** *84* (11), 5133-5139.
102. Wahab, M. F.; Wimalasinghe, R. M.; Wang, Y.; Barhate, C. L.; Patel, D. C.; Armstrong, D. W., Salient Sub-Second Separations. *analytical chemistry* **2016,** *88* (17), 8821-8826.
103. Bleicher, K. H.; Bohm, H. J.; Muller, K.; Alanine, A. I., Hit and lead generation: beyond high-throughput screening. *Nat Rev Drug Discov* **2003,** *2* (5), 369-78.

104. Spacil, Z.; Tatipaka, H.; Barcenas, M.; Scott, C. R.; Turecek, F.; Gelb, M. H., High-throughput assay of 9 lysosomal enzymes for newborn screening. *Clin Chem* **2013,** *59* (3), 502-11.
105. Equitz, T. R.; Rodriguez-Cruz, S. E., High-throughput analysis of controlled substances: Combining multiple injections in a single experimental run (MISER) and liquid chromatography–mass spectrometry (LC-MS). *Forensic Chemistry* **2017,** *5*, 8-15.
106. Wahab, M. F.; Wimalasinghe, R. M.; Wang, Y.; Barhate, C. L.; Patel, D. C.; Armstrong, D. W., Salient Sub-Second Separations. *Anal Chem* **2016,** *88* (17), 8821-6.
107. Horvath, C. G.; Preiss, B. A.; Lipsky, S. R., Fast liquid chromatography: an investigation of operating parameters and the separation of nucleotides on pellicular ion exchangers. *Anal Chem* **1967,** *39* (12), 1422-8.
108. Nguyen, D. T.; Guillarme, D.; Rudaz, S.; Veuthey, J. L., Validation of an ultra-fast UPLC-UV method for the separation of antituberculosis tablets. *J Sep Sci* **2008,** *31* (6-7), 1050-6.
109. Barhate, C. L.; Wahab, M. F.; Breitbach, Z. S.; Bell, D. S.; Armstrong, D. W., High efficiency, narrow particle size distribution, sub-2 mum based macrocyclic glycopeptide chiral stationary phases in HPLC and SFC. *Anal Chim Acta* **2015,** *898*, 128-37.
110. Barhate, C. L.; Wahab, M. F.; Tognarelli, D. J.; Berger, T. A.; Armstrong, D. W., Instrumental Idiosyncrasies Affecting the Performance of Ultrafast Chiral and Achiral Sub/Supercritical Fluid Chromatography. *Anal Chem* **2016,** *88* (17), 8664-72.
111. Ciogli, A.; Ismail, O. H.; Mazzoccanti, G.; Villani, C.; Gasparrini, F., Enantioselective ultra high performance liquid and supercritical fluid chromatography: The race to the shortest chromatogram. *J Sep Sci* **2018,** *41* (6), 1307-1318.
112. Regalado, E. L.; Welch, C. J., Pushing the speed limit in enantioselective supercritical fluid chromatography. *J Sep Sci* **2015,** *38* (16), 2826-32.
113. Patel, D. C.; Breitbach, Z. S.; Wahab, M. F.; Barhate, C. L.; Armstrong, D. W., Gone in seconds: praxis, performance, and peculiarities of ultrafast chiral liquid chromatography with superficially porous particles. *Anal Chem* **2015,** *87* (18), 9137-48.
114. Barhate, C. L.; Joyce, L. A.; Makarov, A. A.; Zawatzky, K.; Bernardoni, F.; Schafer, W. A.; Armstrong, D. W.; Welch, C. J.; Regalado, E. L., Ultrafast chiral separations for high throughput enantiopurity analysis. *Chem Commun (Camb)* **2017,** *53* (3), 509-512.
115. Patel, D. C.; Wahab, M. F.; Armstrong, D. W.; Breitbach, Z. S., Advances in high-throughput and high-efficiency chiral liquid chromatographic separations. *J Chromatogr A* **2016,** *1467*, 2-18.
116. D'Orazio, G.; Kakava, R.; Volonterio, A.; Fanali, S.; Chankvetadze, B., An attempt for fast separation of enantiomers in nano-liquid chromatography and capillary electrochromatography. *Electrophoresis* **2017,** *38* (15), 1932-1938.
117. Thurmann, S.; Lotter, C.; Heiland, J. J.; Chankvetadze, B.; Belder, D., Chip-based high-performance liquid chromatography for high-speed enantioseparations. *Anal Chem* **2015,** *87* (11), 5568-76.
118. Bezhitashvili, L.; Bardavelidze, A.; Ordjonikidze, T.; Chankvetadze, L.; Chity, M.; Farkas, T.; Chankvetadze, B., Effect of pore-size optimization on the performance of

polysaccharide-based superficially porous chiral stationary phases for the separation of enantiomers in high-performance liquid chromatography. *J Chromatogr A* **2017,** *1482*, 32-38.
119. Ismail, O. H.; Pasti, L.; Ciogli, A.; Villani, C.; Kocergin, J.; Anderson, S.; Gasparrini, F.; Cavazzini, A.; Catani, M., Pirkle-type chiral stationary phase on core-shell and fully porous particles: Are superficially porous particles always the better choice toward ultrafast high-performance enantioseparations? *J Chromatogr A* **2016,** *1466*, 96-104.
120. Patel, D. C.; Wahab, M. F.; O'Haver, T. C.; Armstrong, D. W., Separations at the Speed of Sensors. *Anal Chem* **2018,** *90* (5), 3349-3356.
121. Moore, A. W., Jr.; Jorgenson, J. W., Study of zone broadening in optically gated high-speed capillary electrophoresis. *Anal Chem* **1993,** *65* (24), 3550-60.
122. Jacobson, S. C.; Culbertson, C. T.; Daler, J. E.; Ramsey, J. M., Microchip Structures for Submillisecond Electrophoresis. *Analytical Chemistry* **1998,** *70* (16), 3476-3480.
123. Brennen, R. A.; Yin, H.; Killeen, K. P., Microfluidic gradient formation for nanoflow chip LC. *Anal Chem* **2007,** *79* (24), 9302-9.
124. Jaromir, R.; EH, H., Flow Injection Analyses. I. A New Concept of Fast Continuous Flow Analysis. *Anal Chim Acta* **1975**.
125. Ruzicka, J.; Hansen, E. H., Retro-review of flow-injection analysis. *TrAC Trends in Analytical Chemistry* **2008,** *27* (5), 390-393.
126. Ruzicka, J.; Marshall, G. D., Sequential injection: a new concept for chemical sensors, process analysis and laboratory assays. *Analytica Chimica Acta* **1990,** *237* (2), 329-343.
127. Šatínský, D.; Solich, P.; Chocholouš, P.; Karlíček, R., Monolithic columns—a new concept of separation in the sequential injection technique. *Analytica Chimica Acta* **2003,** *499* (1-2), 205-214.
128. Srisawang, B.; Kongtawelert, P.; Hartwell, S. K.; Jakmunee, J.; Grudpan, K., A simple flow injection-reduced volume column system for hemoglobin typing. *Talanta* **2003,** *60* (6), 1163-70.
129. Chocholouš, P.; Dědková, L.; Boháčová, T.; Šatínský, D.; Solich, P., Fast separation of red colorants in beverages using cyano monolithic column in Sequential Injection Chromatography. *Microchemical Journal* **2017,** *130*, 384-389.
130. Koblova, P.; Sklenarova, H.; Chocholous, P.; Polasek, M.; Solich, P., Simple automated generation of gradient elution conditions in sequential injection chromatography using monolithic column. *Talanta* **2011,** *84* (5), 1273-7.
131. Davletbaeva, P.; Chocholous, P.; Bulatov, A.; Satinsky, D.; Solich, P., Sub-1min separation in sequential injection chromatography for determination of synthetic water-soluble dyes in pharmaceutical formulation. *J Pharm Biomed Anal* **2017,** *143*, 123-129.
132. Chocholous, P.; Solich, P.; Satinsky, D., An overview of sequential injection chromatography. *Anal Chim Acta* **2007,** *600* (1-2), 129-35.
133. Hartwell, S. K.; Kehling, A.; Lapanantnoppakhun, S.; Grudpan, K., Flow Injection/Sequential Injection Chromatography: A Review of Recent Developments in Low

Pressure with High Performance Chemical Separation. *Analytical Letters* **2013,** *46* (11), 1640-1671.
134. Idris, A. M., The second five years of sequential injection chromatography: significant developments in the technology and methodologies. *Crit Rev Anal Chem* **2014,** *44* (3), 220-32.
135. Chocholous, P.; Satinsky, D.; Sladkovsky, R.; Pospisilova, M.; Solich, P., Determination of pesticides fenoxycarb and permethrin by sequential injection chromatography using miniaturized monolithic column. *Talanta* **2008,** *77* (2), 566-570.
136. Chocholous, P.; Holik, P.; Satinsky, D.; Solich, P., A novel application of Onyxtrade mark monolithic column for simultaneous determination of salicylic acid and triamcinolone acetonide by sequential injection chromatography. *Talanta* **2007,** *72* (2), 854-8.
137. Chocholous, P.; Kosarova, L.; Satinsky, D.; Sklenarova, H.; Solich, P., Enhanced capabilities of separation in Sequential Injection Chromatography--fused-core particle column and its comparison with narrow-bore monolithic column. *Talanta* **2011,** *85* (2), 1129-34.
138. Zhu, Z.; Chen, H.; Chen, A.; Lu, J. J.; Liu, S.; Zhao, M., Simultaneously sizing and quantitating zeptomole-level DNA at high throughput in free solution. *Chemistry* **2014,** *20* (43), 13945-50.
139. Antonangelo, A. T.; Alonso, D. P.; Ribolla, P. E.; Colombi, D., Microsatellite marker-based assessment of the biodiversity of native bioethanol yeast strains. *Yeast* **2013,** *30* (8), 307-17.
140. Kaliszan, R.; Wiczling, P., Gradient reversed-phase high-performance chromatography of ionogenic analytes. *TrAC Trends in Analytical Chemistry* **2011,** *30* (9), 1372-1381.
141. González-San Miguel, H. M.; Fernández, M.; Estela, J. M.; Cerdà, V., Contribution of multi-commuted flow analysis combined with monolithic columns to low-pressure, high-performance chromatography. *TrAC Trends in Analytical Chemistry* **2009,** *28* (3), 336-346.
142. Adcock, J. L.; Francis, P. S.; Agg, K. M.; Marshall, G. D.; Barnett, N. W., A hybrid FIA/HPLC system incorporating monolithic column chromatography. *Anal Chim Acta* **2007,** *600* (1-2), 136-41.
143. Fernandez, M.; Miro, M.; Gonzalez, H. M.; Cerda, V., Modulation of mobile phase composition in flow-injection/sequential-injection chromatography exploiting multisyringe flow analysis. *Anal Bioanal Chem* **2008,** *391* (3), 817-25.
144. Zhang, B.; Whiteaker, J. R.; Hoofnagle, A. N.; Baird, G. S.; Rodland, K. D.; Paulovich, A. G., Clinical potential of mass spectrometry-based proteogenomics. *Nat Rev Clin Oncol* **2019,** *16* (4), 256-268.
145. Aebersold, R.; Mann, M., Mass-spectrometric exploration of proteome structure and function. *Nature* **2016,** *537* (7620), 347-55.
146. Hein, M. Y.; Sharma, K.; Cox, J.; Mann, M., Proteomic Analysis of Cellular Systems. In *Handbook of Systems Biology*, 2013; Vol. 3, pp 3-25.
147. Zubarev, R. A.; Makarov, A., Orbitrap mass spectrometry. *Anal Chem* **2013,** *85* (11), 5288-96.

148. Hebert, A. S.; Prasad, S.; Belford, M. W.; Bailey, D. J.; McAlister, G. C.; Abbatiello, S. E.; Huguet, R.; Wouters, E. R.; Dunyach, J. J.; Brademan, D. R.; Westphall, M. S.; Coon, J. J., Comprehensive Single-Shot Proteomics with FAIMS on a Hybrid Orbitrap Mass Spectrometer. *Anal Chem* **2018,** *90* (15), 9529-9537.
149. Kelly, R. T.; Tolmachev, A. V.; Page, J. S.; Tang, K.; Smith, R. D., The ion funnel: theory, implementations, and applications. *Mass Spectrom Rev* **2010,** *29* (2), 294-312.
150. Marginean, I.; Page, J. S.; Tolmachev, A. V.; Tang, K.; Smith, R. D., Achieving 50% ionization efficiency in subambient pressure ionization with nanoelectrospray. *Anal Chem* **2010,** *82* (22), 9344-9.
151. Li, S.; Plouffe, B. D.; Belov, A. M.; Ray, S.; Wang, X.; Murthy, S. K.; Karger, B. L.; Ivanov, A. R., An Integrated Platform for Isolation, Processing, and Mass Spectrometry-based Proteomic Profiling of Rare Cells in Whole Blood. *Mol Cell Proteomics* **2015,** *14* (6), 1672-83.
152. Stadlmann, J.; Hudecz, O.; Krssakova, G.; Ctortecka, C.; Van Raemdonck, G.; Op De Beeck, J.; Desmet, G.; Penninger, J. M.; Jacobs, P.; Mechtler, K., Improved Sensitivity in Low-Input Proteomics Using Micropillar Array-Based Chromatography. *Anal Chem* **2019,** *91* (22), 14203-14207.
153. Zhu, Y.; Piehowski, P. D.; Zhao, R.; Chen, J.; Shen, Y.; Moore, R. J.; Shukla, A. K.; Petyuk, V. A.; Campbell-Thompson, M.; Mathews, C. E.; Smith, R. D.; Qian, W. J.; Kelly, R. T., Nanodroplet processing platform for deep and quantitative proteome profiling of 10-100 mammalian cells. *Nat Commun* **2018,** *9* (1), 882.
154. Zhu, Y.; Clair, G.; Chrisler, W. B.; Shen, Y.; Zhao, R.; Shukla, A. K.; Moore, R. J.; Misra, R. S.; Pryhuber, G. S.; Smith, R. D.; Ansong, C.; Kelly, R. T., Proteomic Analysis of Single Mammalian Cells Enabled by Microfluidic Nanodroplet Sample Preparation and Ultrasensitive NanoLC-MS. *Angew Chem Int Ed Engl* **2018,** *57* (38), 12370-12374.
155. Kelstrup, C. D.; Young, C.; Lavallee, R.; Nielsen, M. L.; Olsen, J. V., Optimized fast and sensitive acquisition methods for shotgun proteomics on a quadrupole orbitrap mass spectrometer. *J Proteome Res* **2012,** *11* (6), 3487-97.
156. Tyanova, S.; Temu, T.; Cox, J., The MaxQuant computational platform for mass spectrometry-based shotgun proteomics. *nature protocols* **2016,** *11* (12), 2301-2319.